INTERPRETATION OF CLAY SWELLING VIA NON- CONTACT LINEAR DISPLACEMENT METER (NC-LDM)

ALI RIZA ERDOGAN

INTERPRETATION OF CLAY SWELLING VIA NON-CONTACT LINEAR DISPLACEMENT METER (NC-LDM)

Ali Riza ERDOGAN

Supervisor: Prof. Chris H. Greenwell

Durham University

Department of Earth Sciences

Master by Research Thesis

April 2016

I hereby declare that all information in this document has been obtained and presented in accordance with academic rules and ethical conduct. I also declare that, I have fully cited and referenced all material and results that are not original to this work.

Ali Riza Erdogan

ABSTRACT

Shale instability is one of the ongoing major problems when drilling oil/gas wellbores. The interaction of aqueous drilling fluids or fracturing fluids, with reactive clay minerals in shales causes swelling, in turn causing costly wellbore instabilities. In this study, the swelling of compacted commercial Na-bentonite clay mineral cores was investigated using a novel non-contact displacement meter with various organic solvents and salt solutions as the electrolyte. Swelling results with organic solvents were correlated with the dielectric constant, dipole moment, surface tension and viscosity of the solvent. It was found that swelling rate and total swelling were proportional to dielectric constant and inversely proportional to viscosity, representing the chemical and capillary components of swelling, respectively. Results of swelling tests with salt solutions are discussed in the context of diffuse double layer (DDL) theory. Swelling behaviour of smectite clay minerals were found to be highly affected by cation concentration. Tests with $CaCl_2$ solutions showed that divalent cations were effective at suppressing swelling at low concentrations. At high concentrations KCl and KI solutions were more effective at inhibiting swelling owing to the lower hydration enthalpy of K^+ cations. Repeats of selected tests with non-swelling illite rich shale compacted cores were compared with the swelling Na-bentonite clay mineral compacted cores. Comparison between Na-bentonite and illite swelling shows that, for reconstituted compacted cores, the initial stage of clay swelling is dominated by capillary action. Then, depending on the reactivity of the clay and the medium, chemical swelling occurs. Consequently, the swelling behaviour of compacted clay cores, as used by many drilling fluid research laboratories, is highly dependent on the domination of different swelling components in different time periods as an artefact of the sample preparation and

care should be taken when using ground and compacted shales to assess either reactivity of shale formations to drilling fluids or the effectiveness of swelling inhibitor systems.

ACKNOWLEDGEMENTS

The completion of this project could not have been possible without the participation and contribution of so many people. First, it's been a great pleasure and an honour for me to work with Professor Chris Greenwell who has been very kind and helpful from the moment I walked in. He's made it so much easier for me to carry out a research abroad for the first time in my life.

I would like to thank Turkish Petroleum Association (TPAO) for letting me have such a great working experience in Durham University with the funding and support. I especially thank to my supervisors Selcuk Erkekol and Muzaffer Gorkem Gokdemir, and also Huseyin Ali Dogan from M-I SWACO for helping me take my first steps into a new career in a brand new research field.

Our research group has been very cooperative and enjoyable to work with. Rikan Kareem, Pablo Cubillas, Darren Grocke, Valentina Drulievna, Munira Raji-Idowu and Tom Underwood; and our former members Musarrat Mohammed, Manohara Gudiyor-Veerabhadr, Blanca Racinero Gomez and Josie Mahony made me feel like I am working in United Nations. Hilary Redden and Jack Rowbottom gave a priceless support in the laboratory and made me work in a safer environment. I would also like to thank newborn Yani Kareem, so that his name is mentioned in an academic paper which might lead a way for him to be a scientist like his father and work for peace.

I would personally like to thank Anna Whitford for being a very cheerful co-worker and not using tap water instead of deionized water.

I wish to thank Laura Haswell and many unnamed heroes of Durham University Earth Sciences staff for easing every step of this postgraduate journey. I would also like to thank Stephen Lishman and his team for their technical support in Physics Department workshop.

I am grateful to my family for supporting me with my decisions and being there for me whenever I need them. Finally, I would like to give my biggest thank to my beloved wife Aylin, who has encouraged me for my every single step in the last eight years. She has always led my way to the right choice tirelessly and been the hidden source of my achievements.

TABLE OF CONTENTS

ABSTRACT iii

ACKNOWLEDGEMENTS v

LIST OF TABLES x

LIST OF FIGURES xi

1. INTRODUCTION 1

1.1. Shales & Clay Minerals 3

1.1.1. Properties of Shales 3

1.1.2. Properties of Clay Minerals 5

1.1.3. Smectite Clay Minerals 9

1.1.4. Illite Clay Minerals 11

1.2. Swelling in Shales & Clays 12

1.2.1. Crystalline Swelling 13

1.2.2. Osmotic Swelling 14

1.3. Measuring Swelling of Shales and Compacted Clay Minerals 18

1.3.1. X-Ray Diffraction (XRD) Technique 18

1.3.2. Macroscopic Swelling Tests of Shales and Compacted Clay Minerals 19

1.4. Clay and Shale Swelling in Different Solvents 20

1.5 AIM OF THE STUDY 22

2. EXPERIMENTAL METHODS 24

2.1. Materials 24

2.2. Artificial Core Preparation and Mounting 26

2.3. Swelling Measurements 27

2.3.1. Non-contact Linear Displacement Meter 27

2.3.2 Overall Equilibrium Swelling Tests 30

2.4. Relative Humidity Measurements 30

3. RESULTS AND DISCUSSION 32

3.1 Swelling of Compacted Na-bentonite Cores in Water 33

3.2 Swelling of Compacted Na-bentonite Cores in Different Organic Solvents 37

3.2.1. Short Term Swelling Tests 37

3.2.2. Equlibirium Long Term Swelling Tests 44

3.3. Swelling of Compacted Na-bentonite Cores in Aqueous Electrolyte Solutions 49

3.3.1. Effects of Cation Concentration on Swelling of Compacted Na-bentonite Cores 50

3.3.2. Effect of Group 1 Cations on Swelling of Compacted Na-bentonite Cores 53

3.3.3. Effect of Group 1 Anions on Swelling of Compacted Na-bentonite Cores 56

3.2.4. Effect of Group 2 Cations on the Swelling of Compacted Na-bentonite Cores 58

3.4. Swelling of Illite 62

3.4.1. Swelling in Aqueous Electrolyte Solutions 63

3.4.2. Swelling of Compacted Illite in Organic Solvents.....64

4. FURTHER WORK & LIMITATIONS 67

4.1 Further Possible Tests with NC-LDM.....67

4.2. Development of In-Situ XRD Cell 68

5. CONCLUSIONS.....73

APPENDIX A. XRD Data of Na-bentonite and Illite.....75

APPENDIX B. Definition of the Solvent Properties 77

APPENDIX C. Preparation of Electrolyte Solutions 79

APPENDIX D. Working Principles of Non-Contact Linear Displacement Meter ..81

APPENDIX E. Calibration of Non-Contact Linear Displacement Meter.....83

APPENDIX G. Adjustment of Relative Humidity.....86

APPENDIX F. Data Processing 87

5. REFERENCES.....90

LIST OF TABLES

Table 1. Classes of shales based on methylene blue capacity and water contents (Mondshine, 1969) (M: Montmorillonite, I : Illite, K: kaolin, C: chlorite, ML ; Mixed layer montmorillonite & illite) 4

Table 2. Classes of shales based on hydration and dispersion characteristics (Chenevert and O'Brien, 1973) 5

Table 3: Cation exchange capacities of common clays (Grim, 1953). 9

Table 4. Physical properties of water and the organic solvents used in this study. (Jasper, 1973; Smallwood, 2012) Definitions of the solvent properties are given in Appendix B. 25

Table 5. Physical properties of the salts used in electrolyte solutions 26

Table 6. Hydration enthalpies of the cations used in this study 34

Table 7. Total swelling and approximate swelling time results of equilibrium swelling tests of compacted Na-bentonite cores. 45

Table 8. The amounts of salt required for short term swelling tests 79

Table 9. The amounts of salt required for short term swelling tests 80

Table 10. Relative humidity values at saturated salt solutions 86

LIST OF FIGURES

Figure 1. Schematic description of wellbore drilling operation describing the motion of the drilling fluid throughout the various depths of the borehole. (Murray, 2006).....2

Figure 2: Schematic description of clay structure components: a) An octahedral unit b) sheet structure of octahedral units (Grimm, 1953) 6

Figure 3. Schematic description of clay structure components: a) A tetrahedral unit b) sheet structure of tetrahedral units (Grimm, 1953).....6

Figure 4. Diagrammatic sketch of the montmorillonite structure showing the arrangement of atoms and molecules along with interlayer cations and water (adapted from Grim, 1953).....10

Figure 5. Diagrammatic sketch of the illite structure showing the arrangement of atoms and molecules along with interlayer cations and water (adapted from Grim, 1953).....11

Figure 6. Schematic description of swelling pressure in a shale system, simplified as a single set of clay platelets connected to a pore, including the in-situ vertical and horizontal stresses, the pore pressure, the swelling pressure acting between the clay platelets, and tensile or compressive forces in the cementation developing upon compressive or tensile loading of the shale material, respectively. (Van Oort, 2003) 13

Figure 7. Schematic to show distribution of ions in diffuse double layer (DDL) theory (Soga and Mitchell, 2005).....15

Figure 8. Schematic description of wet-cell XRD technique used in the study of Warr and Berger (2007) 19

Figure 9. Artificial Na-bentonite core prepared by hydraulic press.....27

Figure 10. Schematic description of non-contact linear displacement meter (NC-LDM).....28
Figure 11. The non-contact linear displacement meter (NC-LDM). Inset photograph shows the sample holder along with the perforated metal disk the clay cores are placed on.....29
Figure 12. Application of equilibrium swelling tests.....30
Figure 13. Vaisala HM40s humidity and temperature meter.....31
Figure 14. Short term swelling tests of Na-bentonite cores in water, showing the two main swelling regimes discussed in the main text. 33
Figure 15. Schematic to show possible mechanisms for clay-water interactions: a) Hydrogen bonding, b) Ion hydration, c) Osmosis attraction (forming of double layers) and d) dipole attraction.(Soga and Mitchell, 2005).....35
Figure 16. Short term swelling behaviour of Na-bentonite cores in water with different relative humidity values of air.....36
Figure 17. Linear swelling behaviour of Na-bentonite cores in various organic solvents via NC-LDM with 60 readings/minute frequency. 38
Figure 18. Photographic images of Na-bentonite cores after short term swelling tests in hexane, methanol and water.....39
Figure 19. Correlations of the linear swelling rate of compacted Na-bentonite cores with: a) dipole moment, b) surface tension, c) viscosity and d) dielectric constant of the designated solvent along with linear regression (R^2) values.....40
Figure 20. Short term swelling behaviour of compacted Na-bentonite cores in water and water/propan-2-ol solutions.....42
Figure 21. Short term swelling behaviour of compacted Na-bentonite cores in 1.5 M glycine/water solution 43

Figure 22. Results of equilibrium long term swelling tests of compressed Na-bentonite cores in organic solvents. Water swelling included as a reference point. 44

Figure 23. Correlations of the linear swelling of Na-bentonite cores with: a) dielectric constant, b) dipole moment, c) surface tension and d) viscosity of the designated solvent along with linear regression (R^2) values. 46

Figure 24. Short term swelling behaviour of compacted Na-bentonite cores in aqueous NaCl solutions. 50

Figure 25. Equilibrium swelling behaviour of compacted Na-bentonite cores in aqueous NaCl solutions as a function of concentration. 51

Figure 26. Short term swelling behaviour of compacted Na-bentonite cores in KCl/water solutions. 53

Figure 27. Equilibrium swelling behaviour of Na-bentonite cores in aqueous NaCl and KCl solutions as a function of concentration. 54

Figure 28. Short term swelling behaviour of compacted Na-bentonite cores in aqueous KI and KCl solutions 56

Figure 29. Equilibrium swelling behaviour of compacted Na-bentonite cores in aqueous KI and KCl solutions 57

Figure 30. Short term swelling behaviour of compacted Na-bentonite cores in $CaCl_2$/water solutions. 58

Figure 31. Equilibrium swelling behaviour of compacted Na-bentonite cores in aqueous $CaCl_2$ and KCl solutions 59

Figure 32. Equilibrium linear swelling points of Na-bentonite cores in aqueous solutions of KCl, NaCl, KI and $CaCl_2$ from 0.02 M to 2 M concentrations 60

Figure 33. Short term swelling of Na-bentonite and illite cores in water. 62

Figure 34. Linear swelling behaviour of compacted illite cores in different concentrations of aqueous KCl, NaCl and $CaCl_2$ solutions 63
Figure 35. Swelling behaviour of compacted illite cores in water, methanol, 1-heptanol and 1-decanol.....64
Figure 36. Swelling behaviour of compacted illite cores prepared with different particle sizes 65
Figure 37. XRD peaks showing the varying hydration states of montmorillonite (Warr and Berger, 2007) 69
Figure 38. Schematic description of the *in situ* XRD cell used in this study.....70
Figure 39. Dimensions of the in-situ XRD cell used in this study.....71
Figure 40. XRD Data obtained from the trials of in-situ XRD cell 72
Figure 41. XRD pattern for Na-bentonite cores between a 2-Theta of 2-65°. Where M = Montmorillonite, Q = Quartz, Cr = Cristobalite, F = Feldspar.....75
Figure 42. XRD pattern for illite cores between a 2-Theta of 2-70°. Where I = illite, Q = Quartz, K = Kaolinite, Cr = Cristobalite, F = Feldspar.....76
Figure 43. Photographic image of the calibration of the NC-LDM 84
Figure 44. Calibration curve of 25mm metal disk.....85
Figure 45. Calibration curve of 20mm metal disk.....85
Figure 46. Schematic structure of a single unit of NC-LDM.....87
Figure 47. Swelling data before processing 88
Figure 48. Swelling data after processing 89

1. INTRODUCTION

Drilling of oil and gas wellbores to reach subterranean petroleum reservoirs is a challenging process, mainly because of unstable and non-uniform downhole conditions. Figure 1 shows a schematic illustration of a wellbore drilling operation. (Murray, 2006) In order to perform an optimal wellbore drilling operation, technical drilling fluids (or drilling muds, as they are colloquially called in the industry) are used. Drilling fluid is defined as the circulation fluid used in rotary drilling operations which contacts with the wellbore and performs the needed functions for drilling operations. The functions of drilling fluids are:

-Cooling and lubricating the drill bit,

-Cleaning downhole and transporting drill cuttings,

-Supporting and stabilizing the borehole,

-Balancing the downhole formation pressure.

There are generally two types of drilling muds used; these are oil based drilling muds (OBM) and water based drilling muds (WBM). Despite providing more stability during wellbore drilling operations, the use of OBMs is restricted due to environmental impacts (Mody and Hale, 1993; Hale et al., 1993). As such, a key challenge for the industry has been to develop and produce WBMs having the capacity to stabilize the wellbore conditions with comparable performance to OBMs.

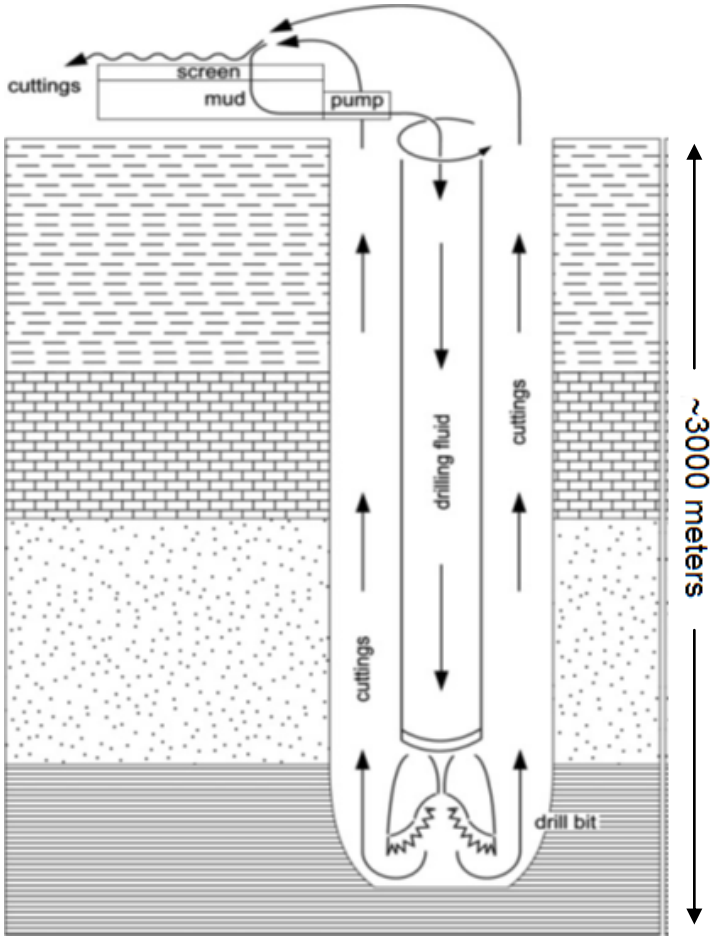

Figure 1. Schematic description of wellbore drilling operation describing the motion of the drilling fluid throughout the various depths (~3000 meters) of the borehole. (Murray, 2006)

Shale instability is an ongoing problem frequently encountered when drilling oil/gas wellbores. Shale is defined as an imprecise heterogeneous argillaceous material ranging from the relatively weak clay-rich gumbo to highly cemented siltstone, with the common characteristic being a matrix of very low permeability that contains clay minerals to some level (Tare and Mody, 2000). The interaction of aqueous drilling fluids, or fracturing fluids, with clay minerals in shales causes a number of effects including;

- *Clay swelling - Well bore disintegration & collapsing*

Adsorption of more water into shales increases shale stresses through the wellbore, which at some point leads to failure and forms cavities along the wellbore. This results as enlargement at the point of drilling, even leading to collapse and loss of wellbores (Chenevert and Osisanya, 1989).

- *Circulation loss & pipe sticking*

  When clay minerals swell and expand into the wellbore, the pre-designed wellbore diameter is reduced and causes an unexpected narrowing. This closure leads to an increase in circulation pressures, lost circulation and sticking of drill collars.

- *Increased plasticity - Bit balling*

  When drilled cuttings in the wellbore adhere to the drill bit assembly due to reactive shales, the rate of penetration (ROP) decreases (Cheatham and Namm, 1990).

Overall, the cost of problems related to unstable shales is estimated as 1 billion $/year (Zeynali, 2012).

1.1. Shales & Clay Minerals

1.1.1. Properties of Shales

There are several factors affecting shale properties, which vary according to the burial depth of the shale formation. The amount and type of the clay minerals in the shale structure defines the water-shale interactions. For instance, shale with more smectite (surface area - 750 m^2/g) has more affinity for water than illite (surface area - 80 m^2/g) or kaolinite (surface area - 25 m^2/g). The properties of shales are also affected by the initial water content, and whether the water is free or bound (Lal, 1999). Bound water refers to the first few water molecule layers attached to the clay surface via osmotic or physical bonding. When the water layer increases,

the strength of the bonds holding water molecules to the clay structure decreases, and the water molecules become more "free" and are able to move within clay structure (Hallikainen et al., 1985).

Table 1. Classes of shales based on methylene blue capacity and water contents (Mondshine, 1969) (M: Montmorillonite, I : Illite, K: kaolin, C: chlorite, ML ; Mixed layer montmorillonite & illite)

Class	Texture	Methylene Blue Capacity (meq/100g)	Water Content	Wt% Water	Clay Content	Wt% Clay	Density (g/cc)
A	Soft	20-40	Free & bound	25-70	M & I	20-30	1.2-1.5
B	Firm	10-20	Bound	15-25	I & ML	20-30	1.5-2.2
C	Hard	3-10	Bound	5-15	Trace of M & high in I	20-30	2.5-2.5
D	Brittle	0-3	Bound	2-5	I & K & C	5-30	2.5-2.7
E	Firm-Hard	10-20	Bound	2-10	I & ML	20-30	2.3-2.7

Shales are classified into groups according to their physical and structural properties, facilitating overcoming shale problems more easily and practically. Table 1 (Mondshine, 1969) shows five different shale properties, mainly classified through their methylene blue capacities. Table 2 (Chenevert and O'Brien, 1973) shows another classification system, based on a combination of clay content and hydration/dispersion characteristics.

Table 2. Classes of shales based on hydration and dispersion characteristics (Chenevert and O'Brien, 1973)

Class	Characteristics	Clay minerals
1	Soft, highly dispersive (Gumbo), mud making	High smectite, some illite
2	Soft, fairly dispersive. Mud making	High illite, fairly high smectite
3	Medium hard, moderately dispersive, sloughing	High in mixed-layer, illite, chlorite
4	Hard, little dispersion, sloughing	Moderate illite, moderate chlorite
5	Very hard, brittle, no dispersion, caving	High illite, moderate chlorite

1.1.2. Properties of Clay Minerals

Clays are ubiquitous naturally occurring layered minerals formed by weathering and decomposition of igneous rocks (Grim, 1953). Synthetic forms of clay may also be prepared, such as laponite or hectorite (Bergaya and Lagaly, 2013). Most of the clay minerals have a mica-like, flaky structure. These flakes consist of small crystal platelets stacking face to face. Each individual platelet is called a "unit layer" and surfaces of these unit layers are "basal surfaces". Depending on the clay mineral, a unit layer consists of an octahedral sheet, comprised of either aluminium or magnesium atoms in octahedral coordination with oxygen atoms of hydroxyl groups (see Figure 2), and one or two tetrahedral sheets, consisting of silicon atoms tetrahedrally coordinated with oxygen atoms (see Figure 3).

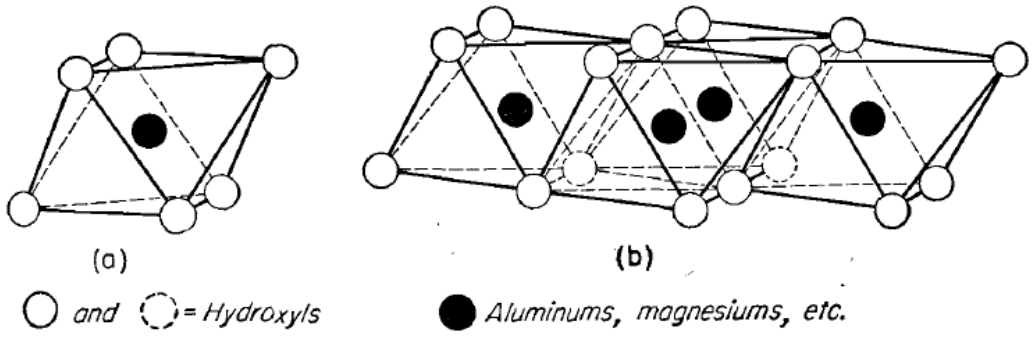

Figure 2: Schematic description of clay structure components: **a)** An octahedral unit **b)** sheet structure of octahedral units (Grimm, 1953)

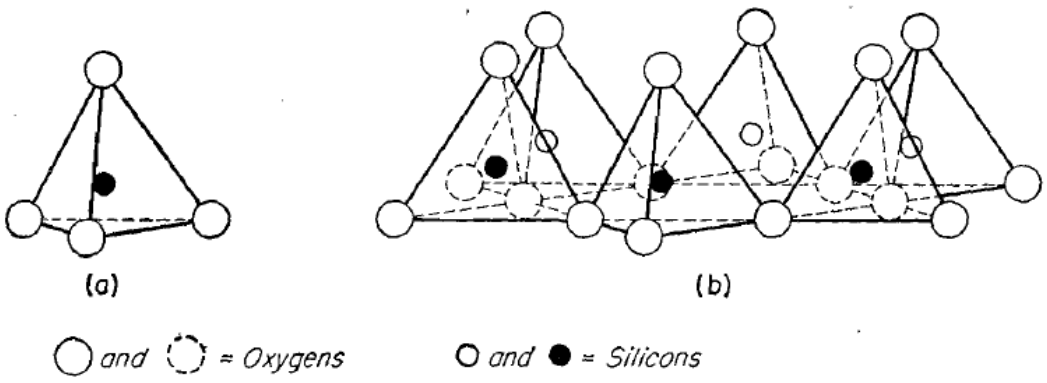

Figure 3. Schematic description of clay structure components: **a)** A tetrahedral unit **b)** sheet structure of tetrahedral units (Grim, 1953)

These octahedral and tetrahedral sheets are tied together by sharing an oxygen atom. When the bonding occurs between octahedral (O) and tetrahedral (T) sheets, one basal surface consists of exposed apical silicate oxygen atoms, while the other surface consists of exposed hydroxyl atoms (OT structure). A typical OT structure is found in the clay mineral kaolinite. In the case of having two tetrahedral sheets, the octahedral sheet is sandwiched between them (TOT structure), as found in montmorillonite, for example (see Figure 4). This structure is also known as a Hoffmann structure (Hoffman et al., 1933) in which both surfaces contain exposed

apical silicate oxygen atoms. There are two types of silicate sheet structures; when the oxygen or hydroxyl ions are surrounded by 3 divalent cations such as Mg^{2+} or Fe^{2+} (e.g. Talc, $Mg_2Si_2O_5(OH)_4$), *trioctahedral*; or when the oxygen or hydroxyl ions are surrounded by 2 trivalent cations such as Al^{3+} (e.g. Pyrophyllite, $Al_2Si_4O_{10}(OH)_2$): *dioctahedral.* (Grim, 1953)

The unit layers are stacked together face-to-face to form the crystal lattice. The distance between two corresponding layers is defined by the crystallographic *c* parameter, sometimes called the 001 or basal spacing. For a dehydrated TOT mineral, the basal spacing is approximately 9.2 Å, while it is 7.2 Å for an OT clay mineral two-layer spacing. The adjacent sheets in a unit layer are held together by covalent bonds which makes them stable, where adjacent unit layers are held together by hydrogen bonding or electrostatic attraction (Darley and Gray, 1988).

Electrical Charge Distribution

When lower or higher formal charge ions isomorphically replace the existing Al^{3+} or Si^{4+} atoms of the tetrahedral and octahedral sheet units, the charge balance is changed. For instance, exchange of Al^{3+} in the octahedral sheet unit with Mg^{2+} or Fe^{2+}, or Si^{4+} with Al^{3+} in the tetrahedral sheet, creates a structural net negative charge, which is the primary reason for the negative charged structure of montmorillonite and the presence of exchangeable charge-balancing cations. Another factor affecting the charge distribution in clays is the hydration of ruptured Si-O and Al-OH bonds. These hydroxyl groups create either positive or negative sites on the clay basal surface and, especially, edge sites, depending on the silicate structure and the pH of the electrolyte medium. This process has a minor effect on the charge distribution of TOT clay minerals such as montmorillonite at most pH, while on the other hand it is critical for the charge distribution of OT clay minerals

such as kaolinite, which have no, or very little, isomorphic substitutions. The pH value where the net electrical charge becomes zero is called as Zero Point Concentration (ZPC) (Morais et al., 1976; Parks and De Bruyn, 1962).

Ion Exchange

In aqueous suspensions, the cations on the clay mineral basal surfaces, and both cations and anions on clay mineral crystal edges may exchange with the ions in the bulk solution. The exchange reaction is mainly controlled by the relative concentration of ions in each phase. In case of two species of monovalent ions, Equation 1 can be written as;

$$[A]_c/[B]_c = K[A]_s/[B]_s \quad (1)$$

where $[A]_s$ & $[B]_s$ and $[A]_c$ & $[B]_c$ are the molecular concentrations of ions in the solution and at the clay, respectively, and K is the exchange equilibrium constant. When two ions of different valences are present, the one with the higher valence is adsorbed preferentially (Darley and Gray, 1988). The order or preference is:

$Ba^{++}>Sr^{++}>Ca^{++}>Cs^{+}>Rb^{+}>K^{+}>Na^{+}>Li^{+}$

However this series may show some changes. Intense adsorption of H_3O^+ ions makes pH a strong influence on cation exchange reactions (Hendriks et al., 1940). The total amount of cation charge adsorbed is termed the cation exchange capacity (CEC), which is expressed in milliequivalents per hundred grams of dry clay. CEC is a good indication of colloidal activity of clay suspensions. Clay minerals such as montmorillonite have a high CEC, which leads to swelling, especially when sodium is the exchangeable cation (see Table 3). On the other hand, clay minerals such as

kaolinite are relatively inert to swelling, regardless of the exchange cation, mainly due to little cation content.

Table 3: Cation exchange capacities of common clays (Grim, 1953).

Clay Type	Cation Exchange Capacity (meq/100g)
Montmorillonite	70-150
Vermiculite	100-200
Illite	10-40
Chlorite	10-40
Attapulgite-Sepiolite	10-35
Kaolinite	3-15

1.1.3. Smectite Clay Minerals

Montmorillonite is the most commonly encountered member of the smectite group of minerals. Montmorillonite is the primary constituent of Wyoming Na-bentonite, and is the active component in the younger argillaceous formations causing swelling problems in drilling operations (Darley et al., 1988). Figure 4 shows the structural arrangements of a single montmorillonite (TOT) layer. The layers are continuous in the crystallographic *a* and *b* directions and are stacked one upon the other in the *c* crystallographic direction. The apical oxygen atom of each silica-alumina-silica stack is adjacent to oxygen atoms of neighbouring stacks, which manifests as weak bonding and good cleavage between the layers. Water and some organic molecules can easily enter (intercalate, if neutral) between unit layers and cause variable lattice expansion along the *c*-axis, depending on the size and the

geometry of the molecules. Exchangeable cations are located between the clay sheets and they play an important role determining the interlayer spacing.

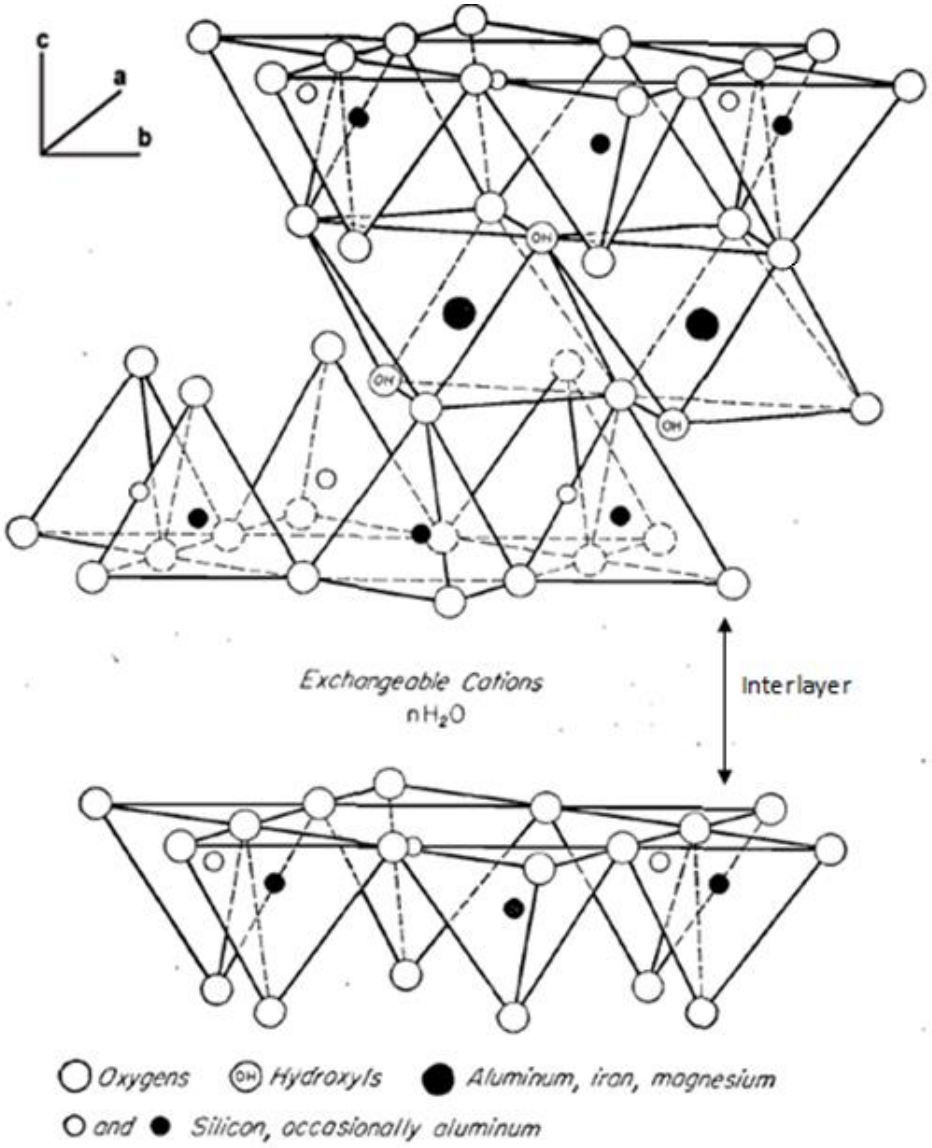

Figure 4. Diagrammatic sketch of the montmorillonite structure showing the arrangement of atoms and molecules along with interlayer cations and water (adapted from Grim, 1953)

The amount of water absorbed depends on the nature of the exchangeable cation. In normal ambient conditions, montmorillonites with Na^+ exchangeable cations

generally have one layer of water molecules and 12.5 Å interlayer spacing, while Ca^{2+} montmorillonites have 15.5 Å interlayer spacing because of two water layers being present (Grim, 1953). Since the interlayer spacing of Na-montmorillonites are highly dependent on relative humidity of air present, the thickness of the spacing may vary.

1.1.4. Illite Clay Minerals

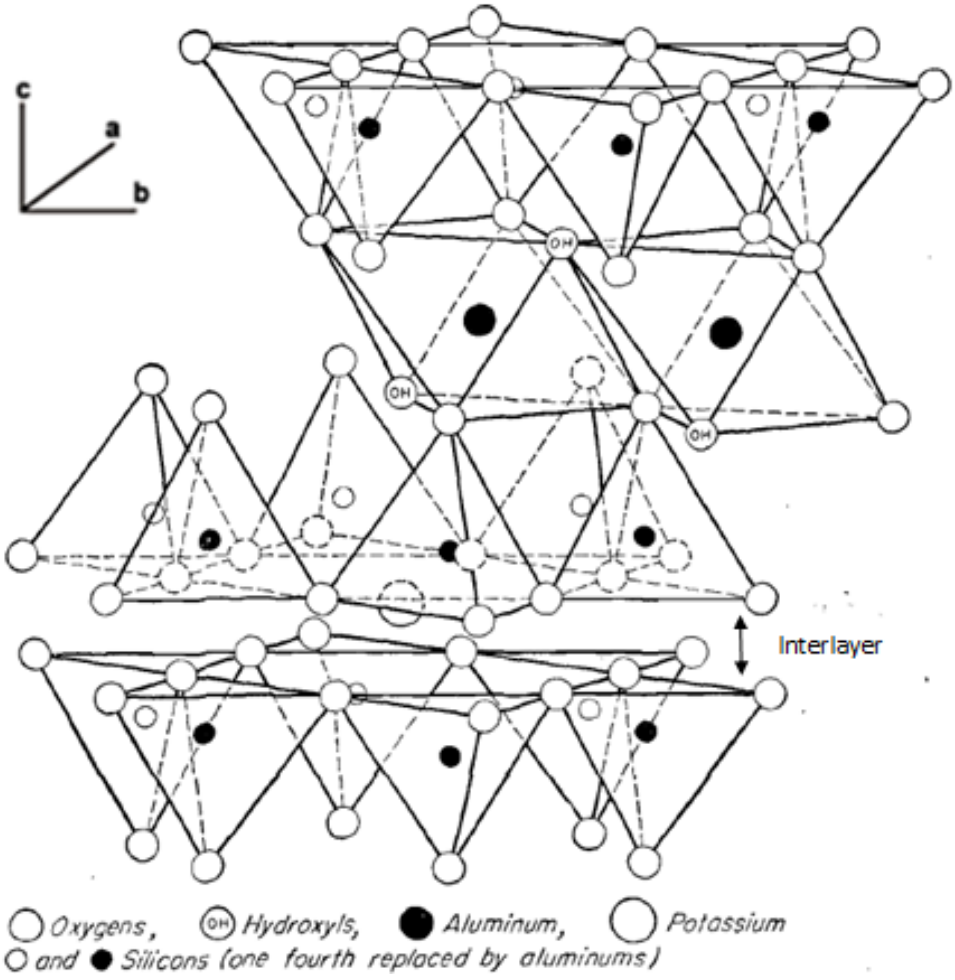

Figure 5. Diagrammatic sketch of the illite structure showing the arrangement of atoms and molecules along with interlayer cations and water (adapted from Grim, 1953)

The basic structural unit of illite is a layer composed of two silica tetrahedral sheets with a central octahedral sheet (TOT). The structure of illite is almost the same as that of montmorillonite, except that some of the silicon atoms are always replaced by aluminium and the resulting charge deficiency is balanced by having potassium ions in the interlayer (Grim, 1953). These potassium ions fit perfectly into the oxygen interlayer and due to lower hydration energy they create a strong bonding between layers, which prevents layers from expanding (Wilson and Wilson, 2014).

1.2. Swelling in Shales & Clays

Technically, swelling is the moving apart or disjoining of clay particles, especially those in aligned in a parallel arrangement, until they reach their equilibrium cleavage under the given pressure or until they fall into the secondary energy minimum. During swelling, water is absorbed and the clay matrix expands but remains intact (Chen et al., 1987).

Over the years many studies have been undertaken to explore the mechanisms of shale failure, a selection of which are presented here; more exhaustive reviews may be found in the work of Anderson et al. (2010) and Wilson and Wilson (2014). Van Oort (2003) described the swelling pressure encountered in drilling as the overwhelming factor for generating *in situ* downhole stresses and overcoming cementation forces via expansion of clay minerals combined with pore pressure effects (see Figure 6). Loret et al. (2002) described clay swelling as a volume increase driven by two forces: (i) chemical swelling, which is distinguishing for smectite-like reactive clays and, (ii) the matrix swelling driven by the capillary forces, which occurs in both reactive and non-reactive clays.

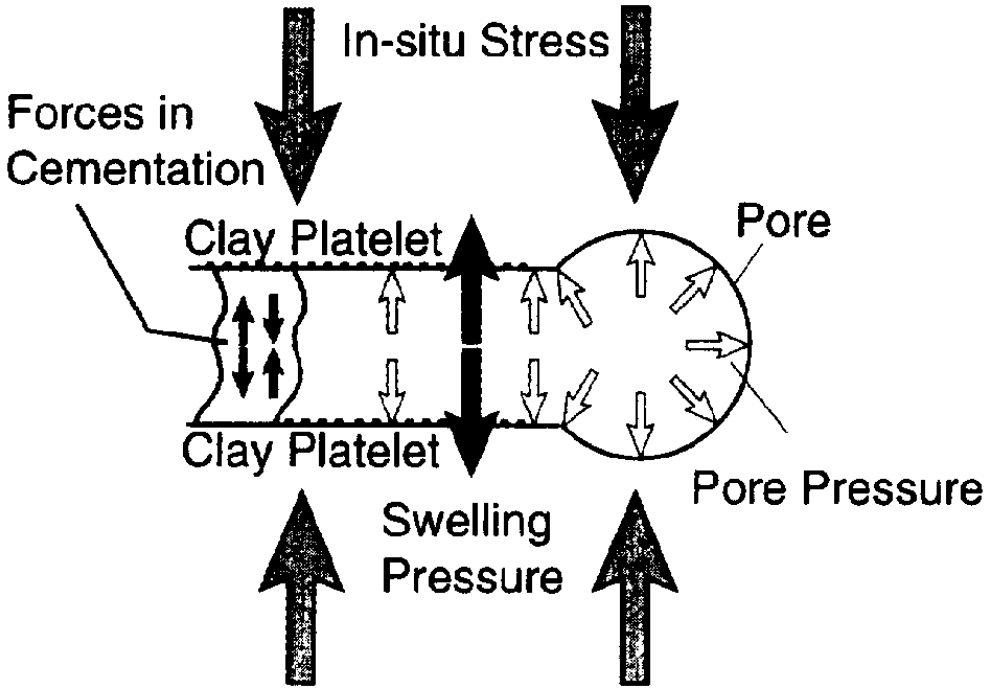

Figure 6. Schematic description of swelling pressure in a shale system, simplified as a single set of clay platelets connected to a pore, including the in situ vertical and horizontal stresses, the pore pressure, the swelling pressure acting between the clay platelets, and tensile or compressive forces in the cementation developing upon compressive or tensile loading of the shale material, respectively. (Van Oort, 2003)

1.2.1. Crystalline Swelling

In crystalline swelling, clay particles absorb up to four layers of water molecules into the interlayer spacing and may expand upto approximately 20 Å. This crystalline swelling occurs in two ways:

-*Surface hydration* is caused by hydrogen bonding of water mo1ecu1es to oxygen atoms of the clay's silicate surfaces. Water molecules bond to basal surface oxygen atoms and form the first water film (Norrish, 1954; Mooney, 1952). Following this, another water film bonds to the first water film and this sequence forms a multi-layered quasi-crystalline water structure on the surface. However, when water

molecules get further away from the clay surface the bonding strength decreases and limits the thickness of the water layer. The type and the valence of the interlayer cation also determine the thickness of the water layer. Exchangeable cations such as Ca^{2+}, Mg^{2+} and H^{+} increases the interlayer attraction forces and reduces swelling, on the other hand exchangeable cations such as Na^{+} and Li^{+}, reduces the attractive forces and causes more expansion.

-*Ion hydration* is brought about by the arrangement of hydration shells around exchangeable cations (Roehl and Hackett, 1982). The size and the position of the cation along with its hydration enthalpy determines the thickness of the water shell adsorbed around the cation. Ions with lower hydration enthalphies such as K^{+} tend to adsorb less water than ions with higher hydration enthalpies suc has Na^{+}, Ca^{+2}, Li^{+}.

Since 1954, there has been a general agreement among researchers that crystalline swelling is controlled by a balance between both Coulombic and Van der Waals attractive forces between clay layers and repulsive forces arising from hydration of the interlayer cations and negative surface charge sites (e.g. Norrish, 1954; van Olphen, 1965; Kittrick, 1969).

1.2.2. Osmotic Swelling

After clay undergoes complete crystalline swelling and is still being exposed to free water, osmotic swelling is initiated (Norrish, 1954). During osmotic swelling, water is adsorbed into the clay mineral particles until the interparticle spaces are isotonic with the bulk solution, with surface hydration leading to formation of electrical double layers, in line with DVLO theory (Loret et al., 2002). This action leads to a 20 to ~130 Å increase of distance between the unit layers. Generally, this volume

increase caused by osmotic swelling is considered as a major contributor in shale instability during drilling (e.g. see review by Anderson et al., (2010)). Interlayer swelling can be determined by X-ray diffraction analysis, while osmotic swelling can be determined by the total volume increase of the clay structure or the swelling pressures generated (Barshad, 1952).

Diffuse Double Layer (DDL) Theory

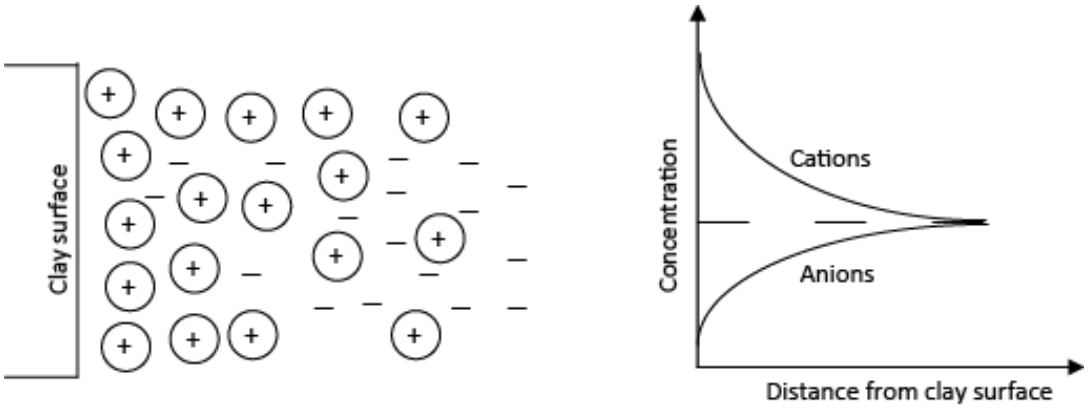

Figure 7. Schematic to show distribution of ions in diffuse double layer (DDL) theory (Soga and Mitchell, 2005).

In dehydrated clays, interlayer cations are strongly held by the negatively charged clay platelets. Excess cations that are required to neutralize the overall negative charge of the clay particles are present as salt precipitates with their associated anions. With the presence of water, these ions tend to move through water in order to balance the ion concentration. The cation movement, however, is restricted by the negative surfaces of clays and the balance between diffusive and electrostatic forces lead to an ion distribution adjacent to the clay surface (see Figure 7). The phenomena, including the charged surface and the distribution of ions adjacent to the surface is termed as diffuse double layer, which was described by Louis Georges Gouy (1910) and David Leonard Chapman (1913), then refined by Otto Stern (1933).

Influences of the system variables on the thickness of the double layer are described in Equation 2:

$$\frac{1}{\kappa} = \sqrt{\left(\frac{\varepsilon DkT}{2n_0 e^2 v^2}\right)} \quad (2)$$

where $\frac{1}{\kappa}$ is Debye length (m) (where κ is the Debye-Huckel parameter), n_0 is electrolyte concentration (mol/m^3), *v* is cation valence, *D* is dielectric constant of the medium, and T is temperature (K), *ε* is the permittivity of the vacuum, *k* is the Boltzmann constant (1.38 x 10^{-23} $\mathring{J}K^{-1}$) and *e* is the electronic charge (1.602 x 10^{-19} coulomb). At constant temperature, the thickness of the double layer is proportional to dielectric constant, and inversely proportional to cation valence and the square root of electrolyte concentration. In general, the thicker the diffuse double layer, the higher the swelling of reactive clays.

1.2.3. Pore Swelling in Shales and Compacted Clay Minerals

Conceptually, permeable rocks are similar to a pack of capillary tubes. In real shales, the structure of the pores is far more complicated yet the capillary phenomena still applies. The pore size is described as the radius of the pore which is assumed to be cylindrical. The widths of micropores are < 2 nm, mesopores vary between 2 and 50 nm, and macropores are > 50 nm (Gregg and Sing, 1982).

When a wetting fluid, (water) and a non-wetting fluid (air) come into contact, tension forces 'γ are developed at the interface. These forces are balanced by a pressure drop (ΔP) under equilibrium conditions. Adaptation of the Laplace law gives Equation 3:

$$\Delta P = Pc = u_a - u_w = \frac{2 \cdot \gamma \cdot cos\theta}{r} \quad (3)$$

where Pc is capillary pressure (Pa), u_w is the pressure in water, (Pa), u_a is the pressure in air, (Pa), γ is the interfacial tension (N/m), θ is the contact angle between the fluids interface and the solid (tube) surface and r is the pore radius (m) (Schmitt et al., 1994).

In the case of "capillary rise" in a tube, where air is at a fixed pressure, a depression occurs at the interface which increases the water level until this depression is compensated by the hydrostatic pressure of the water column. By analogy, any water trapped between the grains of unsaturated shales will be subject to a pressure decrease, thus giving rise to “capillary suction”. The contact between an unsaturated shale sample and a water-based fluid, due to the attraction of shales for water, will result in the development of capillary pressures in the air filled pores. The extent of capillary pressures depends on the pore size, as well as the initial moisture content as the more hydrated the sample, the lower the developed capillary pressure. The development of capillary pressures will also depend on the affinity of the shale for the contacting fluid and on its interfacial tension. Hence the determination of the wettability of the shale with respect to the pore fluid is essential. However, in general shale-wetting ability of the fluids is expected to increase with polarity. This means that organic compounds will get less attracted than aqueous solutions and wettability will decrease with increasing concentration in aqueous solutions of water soluble organic compounds. In addition, the kinetics of the development of capillary pressures will depend on the rate of· penetration of the mud filtrate, hence of its viscosity (Forsans and Schmidt, 1994).

1.3. Measuring Swelling of Shales and Compacted Clay Minerals

1.3.1. X-Ray Diffraction (XRD) Technique

X-ray diffraction is the most favourable analysis to investigate the fundamental background of clay swelling. It is used to reveal the (001) interlayer spacing (basal *c*-spacing) of the silicate layers of clay minerals, which expand during swelling. The principle of using XRD for clay swelling studies was discussed by many researchers in the early literature (Norrish, 1954; Foster et al., 1954; Mooney et al., 1952; Barshad, 1952; Brindley et al., 1969, 1980; Olejnik et al., 1974; Berkheiser and Mortland 1975). Most notably, Norrish (1952) measured the *c*-spacing of mono-ionic montmorillonites in saturated and diluted aqueous salt solutions and described the changes in *c*-spacing in terms of repulsive swelling forces resulting from hydration of the interlayer cations, and opposing attractive forces resulting from electrostatic interactions between the negatively charged layer surface and the interlayer cations.

Wet-cell XRD is an improved way of taking *in situ* XRD measurements of fine grained particles in percolated solutions (see Figure 8). The wet cell allows the changes in basal spacing through time to be recorded, enabling kinetic measurements of rapid and low temperature crystalline swelling reactions (Laurence and Hofmann, 2003) (Laurence and Berger, 2007). This is more useful for observing clay swelling than the classical XRD approach, as it gives the output of time dependent expansion of clay sheets, instead of stable final conditions after basal displacement.

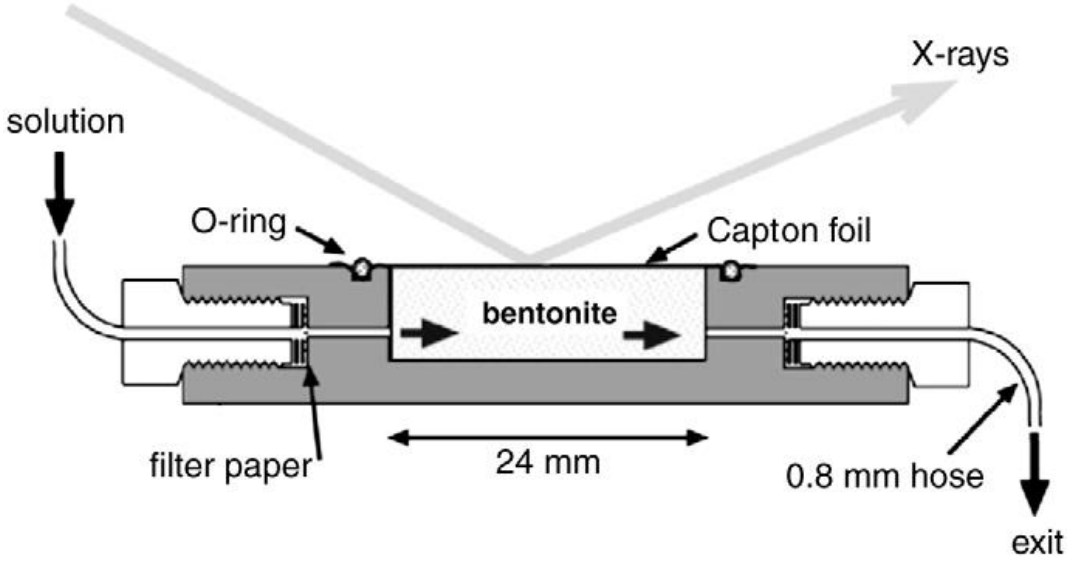

Figure 8. Schematic description of wet-cell XRD technique used in the study of Warr and Berger (2007)

1.3.2. Macroscopic Swelling Tests of Shales and Compacted Clay Minerals

Macroscopic swelling data can be obtained by measuring the volumetric expansion of clay particles in a single- or multi-dimensional perspective. With the output of this method, a swelling index can be predicted. Prediction of swelling indexes of commercial Na-bentonites via macroscopic tests has been reported by Besq et al. (2003) and Christidis et al. (2006). Continuous measurement of one-dimensional expansions of Ca^{2+} montmorillonites in the presence of polymeric inhibitors was carried out by Zhang and Sun (1999) and Liu et al. (2004). A variation of this method is also the main experimental technique in the present study.

Swelling pressure tests are also another technique to study clay swelling in macroscopic scale. Swelling pressure of clays is defined as the pressure required to keep the clay particles at the original volume upon the absorption of a certain liquid. Determination of swelling pressures is described in detail in the study of Sridharan and Puvvadi (1986).

1.4. Clay and Shale Swelling in Different Solvents

The control of clay mineral swelling has been a subject of significant and longstanding research interest. These studies have included the effect of the fluid composition and/or type in contact with the shale/clay minerals. Barshad (1952) examined the interlayer spacing of montmorillonite and vermiculite in different organic solvents and water-organic mixtures and concluded that interlayer spacing decreased with decreasing dielectric constant or dipole moment. Brindley et al. (1969) studied the interlayer spacing of Ca-montmorillonite in water-organic mixtures and concluded that at critical compositions of the water-organic mixtures, a sudden decrease of interlayer spacing occurs because of the increased Coulombic attractions due to the diminished dielectric constant of the organic-water mixtures. Murray and Quirk (1982) studied the changes in the bulk volume of two illitic shale samples (Urrbrae B and Willalooka illite) in water and organic solvents and claimed that the bulk swelling increased with increasing dielectric constant of the liquid. Berkheiser and Mortland (1975), however, observed little relationship between crystalline swelling and dipole moment of the liquid. Olejnik et al. (1974) studied the swelling of montmorillonite in polar organic liquids with high dielectric constant such as N-methylformamide and concluded that in general the swelling behaviour of montmorillonite is affected by dielectric constant, on the other hand chemical changes in the solvent molecule such as methyl substitution may prevent the development of diffuse double layers despite a solvent having high dielectric constants.

The effect of cation properties on clay swelling has also been studied widely in the early literature (Falconer and Mattison (1933); Lutz, (1935); Norrish, (1954);

Mooney et al., (1952); Hendricks et al, (1940); Bradley, et al., (1937)). Most notably, Mooney et al. (1952) revealed that larger monovalent cations such as cesium (Cs) or rubidium (Rb) decreased water absorption into clay interlayers (i.e. supressed swelling). XRD studies by Norrish (1954) also showed a correlation between the hydration energies of monovalent cations and clay mineral swelling. In the Monte Carlo simulations of Boek et al. (1995) the behaviour of interlayer cations at high water content was displayed and it was revealed that compared to Na^+ and Li^+, K^+ ions provide better suppression of clay expansion by migrating and binding to clay surface as well as having low hydration enthalpy. Liu and Lu (2006) showed that K^+ montmorillonite only showed swelling corresponding to one layer of hydration in the clay interlayer. Suter et al. (2011) devised a set of rule-based design criteria for cationic and polyether based clay-swelling inhibitors by using a range of computational techniques and analysis, combined with known experimental results. The weak hydration enthalpy of potassium salts has resulted in their use in drilling fluids, as described in detail by O'Brien and Chenevert (1973) and Steiger (1982).

In the detailed review of Wilson and Wilson (2014), an alternative viewpoint for the failure of smectite and illitic shales was developed and a mechanism leading to a forming of pore and hydration pressures related to overlapping of the diffuse double layers linked with the charged external surfaces of the clay minerals exposed in opposite walls of pores of the shale was described.

Contrary to the view that clay mineral swelling underpins shale failure in well bores, Santarelli and Carminati (1995) showed that laboratory tests on shales are generally not representative of downhole conditions and any swelling observed is mainly because of capillary effects. In the studies they conducted, there was no

difference observed between the effects of inhibitive KCl and non-inhibitive lignosulfonate muds. Forsans and Schmitt (1994) stated that when shales are unsaturated, formation of capillary pressures is inevitable and it is directly affected by the pore size distribution and the moisture content of the shale. This needs to be accounted for when undertaking swelling experiments in the laboratory.

1.5 AIM OF THE STUDY

In order to assess shale stability, as well as to develop chemical inhibitor systems, an understanding of shale stability is essential. A challenge arises in that to assess swelling representative rock units are needed. However, obtaining intact cores of shale during drilling operations is expensive and laborious, requiring extraction of the main drill bit and reattachment of a coring bit. Furthermore, even when core is obtained it is removed from its original constraining envrionment and effectively depressurised. Thus, it is common practice to use either cores from onshore analogue rocks, drilling cuttings (small 2 ~mm rock cuttings from the sieves on board the oil platform, obtained when the fluid is recirculated), or model clays. The latter two sample sets are typically ground up and then compacted into a model core using a hydraulic press. Conceptually, water ingress in a shale stability test will flood the test core through intra-grain pores, and then enter the far smaller intra-grain interlayers of clay minerals. The interplay between the relative initial composition of brines in the clay mineral interlayers (of swelling types), in micropores between small clay mineral particles and in more macroscopic pores will influence the swelling behaviour upon ingress. It is convenient, in terms of the literature, to separate out clay mineral swelling from bulk shale swelling.

The study presented here explores the short term (< 1 hour) swelling of “artificial” cores through using a new non-contact linear swelling meter which offers high

resolution (60 scans per minute) and reproducible (4 simultaneous measurements) data sets. To provide comparison the long-term swelling of similar clay tablets was assessed in the same solvents. The study undertaken examines core flooding in different electrolytes/solvents and correlations are made between the measured swelling rates and the bulk properties of the organic solvents and ion type and concentration of salt solutions. A subset of experiments was also conducted with non-reactive illitic shales for comparison and better interpretation of clay swelling. Results of these experiments are expected to give fundamental assistance for the development of appropriate drilling fluids to a given shale type.

2. EXPERIMENTAL METHODS

2.1. Materials

The clay minerals used in this study were montmorillonite (as Na-bentonite) and illite.

The Na-bentonite used in this study was the Wyoming Na-bentonite GDM purchased from Steetley Na-bentonite & Absorbents Ltd, Retford, U.K. and used as supplied. Particle size was constrained by sieving into different mesh sizes and determined as 150 μm. The BET Surface Area was determined by nitrogen gas adsorption isotherm method to be 30.33 m^2/g (Ratcliffe et al., 2009). (See Appendix A)

The illite used in this study was 85% illitic shale is a Mapplewood Shale from Neahga, U.S., supplied by Ward's Science. It was prepared by grinding and then sieved to 150 μm particle size for a consistent comparison with the Na-bentonite. (See Appendix A)

Organic solvents were laboratory reagent-grade solvents and used as obtained from Sigma-Aldrich. Table 4 shows the common physical properties of the solvents used in this study. Properties of water are also included for comparison. As the investigation of effects of solvent properties on swelling was the main focus in the first part of this study, the organic solvents were chosen in order to provide diversity in their physical properties. In addition to this, solvents were chosen among non-corrosive and non-toxic chemicals in order to be in compliance with laboratory safety. The definitions of the solvent properties are given in Appendix B.

Table 4. Physical properties of water and the organic solvents used in this study. (Jasper, 1973; Smallwood, 2012) Definitions of the solvent properties are given in Appendix B.

Solvent	Chemical Structure	Viscosity (mPa.s)	Dipole moment (D)	Dielectric constant	Surface tension (N/m)
Hexane	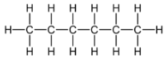	0.297	0.08	1.88	17.91
Water	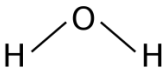	0.890	1.87	80.1	72.80
Methanol	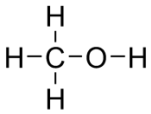	0.551	2.87	32.7	22.55
Ethanol	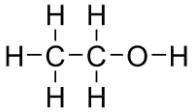	1.090	1.66	24.55	22.32
Propan-2-ol	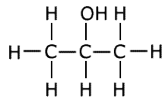	1.960	1.66	19.92	21.79
1-butanol	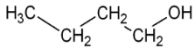	2.571	1.66	24.2	17.81
1-heptanol	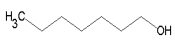	5.758	1.71	6.7	26.20
Benzyl alcohol	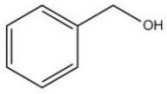	5.47	1.7	13	39.00

Acetone	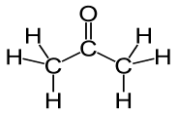	0.32	2.69	20.7	23.32
1-decanol		12.05	1.6	8.1	28.5

KCl, NaCl, KI and $CaCl_2$ salts were all purchased from Sigma Aldrich and used as received. Table 5 shows the physical properties of the salts used in this study. The calculation of the amount of the salt required for each test is given in Appendix C.

Table 5. Physical properties of the salts used in electrolyte solutions

Salt	**Chemical Formula**	**Solubility in water (at 20 °C) (g/100g water)**	**Molar mass (g/mol)**
Potassium Chloride	KCl	34.2	74.6
Sodium Chloride	NaCl	35.9	58.4
Potassium Iodide	KI	144	166.0
Calcium Chloride	$CaCl_2$	74.5	110.9

2.2. Artificial Core Preparation and Mounting

Clay mineral "cores" having 3.8 mm thickness and 20 mm diameter were prepared by applying a load of 4 tons (31.22 MPa estimated pressure) to 100 mesh size sieved clay mineral powders using a hydraulic press (See Figure 9). Note that the term "core" is not used for the actual samples cored from underground, but compressed from clay powder and having the shape of "artificial cores". Four artificial clay cores were used in each test to check for consistency. The process was carried out by applying 4 tons of pressure to 2.5 g of clay between stainless steel disks for 2 minutes. Disk surfaces were cleaned after each process to keep the

surfaces of the cores smooth for consistent surface area in each test, and in order to prevent sticking of cores onto the metal surfaces due to impurities.

The artificial cores were placed into the sample holders (component 2 in Figure 10), which in turn were placed into the holes (marked 13 in Figure 10) present in the water bath shelf (component 3 in Figure 10). 0.7 mm thick metal disks were placed onto the pressed clay cores.

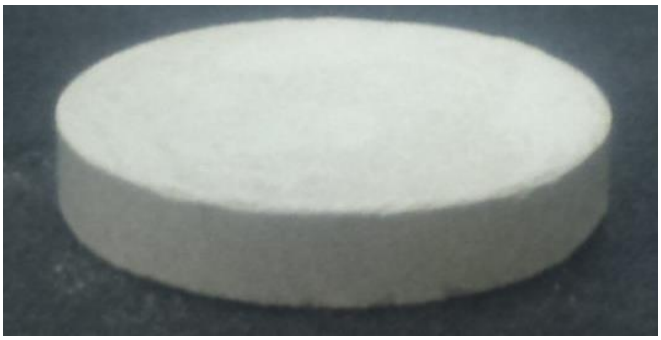

Figure 9. Artificial Na-bentonite core prepared by hydraulic press

2.3. Swelling Measurements

2.3.1. Non-contact Linear Displacement Meter

In this study, a novel non-contact linear displacement meter (NC-LDM), based on induction sensors was used to investigate linear swelling behaviour of compacted clay cores. The NC-LDM is shown in Figure 10, and comprises 4 non-contact linear displacement meters (1 in Figure 10), which sits above teflon sample holders (2 in Figure 10) that are held in place by a stainless steel shelf (3 in Figure 10). The core sits on a porous shelf (4 in Figure 10) in the holder sample and holes around the base (5 in Figure 10) allow fluids to ingress into the core. A clear lid (6 in Figure 10) allows the sample to be observed and a valve allows introduction of the flooding fluid. The samples are flooded by introduction of the contacting salt

solution or organic solvent into a raised bath (8 in Figure 10) in which the sample holders sit. This raised bath sits on a porous shelf above a further bath in which saturated salt solutions can be placed to control the humidity on the upper part of the vessel, if desired. The data from the sensors was collected and processed via LabVIEW software (Johnson, 1997). A photograph of the device is shown in Figure 11.

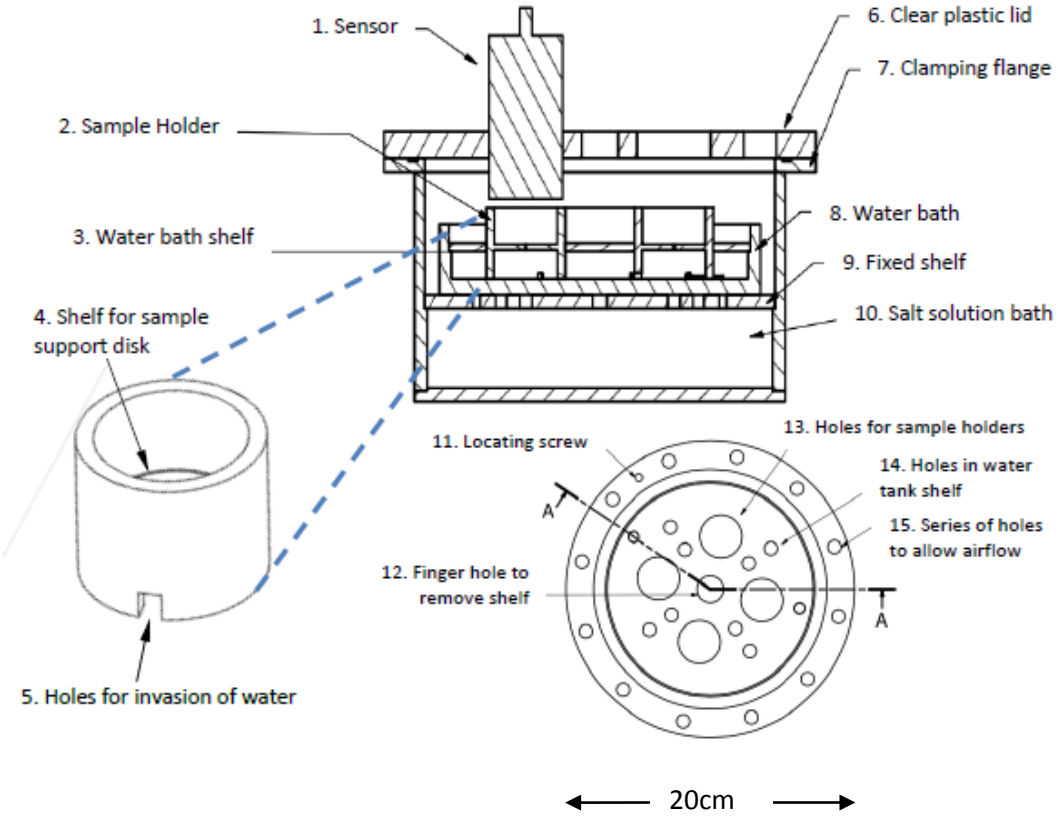

Figure 10. Schematic description of non-contact linear displacement meter (NC-LDM)

In short term swelling tests, core samples were partly immersed in 200 mL of the designated solvent. The experiment time was kept between 30-60 minutes, depending on the swelling response of clay cores in the medium. In each experiment, four individual sensors gave four individual data and the average of

these data used as the result of the experiment. In case of any faulty or inconsistent data, another test was performed and these data are replaced with new ones. Thus it was made sure that in each test the average of at least four individual data was used (see Appendix G).

The working principle and calibration of the device is explained in Appendix D and Appendix E respectively.

Figure 11. The non-contact linear displacement meter (NC-LDM). Inset photograph shows the sample holder along with the perforated metal disk the clay cores are placed on.

2.3.2. Overall Equilibrium Swelling Tests

A simple volumetric method was applied to examine the equilibrium swelling behaviour of Na-bentonite cores in the designated solvents. Clay cores were put and fully immersed into flat bottom vials with 20 mL of designated solvent. The change in levels due to swelling was recorded every five minutes in the first hour, then every hour in the first 8 hours, and then every 24 hours for each day. The point where clay expansion is balanced and no further swelling is observed in calliper measurements was designated as the overall equilibrium swelling. Figure 12 shows a photographic image of equilibrium swelling tests. As the progress of the experiment could be observed throughout the experiment, no repetition was applied as long as no human error occurred during handling the samples.

Figure 12. Application of equilibrium swelling tests

2.4. Relative Humidity Measurements

Humidity measurements were carried out by a "Vaisala HM40s Humidity and Temperature Meter" supplied by Vaisala Inc. In order to achieve a consistent humidity value, the salt solution bath of the swelling meter (see Figure 13) was filled with a designated salt solution to attain the desired humidity (see Appendix

F). The probe of the device was placed into the top of the swelling meter then sealed with cling film in order to prevent air flow. The device was left overnight to reach a humidity balance and as well as for clay cores to reach equilibrium saturation. When clay particles absorbed water from the air, the clay cores slightly expanded so that the position of the metal disks rose. The saturation was confirmed when the position of the metal disk was fixed. When the designated humidity value and saturation of clay cores were reached, swelling tests were carried out with the same procedure described above.

Figure 13. Vaisala HM40s humidity and temperature meter

3. RESULTS AND DISCUSSION

Short term and equilibrium swelling tests of the compacted Na-bentonite artificial cores were carried out using two main solvents: “tests with organic compounds” and “tests with aqueous electrolyte solutions”. Results of each set of experiments are presented and discussed in turn below. The swelling behaviour of compacted Na-bentonite cores in water was examined first, along with the effects of initial moisture content in order to lay the groundwork for comparison. This is followed by the bulk of the results, using the compacted Na-bentonite cores. In the final part, selected tests were repeated with non-reactive illite cores and results are compared with the results of the tests with Na-bentonite cores.

It should be noted that there was no external pressure applied to the experimental system in these tests, though the NC-LDM is capable of working under elevated pressure and temperature. The movement of fluids throughout the clay cores arose because of the physical and physicochemical interactions between the clay minerals and the solvent/electrolyte system. In short term tests the cores were partially immersed into the swelling medium, while in equilibrium swelling tests they were fully immersed. Thus, short term response of equilibrium swelling tests was different than results of short term swelling tests.

The Na-bentonite cores used in this study contain some residual water at room temperature and humidity, therefore there is already water existing (estimated 6-7% w/w) in the core structure.

3.1 Swelling of Compacted Na-bentonite Cores in Water

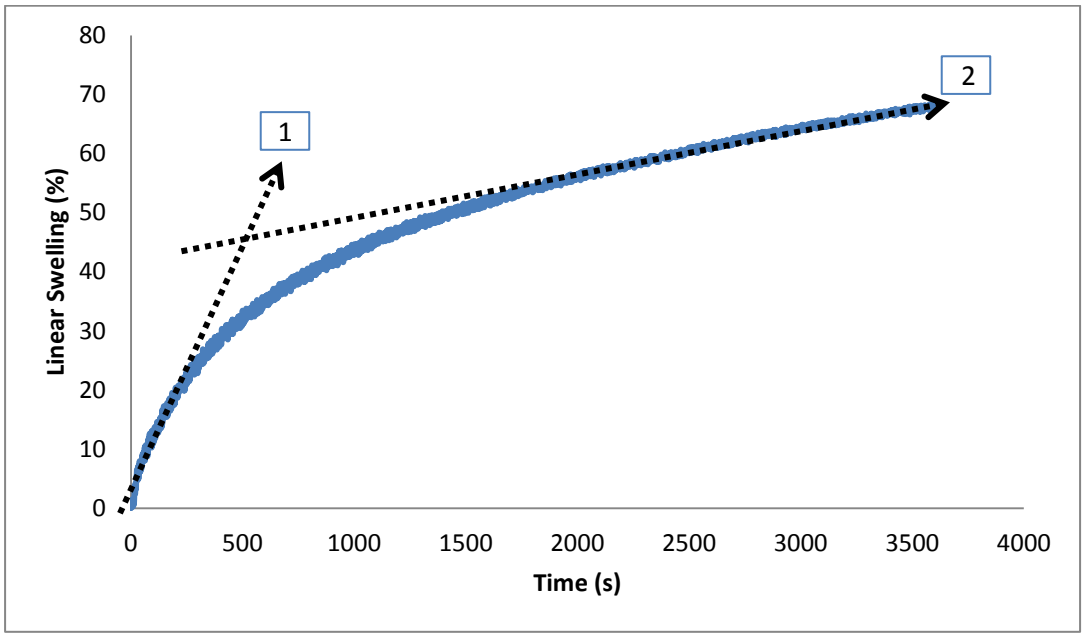

Figure 14. Short term swelling tests of Na-bentonite cores in water, showing the two main swelling regimes discussed in the main text.

Short term swelling tests showed that swelling of Na-bentonite cores in water occurs in two regimes. In Figure 14, it is seen that the slope of linear swelling changes after a point and remains constant until the end of the experiment. Note that the slope of the second regime didn't change when the experiment time was extended. This shows that swelling of Na-bentonite in water is dominated by different effects and therefore the rate changes throughout swelling.

Clays are negatively charged particles and water molecules are attracted to the clay surfaces in multiple possible ways under normal circumstances. As discussed in the introduction section, clays swell through a combination of capillary and chemical forces. Water enters the pores via capillary forces and causes pore swelling. Then water interacts with clay surface and causes surface hydration. Figure 15 shows the possible adsorption mechanisms of water onto clay mineral surfaces. Through the

uneven charge distribution on clay surfaces and dipole of water molecules, they are attracted to cations attached to the clay surface, leading to ion hydration. Ion hydration is important especially at low water contents. Hydration is strongly dependent on the size and the charge (or electronegativity) of the cation. The hydration enthalpies of the cations used in this study are given below in Table 6 (Smith, 1977). The reason why there are two different regimes can be interpreted as following; there are two swelling processes occurring simultaneously with different rates at through time; capillary forces and surface adsorption & hydration forces. The first regime is dominated by capillary forces and occurs immediately when water enters the pores and starts interacting with clay surfaces. When pore saturation is completed, capillary forces are no longer effective and therefore swelling only occurs via adsorption and hydration forces described in Figure 15. So that the swelling rate of the Na-bentonite cores change.

The effects of different swelling forces will be discussed in detail in the following parts.

Table 6. Hydration enthalpies of the cations used in this study (Norrish, 1954; Bergaya and Lagaly, 2013)

Cation	Dehydrated ionic radius (Å)	Hydrated ionic radius (Å)	Hydration Enthalpy (kJ/mol)
Na^{+}	0.9	3.6	409
K^{+}	1.3	3.3	322
Ca^{+2}	1	4.1	1577

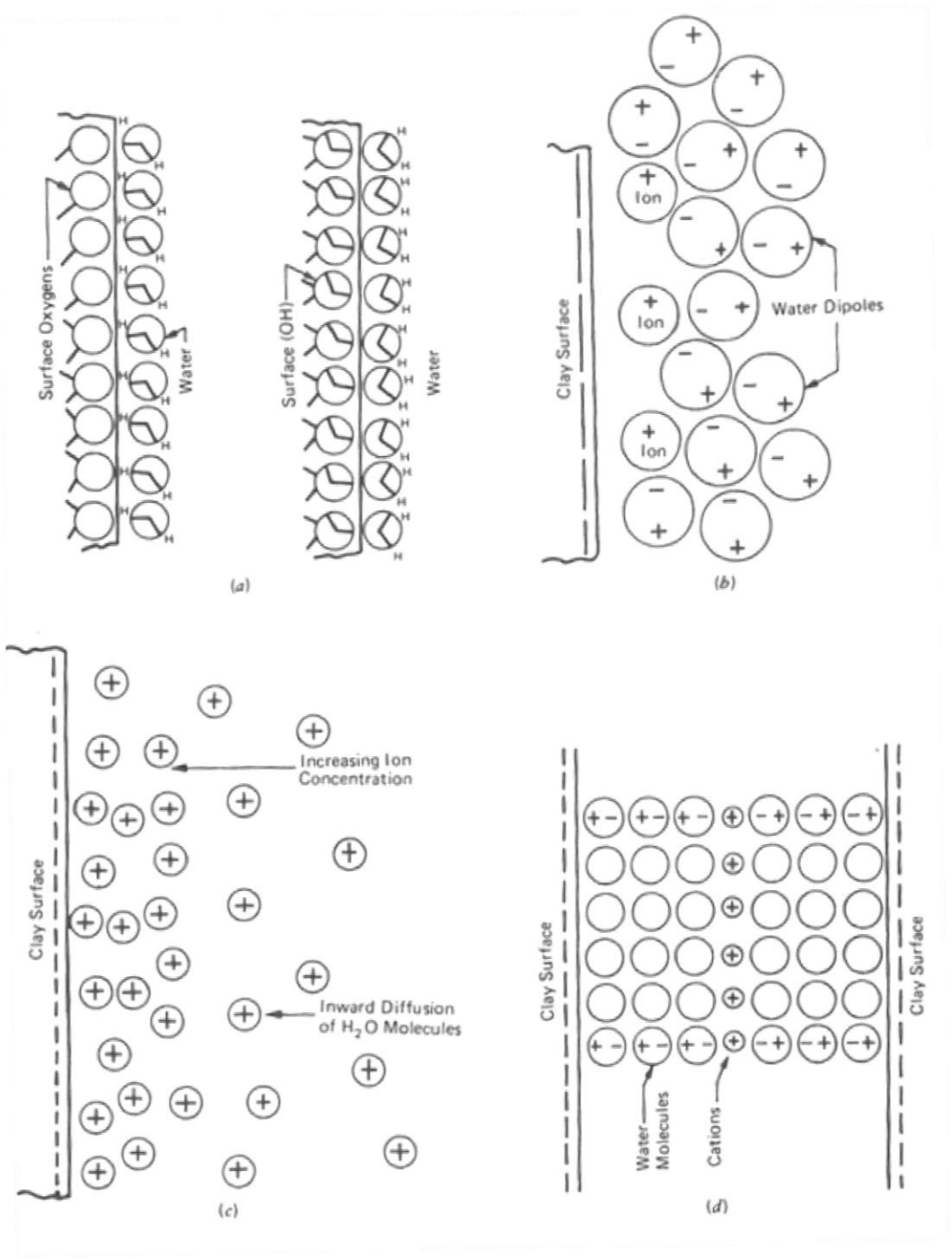

Figure 15. Schematic to show possible mechanisms for clay-water interactions: a) Hydrogen bonding, b) Ion hydration, c) Osmosis attraction (forming of double layers) and d) dipole attraction.(Soga and Mitchell, 2005)

Effects of Relative Humidity on Swelling

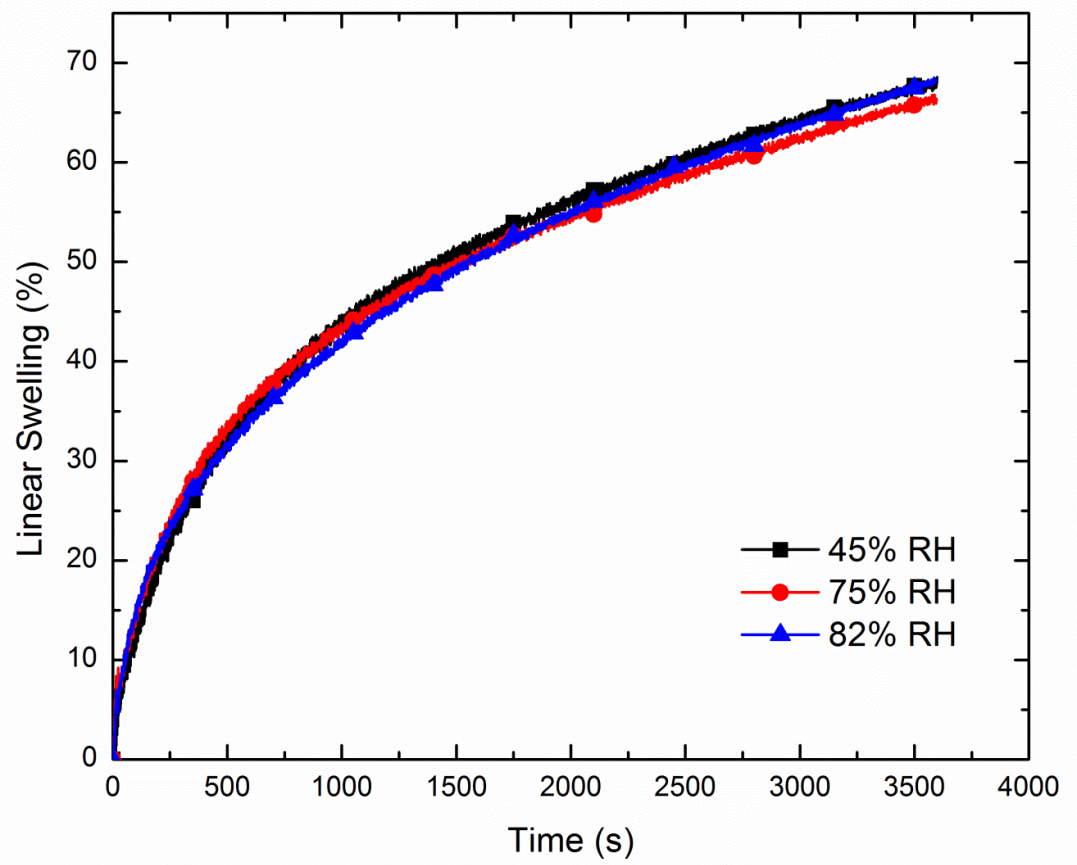

Figure 16. Short term swelling behaviour of Na-bentonite cores in water with different relative humidity values of air

Figure 16 shows the short term swelling behaviour of Na-bentonite cores in water with different degrees of atmospheric relative humidity (RH). 45% RH value was the average humidity of the laboratory environment. Atmospheres with 75% and 82% relative humidity were achieved by using appropriate saturated solutions. Note that only the saturation of the atmosphere was controlled the water content of the clay tablets after altering the relative humidity was unclear. The saturation of clay tablets was controlled by observing the expansion and therefore the level change of metal disks via NC-LDM. (see Section 2.4 and Appendix F).

It is seen that there is no observable difference in the short term behaviour of Na-bentonite cores in different relative humidity. It was, however, expected that increasing moisture content would decrease pore swelling with respect to capillary pressures developed, which is a major contributor to the bulk swelling of clays. It is assumed that the pore saturation of Na-bentonite cores occurred at the very beginning of the experiment; therefore the effects of different initial moisture content couldn't be captured by the device. Moreover, saturation of clay cores was only predicted via displacement of the metal disks. This method could be improved to a more precise gravimetric analysis.

3.2 Swelling of Compacted Na-bentonite Cores in Different Organic Solvents

3.2.1. Short Term Swelling Tests

Figure 17 shows the short term swelling behaviour of Na-bentonite cores in water and various organic solvents over a 30 minute period. First, it is clearly seen that there was no swelling observed in hexane. Clay cores swelled to the device limit (the sensors can only measure a 6 mm of displacement, see Appendix E) in less than just 5 minutes with a very fast swelling rate in acetone, methanol, ethanol, propan-2-ol, 1-butanol and benzyl alcohol. The fastest swelling was observed in acetone, in which the clay cores swelled up to the device limit just in 2 minutes. The slowest swelling was observed in 1-decanol.

Expansion of Na-bentonite cores in organic solvents showed a linear behaviour and was completed in a single swelling regime. Even though the equilibrium end point of swelling is not observable in the results because of the limited sensor height, it is predicted from the times of equilibrium swelling tests (see Table 7) that clay cores swell to a single point linearly and stopped swelling in the organic solvents used in

this study. Equilibrium swelling in all the organic solvents was completed in a very short time.

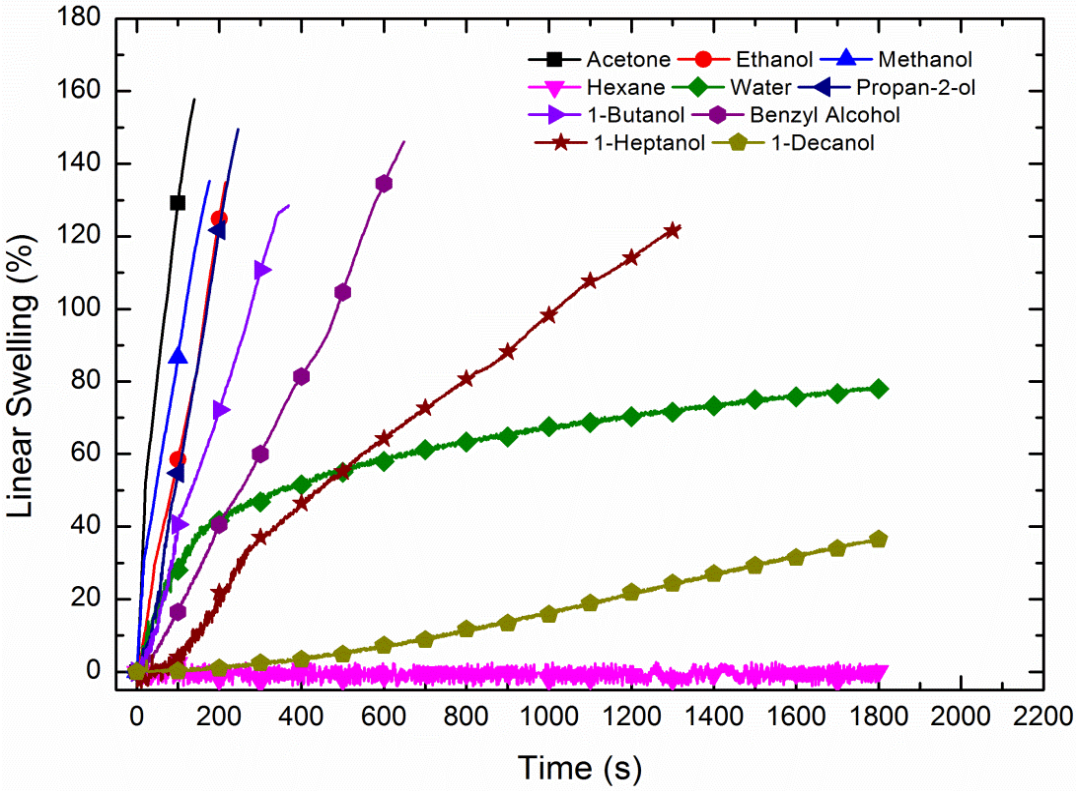

Figure 17. Linear swelling behaviour of Na-bentonite cores in various organic solvents within the range of sensor height (6mm) via NC-LDM with 60 readings/minute frequency.

Photographic images in Figure 18 show that the clay core surfaces were not even wetted by hexane molecules and remained dry after immersion. On the other hand, after swelling in methanol, clay cores became friable and easily dispersed. This behaviour of clay cores was also observed in all the organic solvents (with the exception of hexane). Unlike the behaviour observed in organic solvents, the clay mineral cores became sticky after swelling in water, forming a coherent structure.

Figure 18. Photographic images of Na-bentonite cores after short term swelling tests in hexane, methanol and water.

Results of short term swelling tests were correlated with dielectric constant, dipole moment, surface tension and viscosity of the solvents (see Table 3) in order to elucidate the effects of solvent parameters on the clay swelling behaviour. Due to limited sensor height leading to uncertainty in results in short term swelling tests, swelling rate data was used for correlations (See Appendix G). Note that swelling rate correlations were only applied for the bulk properties of organic compounds since swelling in water didn't show linear behaviour. Figure 19 shows the effects of bulk solvent parameters on the linear swelling rate of Na-bentonite cores obtained in short term swelling tests.

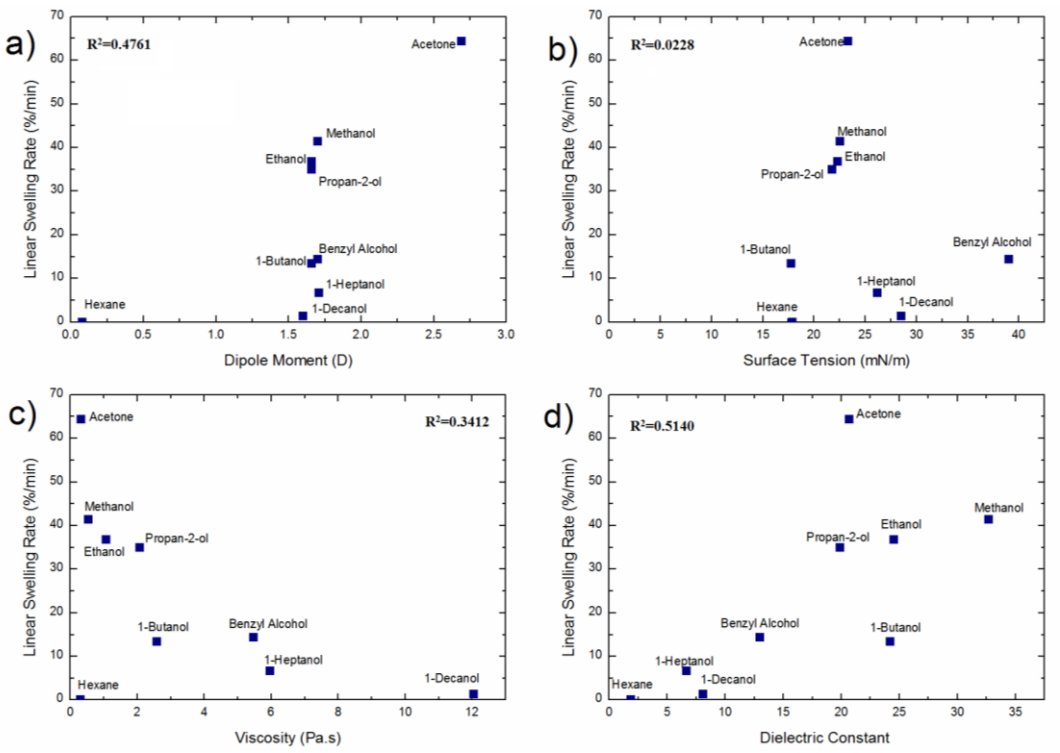

Figure 19. Correlations of the linear swelling rate of compacted Na-bentonite cores with: a) dipole moment, b) surface tension, c) viscosity and d) dielectric constant of the designated solvent along with linear regression (R^2) values

Figure 19a shows that there are no clear correlations of dipole with swelling rate. Swelling rate is at zero in hexane, having no polarity (i.e. dipole moment = 0), and is the highest in acetone, which has the highest dipole moment among all the solvents. However, swelling rate is variable between the alcohols having a similar dipole moment, which makes the relationship between dipole moment and swelling rate unclear.

Figure 19b shows that there are also no clear correlations of surface tension with clay swelling rate. This is an unexpected finding as with increasing surface tension, capillary forces developed in the pores leading to pore swelling are expected to increase, according to Equation 3. On the other hand, when the solvents are divided into two groups as water miscible (acetone, methanol, ethanol, propan-

2-ol and 1-butanol) and water immiscible (hexane, 1-heptanol, 1-decanol and benzyl alcohol), there seems to be two distinct relation leading to viable correlations. However it is not possible to interpret this relationship with the data present in this study.

Figure 19c shows that swelling rate is strongly dependent on the viscosity of the medium. Besides apolar hexane, swelling rate is minimal in highly viscous 1-decanol and increases non-linearly with decreasing viscosity. Swelling rate is also the highest in acetone, which has the lowest viscosity. The viscosity of pore fluid has an essential role in formation of pore pressures in the compacted Na-bentonite clay fabric. The faster the fluid is drawn into the pores, the higher the pore pressure becomes. Thus, solvents with lower viscosities are expected to lead to higher pore pressures and faster swelling rates at the initial stage (i.e. pore swelling).

In Figure 19d, it is seen that there is a relationship between dielectric constant and swelling rate as there is an increasing trend of swelling rate with increasing dielectric constant. Dielectric constant is essentially an indication of how well the medium can separate the charges present in the medium. The Debye equation (see Appendix B) shows that dipole moment and dielectric constant are proportional, yet the polarizability of the medium also affects the value of dielectric constant as a variable. Therefore solvents with similar dipole moments can have different dielectric constants. Even though there seems to be a relationship between swelling rate and dielectric constant, it is assumed that the proportionality between swelling rate and dielectric constant is because the solvents with higher viscosity tend to have lower dielectric constants, or vice versa, since the initial stage of swelling is expected to be mostly pore swelling and only affected by capillary forces.

In order to discuss the effects of dielectric constant in more detail further short term tests were applied.

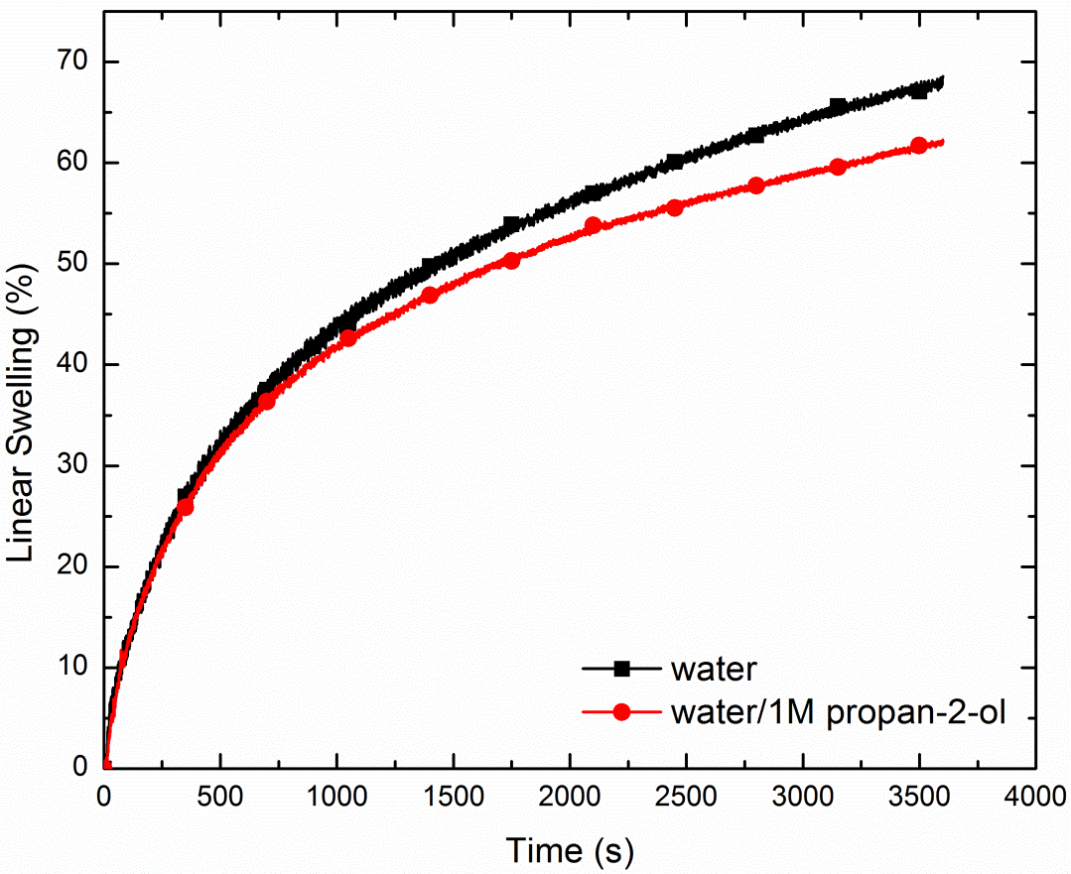

Figure 20. Short term swelling behaviour of compacted Na-bentonite cores in water and water/propan-2-ol solutions.

Figure 20 shows the short term swelling behaviour of Na-bentonite cores in water and 1M propan-2-ol/water solution. Note that the dielectric constant of 1 M propan-2-ol/water solution is approximately 65. It is seen that in water/propan-2-ol mixture, there is a decrease in the slope of the second regime of swelling. This decrease could be attributed to the decrease in dielectric constant of the swelling medium resulting from the addition of propan-2-ol to water, which would increase electrostatic forces of attraction between interlayers and screening of the longer range negative-negative repulsion.

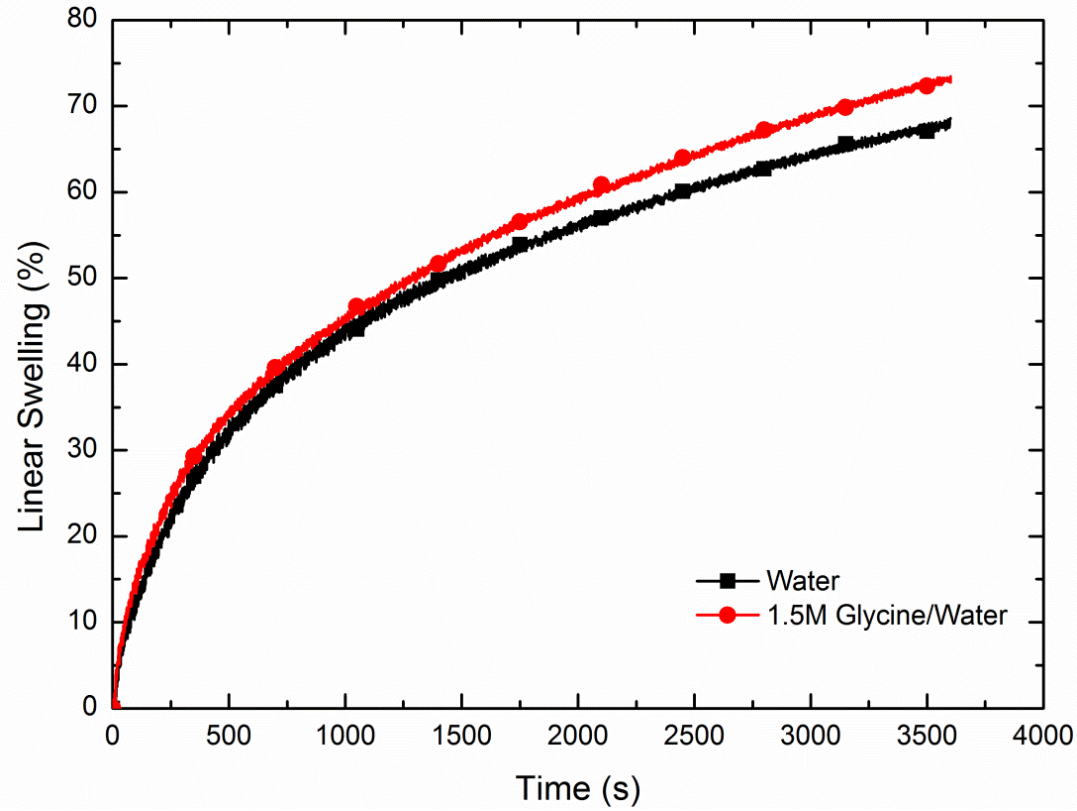

Figure 21. Short term swelling behaviour of compacted Na-bentonite cores in 1.5 M glycine/water solution

Water has the highest dielectric constant in the solvents used in this study thus far. In order to see the effects of higher dielectric constants, an amino acid "glycine" was added to the deionised water. In 1.5 M glycine/water solution, the dielectric constant increases from 80.1 for water, to 109.9 (Barshad, 1952). Figure 21 shows the short term swelling behaviour of Na-bentonite cores in water/glycine solutions. The first swelling regime is nearly the same with water, which is also similar to water/propan-2-ol solutions. This time there is an increase in the second regime on swelling, which can be attributed to the increased dielectric constant.

3.2.2. Equlibirium Long Term Swelling Tests

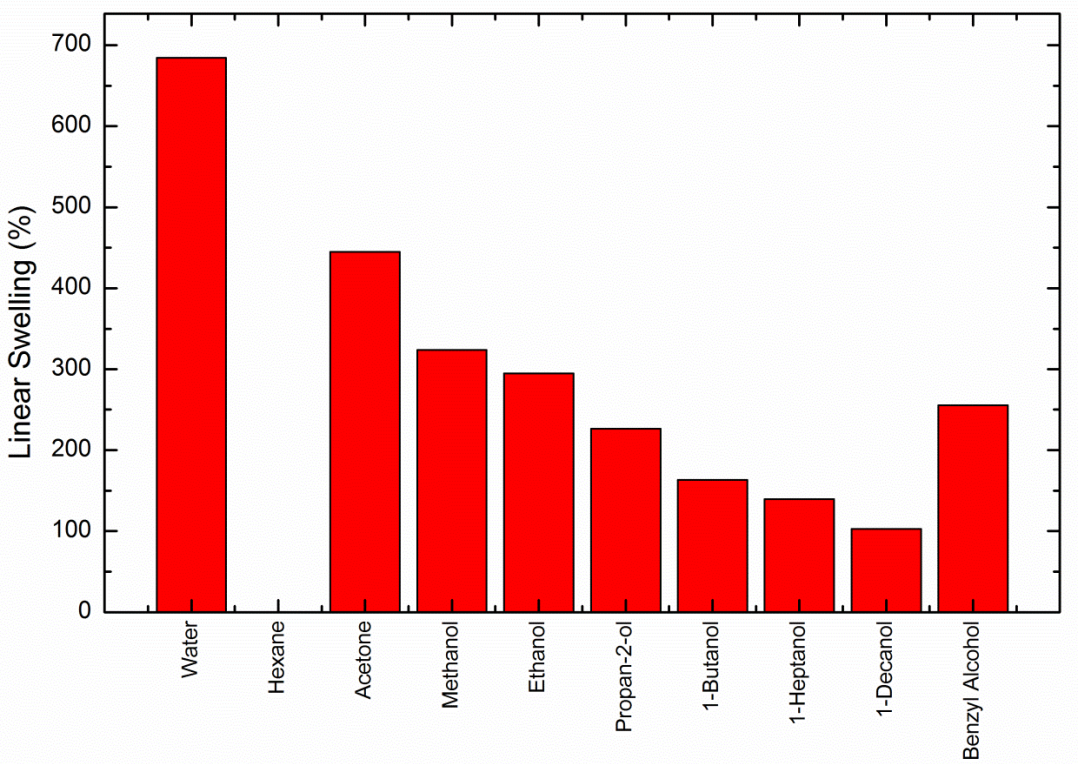

Figure 22. Results of equilibrium long term swelling tests of compressed Na-bentonite cores in organic solvents. Water swelling included as a reference point.

The results of equilibrium swelling tests of Na-bentonite cores in organic solvents are shown in Figure 22. Note that the cores were fully immersed into the designated solvents and the linear expansion was recorded periodically until they reached a balance and stopped swelling. Since the readings were recorded manually, the swelling times (see Table 7) are not exact, but approximate values between two recordings. For instance if the swelling stopped between two readings (i.e. between 40 and 45 minutes), the swelling time is recorded as the lower value (in this case 40). It is seen that the equilibrium swelling time of Na-bentonite cores correspond to the linear approximation of short term swelling and therefore the use of linear approximation in short term swelling experiments to calculate the swelling rate was valid.

Table 7. Total swelling and approximate swelling time results of equilibrium swelling tests of compacted Na-bentonite cores.

Solvent	Total Linear Swelling (%)	Approximate Time of Swelling
Hexane	-	-
Water	684.2	2 weeks
Ethanol	294.7	10 min
Methanol	323.7	10 min
Propan-2-ol	226.3	10 min
Acetone	444.7	10 min
1-butanol	163.2	10 min
Benzyl alcohol	239.4	45 min
1-Heptanol	139.7	30 min
1-Decanol	102.9	60 min

Figure 23a shows that equilibrium swelling points of Na-bentonite cores increased with increasing dielectric constant. The relationship between dielectric constant and clay swelling was explained in early studies. Barshad (1952) explained the dependence of swelling on dielectric constant by claiming that the absorbed liquid phase acts as a dielectric medium weakening the interlayer attractive forces of the crystal lattice. This action could be interpreted from Coulomb's law, that the greater the dielectric medium separating the charges, the weaker would be the interlayer attractive forces of the crystal lattice itself. Norrish (1954), made a deduction of swelling index described by $U\varepsilon/v^2$ in which U is the solvation energy and v is the valence of the interlayer cation, while ε is the dielectric constant of the interlayer

liquid. For a given cation valence, swelling increases with increased solvation energy and dielectric constant. Since these theories apply only for layer expansion phase of clay swelling, the effects of pore swelling on total bulk swelling of clays should also be considered. The disruption of the linear correlation between dielectric constant and swelling in acetone or 1-butanol can be explained with the previous effects of pore swelling due to viscosities.

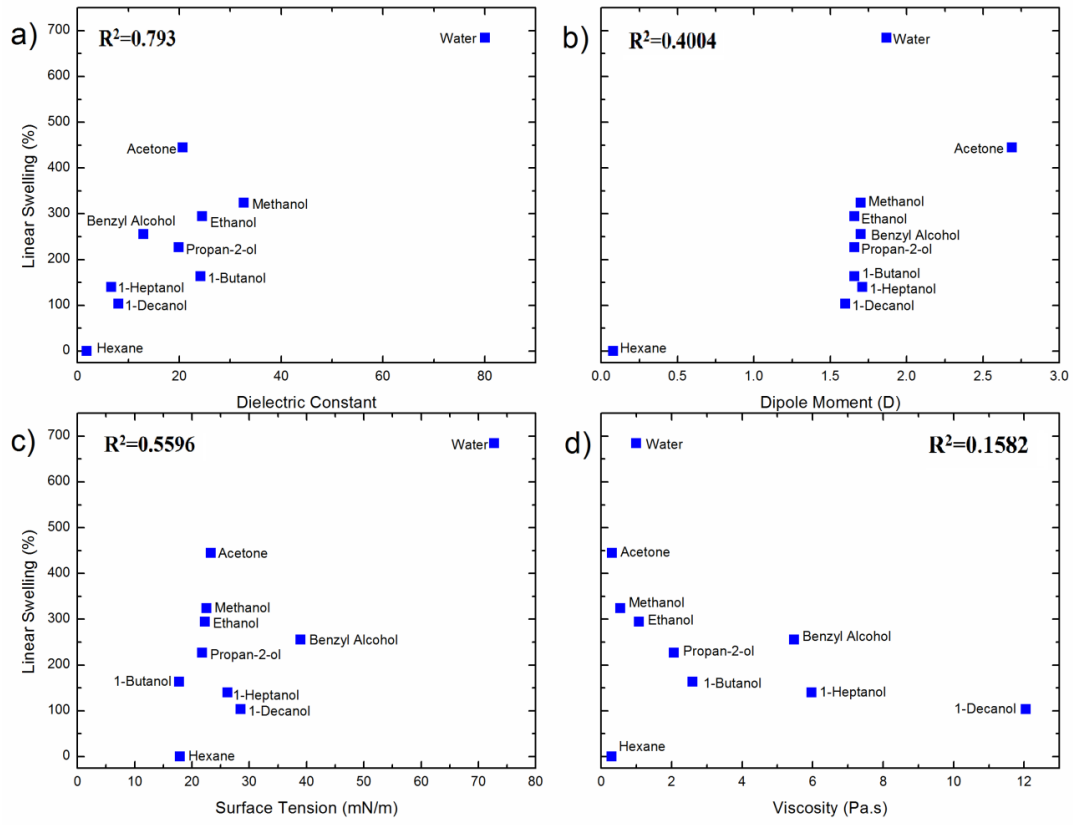

Figure 23. Correlations of the linear swelling of Na-bentonite cores with: a) dielectric constant, b) dipole moment, c) surface tension and d) viscosity of the designated solvent along with linear regression (R^2) values.

Figure 23b shows no clear relationship between dipole moment and total swelling. However, since there is no swelling in hexane which has no dipole moment (μ=0), it can be said that polarity is essential for swelling. With presence of water in the clay interlayer, non-polar molecules can't cause interlayer expansion as they can't

replace water molecules. On the other hand, solvents with sufficient dipolar activity (in this case solvents with μ>1.5D) can cause swelling. Polar compounds can compete with water to be adsorbed in the interlayer and replacement of water with larger molecules may cause higher interlayer expansions. However, this replacement is unlikely to occur if the molecular size of the organic compound is larger than the interlayer spacing, and the dipole low. Molecules of organic compounds might hydrogen bond with water or interact with water through dipole-dipole forces and can have a tendency to become solubilized in the core pore water and therefore cause bulk clay expansion. (Green et al., 1983)

For a given organic-clay complex, the expansion of layers are dependent on the solvation of exchangeable cations, therefore ion-dipole interactions. Increasing dipole moment of the solvent is expected to increase the interactions and lead to development of diffuse layers. According to Onikata et al. (1999), since the driving force governing the intercalation of solvent molecules into the clay interlayer is primarily due to the solvation of the interlayer cations then the electron donor ability of the solvents should be considered for correlation, rather than the dipole moment. However, these studies revealed that there was also no direct correlations between layer expansion and electron donor ability either. In summary, it can be stated that here is no direct relationship between dipole moment and layer expansion, yet the dipole moment can be related to dielectric constant according to the Debye equation (see Equation 4).

The correlations of surface tension with swelling in Figure 23c were similar to previous swelling rate correlations, and there was no discernible relationship. The correlations of viscosity were also similar to previous swelling rate correlations, as swelling decreased with increasing viscosity in Figure 23d. Note that hexane can be

excluded from viscosity correlations as it is a non-polar solvent and there is no physical swelling in hexane. Since the equilibrium swelling is not related to viscosity these results can be interpreted in two ways. First, it can be observed that the effect of pore swelling is dominating the bulk swelling in organic solvents and therefore the effects of viscosity still applies, as in swelling rate calculations. Second, the tendency of low viscosity fluids having high dielectric constants overlaps with the effects of dielectric constant.

The results can be interpreted as that the swelling at first is driven by capillary forces and mainly pore swelling, then interlayer swelling occurs and the dielectric constant of the medium becomes a determinant parameter. As a result, a combination of having lower viscosity and higher dielectric constants leads to both more rapid swelling owing to capillarity and an overall greater final equilibrium swelling in acetone and methanol among the organic solvents. The apparent difference between the short term and the equilibrium swelling behaviour of water and polar organics might be explained by the following argument. At the initial swelling state, interlayer water is replaced by larger organic molecules which lead to higher interlayer swelling. In the latter state, due to osmotic swelling, forming of double layers occurs and the influence of the dielectric constant arises. More detailed interpretation of the Na-bentonite clay swelling in water will be discussed in the results of the aqueous electrolyte solutions.

3.3. Swelling of Compacted Na-bentonite Cores in Aqueous Electrolyte Solutions

Swelling tests of the prepared compacted Na-bentonite cores (see Section 2.2) in different electrolyte concentrations were performed in order to examine the effects of brine ion type and concentration. For this purpose, solutions of KCl, NaCl, KI and $CaCl_2$ salts were prepared from 0.02 M up to 2 M. Short term swelling tests were carried out for 1 hour, while equilibrium swelling tests were applied for 2 weeks. Results are presented below and discussed under four main conditions:

1. As bentonites used in this study are Na-bentonites, the effects of cation concentration are discussed via using different concentrations of aqueous NaCl solution.
2. The effects of group 1 cation type are discussed through experiments keeping the anion same and changing the cation into another group 1 cation; therefore results of different concentrations of aqueous KCl solutions were compared with the NaCl results.
3. Effects of group 1 anion type were discussed by keeping the cation the same and changing the anion into another group 1 one, therefore results of different concentrations of aqueous KI solutions were compared with KCl results.
4. Finally, the effects of Group 2 cation were discussed by changing the cation into Group 2 and keeping the anion the same. Therefore, results of different concentrations of aqueous $CaCl_2$ solutions were compared with KCl results

3.3.1. Effects of Cation Concentration on Swelling of Compacted Na-bentonite Cores

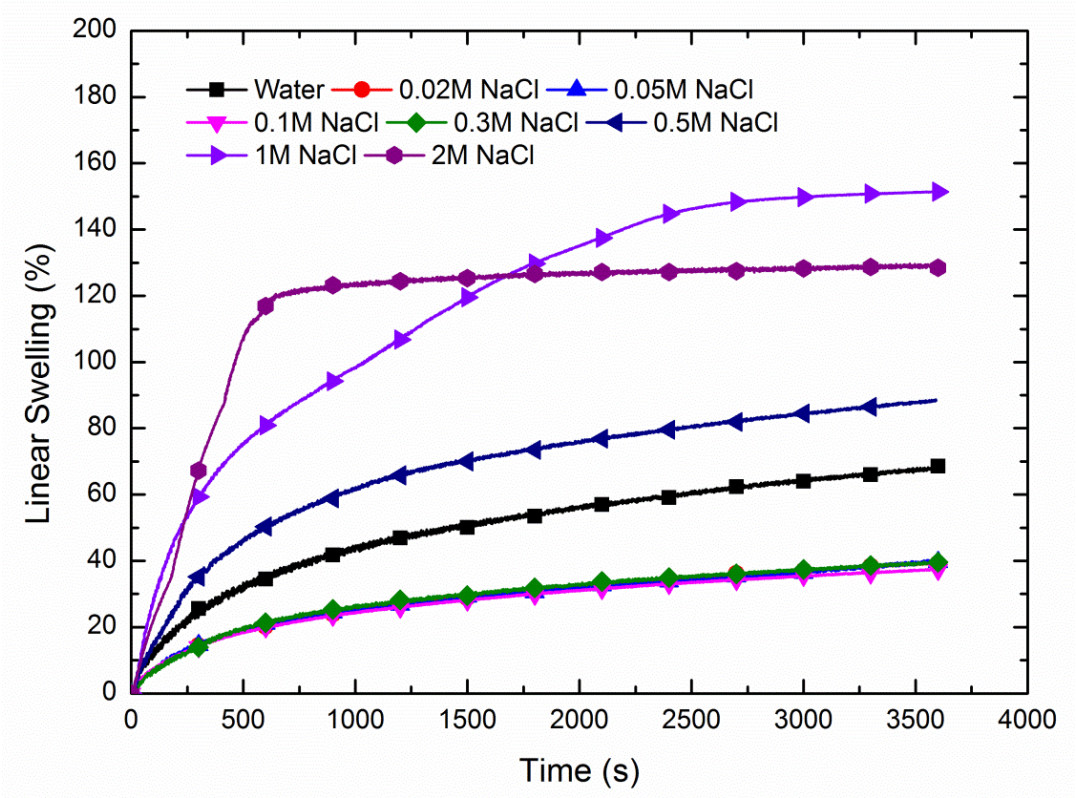

Figure 24. Short term swelling behaviour of compacted Na-bentonite cores in aqueous NaCl solutions.

Figure 24 shows the short-term swelling behaviour of Na-bentonite cores in various concentrations of NaCl–water solutions. In short term swelling tests, the highest suppression of swelling is found in 0.1 M concentrations, which resulted in a 46 % decrease in swelling compared to water. Swelling in NaCl brine is lower than the observed swelling in water from 0.02 M up to 0.3 M NaCl. The expansion of the cores exceeds the device limit in 1 M concentration in approximately 40 minutes, and that is the highest swelling observed in short term experiments in NaCl solutions. On the other hand, in 2 M NaCl solution the swelling trend of Na-

bentonite changes as the linear expansion reaches to 129% after a fast swelling completed in approximately 10 minutes, then swelling stops and remains the same until the end of the experiment.

At low concentrations, short term swelling in aqueous NaCl solutions is similar to swelling in water, though the rate of swelling is generally lower. The first swelling regime is faster with a higher slope and is completed in between 10-15 minutes. In the second regime, swelling is slower compared to first one, and increased with a constant slope until the end of the experiment. On the other hand, interestingly, when salt concentration is higher than 0.5-1 M limit the swelling trend changes. In general, at 2M electrolyte concentrations, the swelling of Na-bentonite cores occurs only in a single regime. After a fast swelling, the expansion stops and core thickness remains constant. This brings out the concept of a critical salt concentration (CSC) at which interlayer swelling is suppressed.

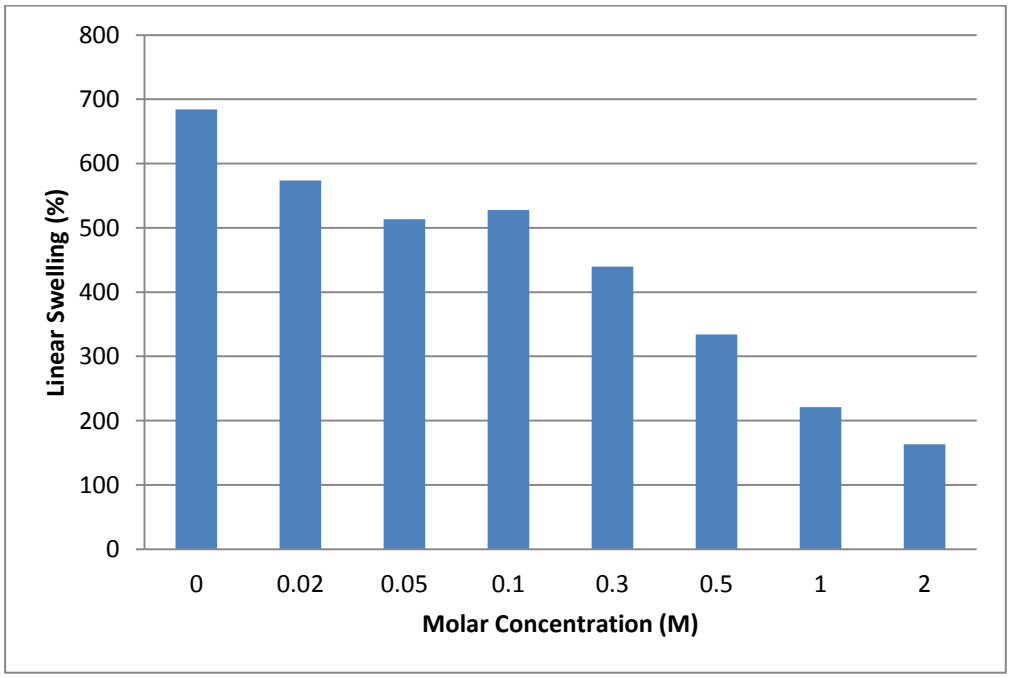

Figure 25. Equilibrium swelling behaviour of compacted Na-bentonite cores in aqueous NaCl solutions as a function of concentration.

Figure 25 shows the equilibrium swelling behaviour of Na-bentonite cores in various concentrations of NaCl-water solutions. In the equilibrium state, NaCl is not effective at suppressing clay swelling, especially when at low concentrations. Addition of 0.02 M NaCl into water resulted in a 16% decrease in Na-bentonite swelling. The lowest linear expansion is reported in 2 M NaCl solution at 163%. In contrast, with short term tests it is seen that swelling is inversely proportional to electrolyte concentration in equilibrium swelling tests.

As was mentioned in the introduction, osmotic swelling is described with the DDL equation. To recap, the thickness of the diffuse double layer 1/κ, is described with Equation 2:

$$\frac{1}{\kappa} = \sqrt{\left(\frac{\varepsilon DkT}{2n_0 e^2 v^2}\right)} \qquad (2)$$

where n_0 is electrolyte concentration, v is cation valence, D is dielectric constant of the medium, and T is temperature., ε is the permittivity of the vacuum, k is the Boltzmann constant (1.38 x 10^{-23} $\mathring{J}K^{-1}$) and e is the electronic charge (1.602 x 10^{-19} coulomb). The results of equilibrium swelling tests agree with DDL theory, therefore it can be said that during equilibrium long term swelling, osmotic forces dominate the clay core expansion and can be suppressed by electrolyte concentrations with high concentrations.

It is known that increasing electrolyte concentration decreases the dielectric constant of the medium. Early studies of Haggis et al (1952) show that addition of 1 M KCl and 1 M NaCl to water decreases the dielectric constant from 80.1 to 64.9 and 63.0, respectively. Hasted et al (1948) showed that dielectric constant of water decreased to 58.5 in 2 M KCl solutions. In this study, methanol has the second highest dielectric constant (32.7) between the organic solvents used, after water

(80.1). There is a large difference between the dielectric constants of methanol and water, and the swelling behaviours of Na-bentonite cores in these two solvents are completely different. It is seen that swelling behaviour in 2 M KCl solution is similar to swelling behaviour of the compacted clay core in methanol. This can be interpreted as that below a critical dielectric constant, swelling behaviour of the compacted Na-bentonite cores changes, regardless of the cation type.

3.3.2. Effect of Group 1 Cations on Swelling of Compacted Na-bentonite Cores

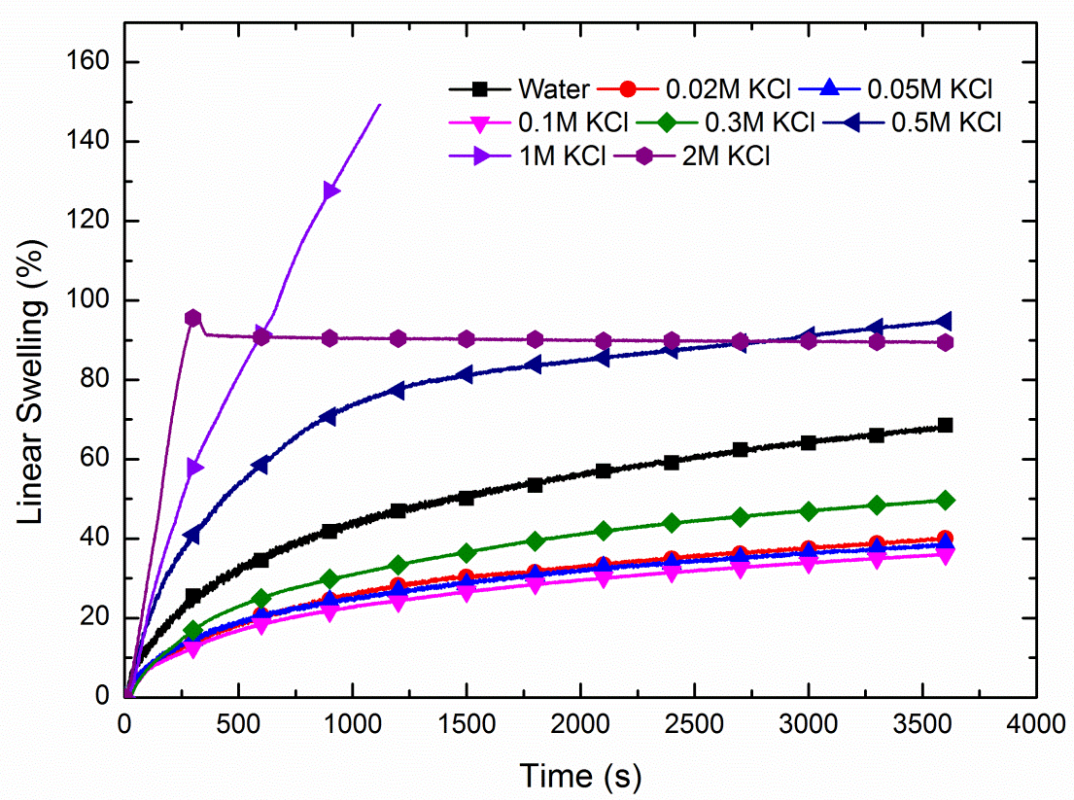

Figure 26. Short term swelling behaviour of compacted Na-bentonite cores in KCl/water solutions within the range of sensor height (6 mm)

Figure 26 shows the short-term swelling behaviour of Na-bentonite cores in various concentrations of aqueous KCl solutions. In the short term, the highest suppression of swelling is derived in 0.1 M concentrations which resulted in a 47 % decrease in swelling relative to swelling in water. Similar to the NaCl solutions, from 0.02 M up to 0.3 M, swelling in KCl solutions is lower than the swelling in water. In

concentrations lower than 1 M, the swelling trend is the same as in water and there are two observable regimes with two different slopes. The expansion of the Na-bentonite cores exceeds the device limit in 1 M concentration in approximately 20 minutes, and that is the highest swelling observed in short term experiments in KCl solutions. On the other hand, in 2 M KCl solution, the swelling trend of the compacted Na-bentonite core changed as the linear expansion reaches to 112% after a fast swelling completed in approximately 5 minutes, then swelling stops and remains the same until the end of the experiment.

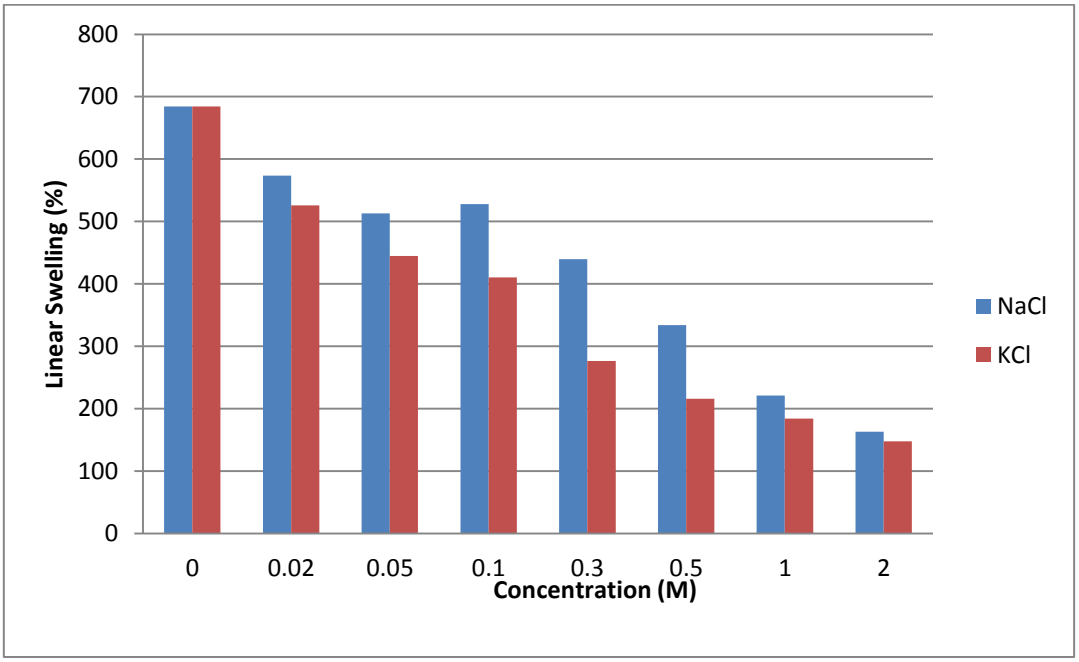

Figure 27. Equilibrium swelling behaviour of Na-bentonite cores in aqueous NaCl and KCl solutions as a function of concentration.

Figure 27 shows the equilibrium swelling behaviour of Na-bentonite cores in various concentrations of aqueous NaCl and KCl solutions. It is clearly seen that the effect of cation type changes the equilibrium swelling of Na-bentonite cores, with aqueous KCl solutions suppressing swelling better than NaCl solutions, especially between the 0.5-1 M concentration ranges.

Inhibition through cation exchange is a very well-known effect in the clay swelling literature. Depending on the adsorption and hydration properties, saturation of different cations affects the expansion of clays differently. Adsorption of cations were classified by Sposito et al. (1999) as inner- and outer-sphere, in which an inner-sphere surface complex has no water molecule interposed between the mineral surface functional group and the small cation or molecule it binds, whereas an outer-sphere surface complex has at least one such interposed water molecule. Na^+ cations initially form inner-sphere complexes with interlayer water molecules that are strongly bound to the tetrahedral substitution sites of the clay layer. A large amount of these inner-sphere complexes transform to outer-sphere complexes upon the addition of more water. On the other hand the K^+ cation forms only inner-sphere complexes. Moreover, K^+ ions have smaller degree of hydration compared to Na^+ (See Table 6), and are less hydrated at high water content. In addition, the ionic radius of K^+ is larger and very close to the size of the hexagonal gap between montmorillonite sheets, and they fit almost perfectly (Sposito et al., 1999; Boek et al. (1995). Having low hydration enthalpy, exchange with larger K^+ ions can control expansion of interlayers and formation of double layers leading to osmotic swelling. Due to the reasons explained above, potassium based salts are used in the drilling industry as once they are exchanged by the interlayer cation, they keep the expandable sheets together and keeps water molecules out of it. Hence, crystalline swelling can be suppressed (O'Brien and Chenevert, 1973).

3.3.3. Effect of Group 1 Anions on Swelling of Compacted Na-bentonite Cores

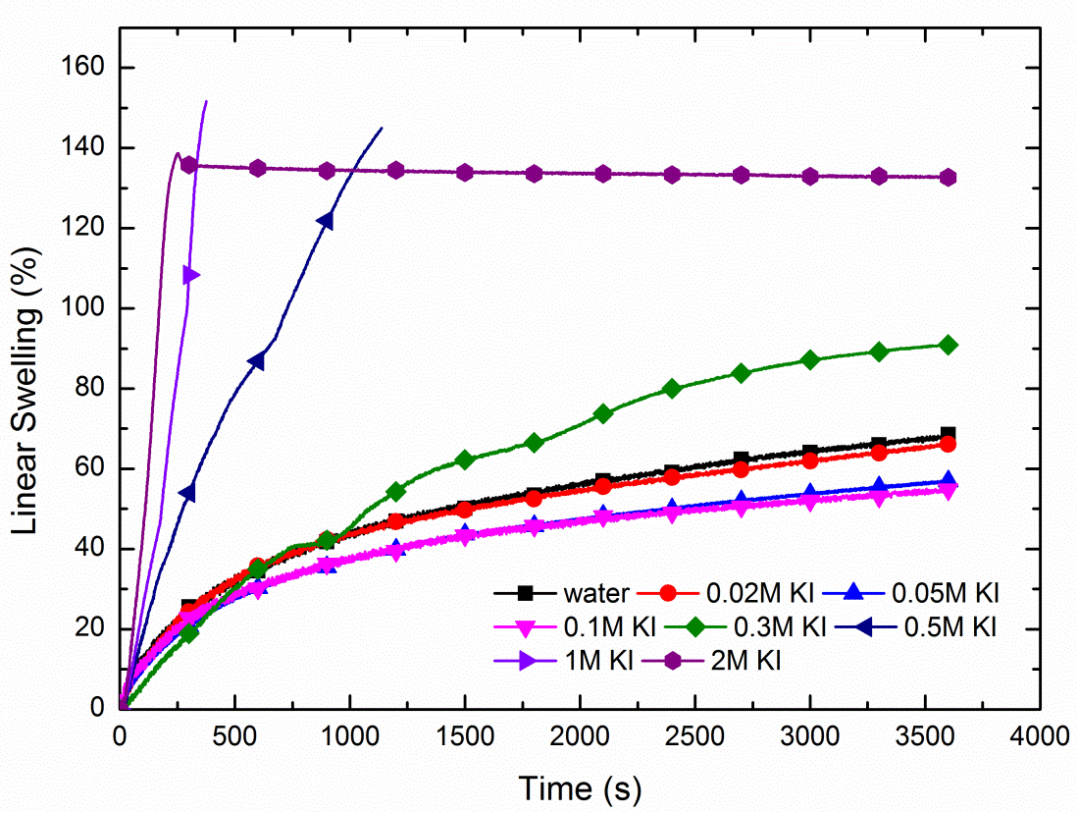

Figure 28. Short term swelling behaviour of compacted Na-bentonite cores in aqueous KI and KCl solutions within the range of sensor height (6mm).

Figure 28 shows the short-term swelling behaviour of Na-bentonite cores in various concentrations of aqueous KI and KCl solutions. In the short term, similar to previous results the highest suppression of swelling is derived in 0.1 M concentrations, which resulted in a 20 % decrease in swelling relative to water. The expansion of the cores exceeds the device limit in 0.5 M and 1 M concentrations in approximately 20 minutes and 5 minutes, respectively.

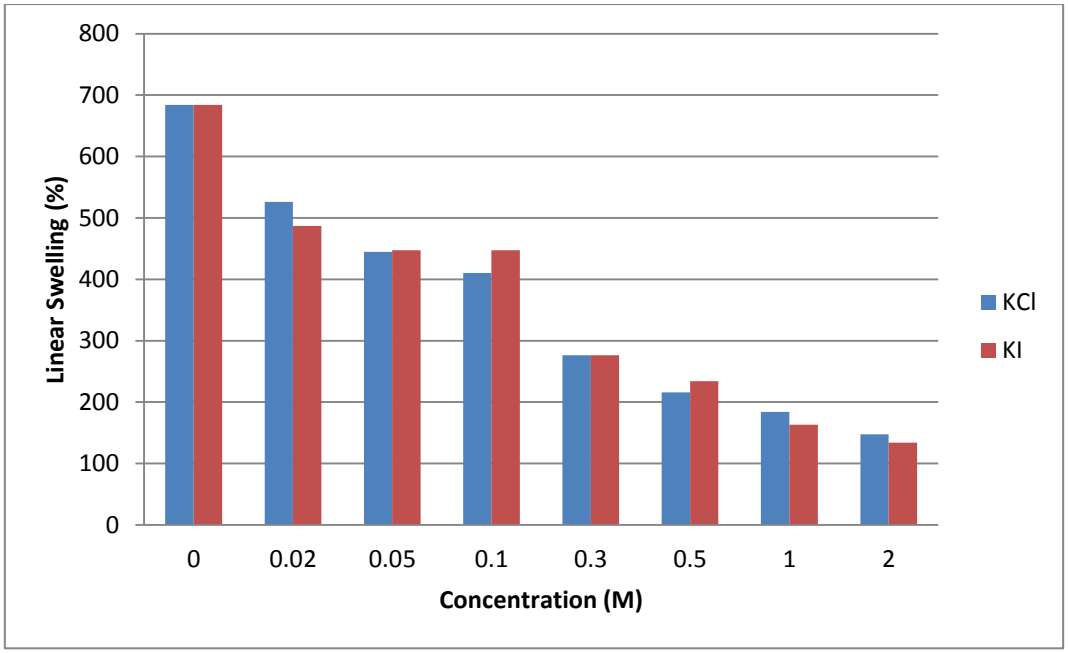

Figure 29. Equilibrium swelling behaviour of compacted Na-bentonite cores in aqueous KI and KCl solutions

Figure 29 shows the equilibrium swelling behaviour of Na-bentonite cores in various concentrations of aqueous KI and KCl solutions. The linear expansion was observed to be 134% in 2 M KI solution, which is the lowest swelling observed in overall equilibrium swelling tests of aqueous salt solutions. It is seen that the swelling in KCl and KI are almost the same, which shows that the variation of anion in the structure doesn't have any observable effects on equilibrium swelling of Na-bentonite. As the diffuse double layer model has no relationship with anion type, the results are in accord with theory.

3.2.4. Effect of Group 2 Cations on the Swelling of Compacted Na-bentonite Cores

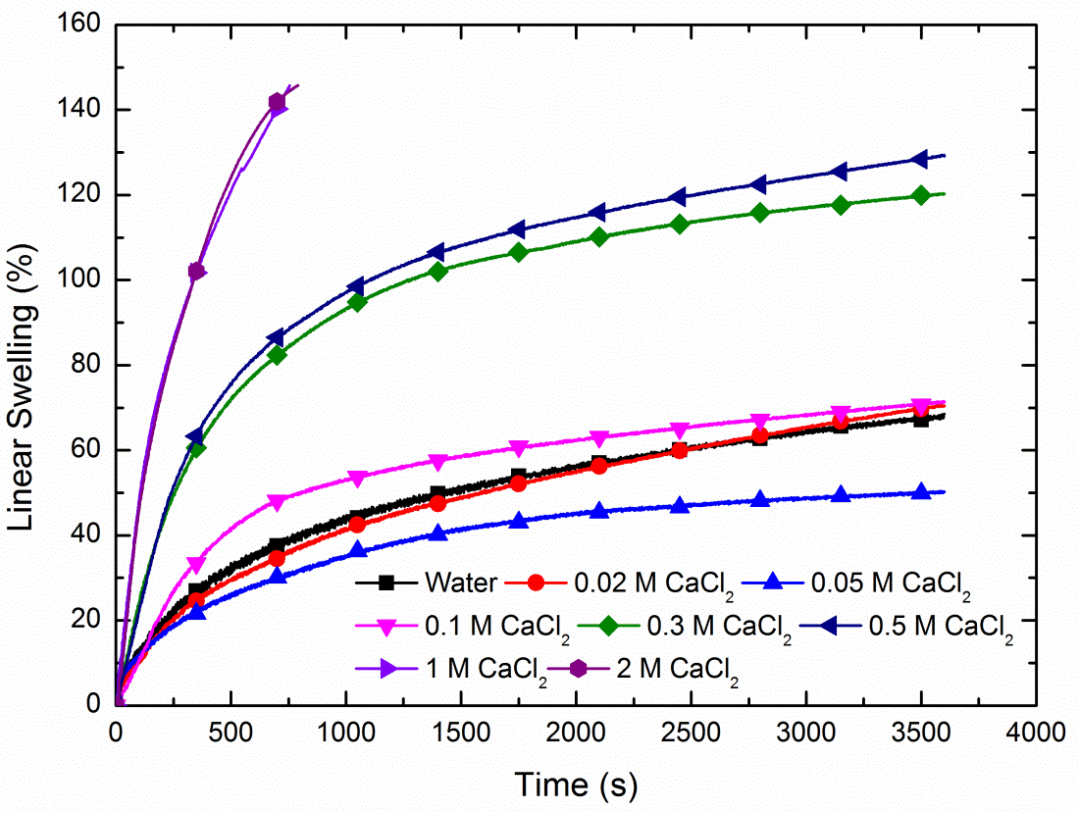

Figure 30. Short term swelling behaviour of compacted Na-bentonite cores in $CaCl_2$/water solutions within the range of sensor height (6mm).

Figure 30 shows the short term behaviour of Na-bentonite cores in $CaCl_2$ solutions from 0.02 M up to 2 M concentrations. The highest suppression of swelling was observed in 0.05 M concentrations which resulted as 26% decrease. Only in 0.05 M concentrations was the expansion of the cores lower than the expansion found in water. Swelling exceeds the device limit in 1 M and 2 M concentrations in approximately 12 minutes. Unlike KCl, the possible change in swelling trend in 2 M $CaCl_2$ solution is not observable in this experiment since the swelling exceeds the device limit. Results show that during short term swelling, in which the water content is lower, the expansion of Na-bentonite cores is faster and therefore higher

in $CaCl_2$ solutions because of the greater hydration enthalpy of Ca^{2+} ions (see Table 6).

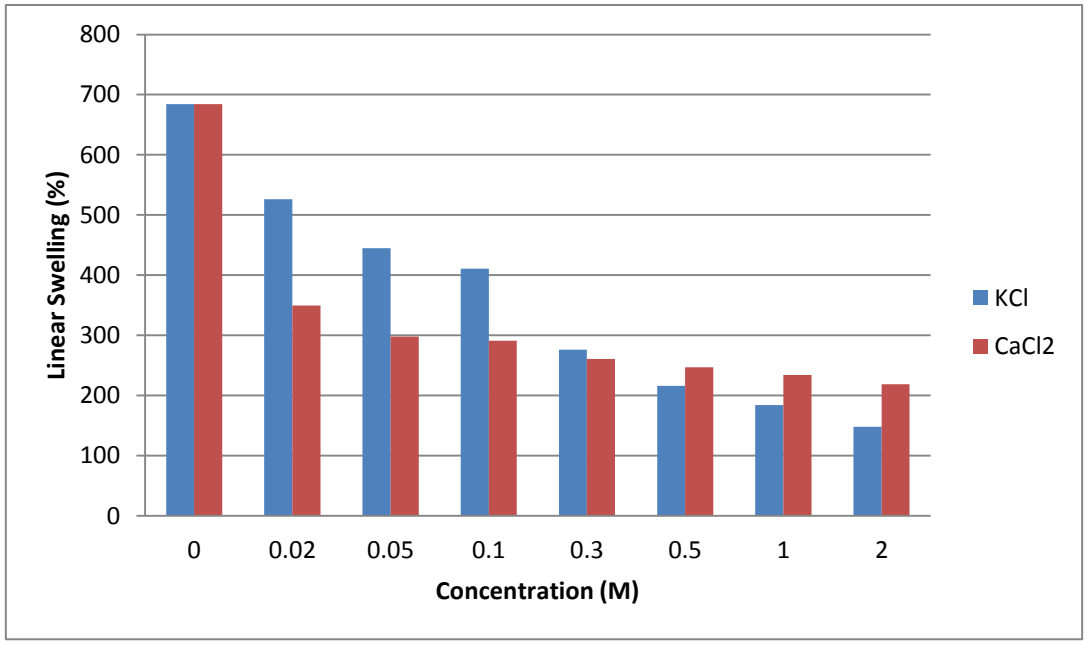

Figure 31. Equilibrium swelling behaviour of compacted Na-bentonite cores in aqueous $CaCl_2$ and KCl solutions

Figure 31 shows the equilibrium swelling behaviour of Na-bentonite cores in various concentrations of aqueous $CaCl_2$ and KCl solutions. It is seen that the change in swelling with presence of $CaCl_2$ is different than the swelling in KCl solutions. Addition of only 0.02 M $CaCl_2$ into water resulted as a 49% decrease in Na-bentonite swelling. On the other hand there is no apparent change in swelling with increasing electrolyte concentration as linear expansion in 0.02 M is 349% while it is 218% in 2 M. Despite having high hydration energy, Ca^{2+} ions can prevent formation of double layers, especially at high water contents. Compared to monovalent cations, multivalent cations cause greater dielectric saturation (Millen and Watts, 1967); which results as the increase in the attractive potential due to lower dielectric medium thereby reduced swelling. Hence, besides the advantage of

higher dielectric saturation, the higher valence of calcium also provides a better suppression of osmotic swelling, agreeing with DDL theory. Since osmotic swelling is a secondary stage after interlayer saturation of smectite minerals, it can be said that during short term, the effects of crystalline swelling is more dominant than the effects of osmotic swelling.

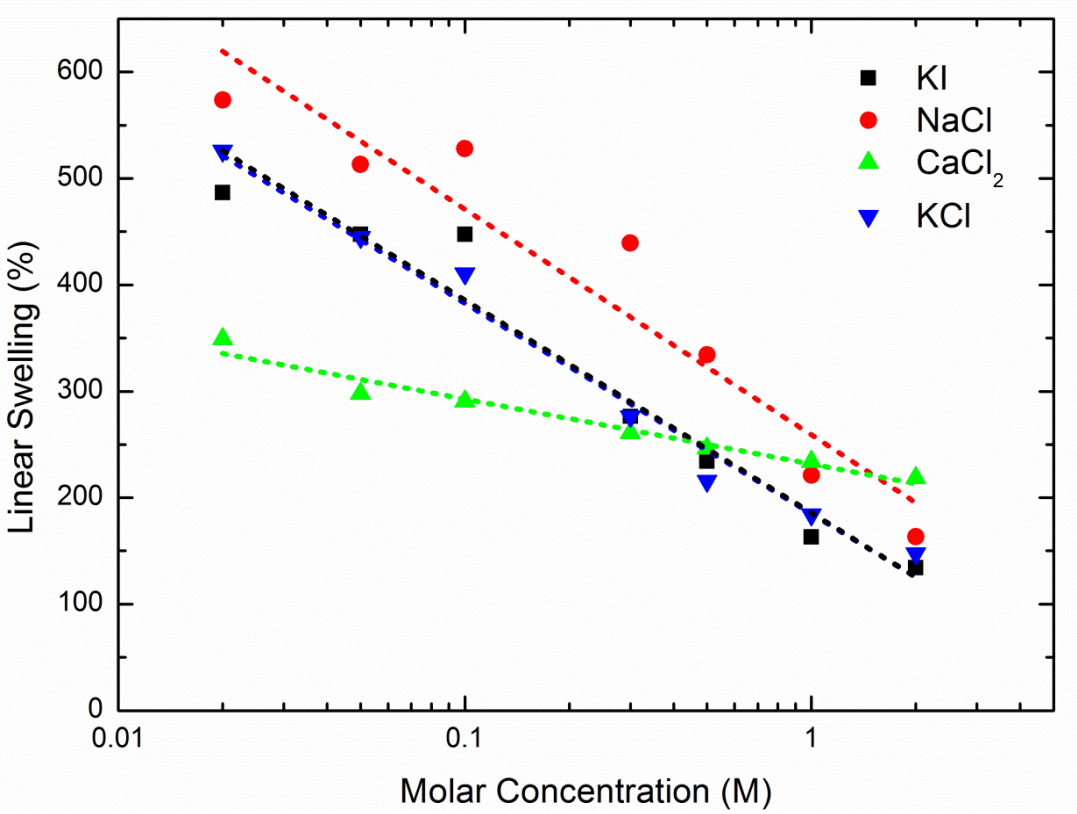

Figure 32. Equilibrium linear swelling points of Na-bentonite cores in aqueous solutions of KCl, NaCl, KI and $CaCl_2$ from 0.02 M to 2 M concentrations

From the point of view of equilibrium swelling (where equilibrium is attained), the difference between the effects of different electrolytes can be seen in Figure 32. At lower concentrations, due to the effectiveness of Ca^{+2} ions against forming double layers, the swelling is lower in $CaCl_2$ solution. It is known that increasing electrolyte concentrations decreases the DDL thickness and therefore the osmotic swelling, yet electrolyte concentration slightly effects surface hydration properties

of cations (Roehl and Hackett, 1982). As such, at high concentrations of brine, osmotic swelling is suppressed in all the electrolyte solutions, regardless of the cation properties. In addition, due to having higher hydration affinity, equilibrium swelling of Na-bentonites is higher at high concentrations of $CaCl_2$.

Short and equilibrium swelling tests of aqueous electrolyte solutions showed that swelling of compacted Na-bentonite is dependent on cation type and the electrolyte concentration, as well as the valence of the cation.

3.4. Swelling of Illite

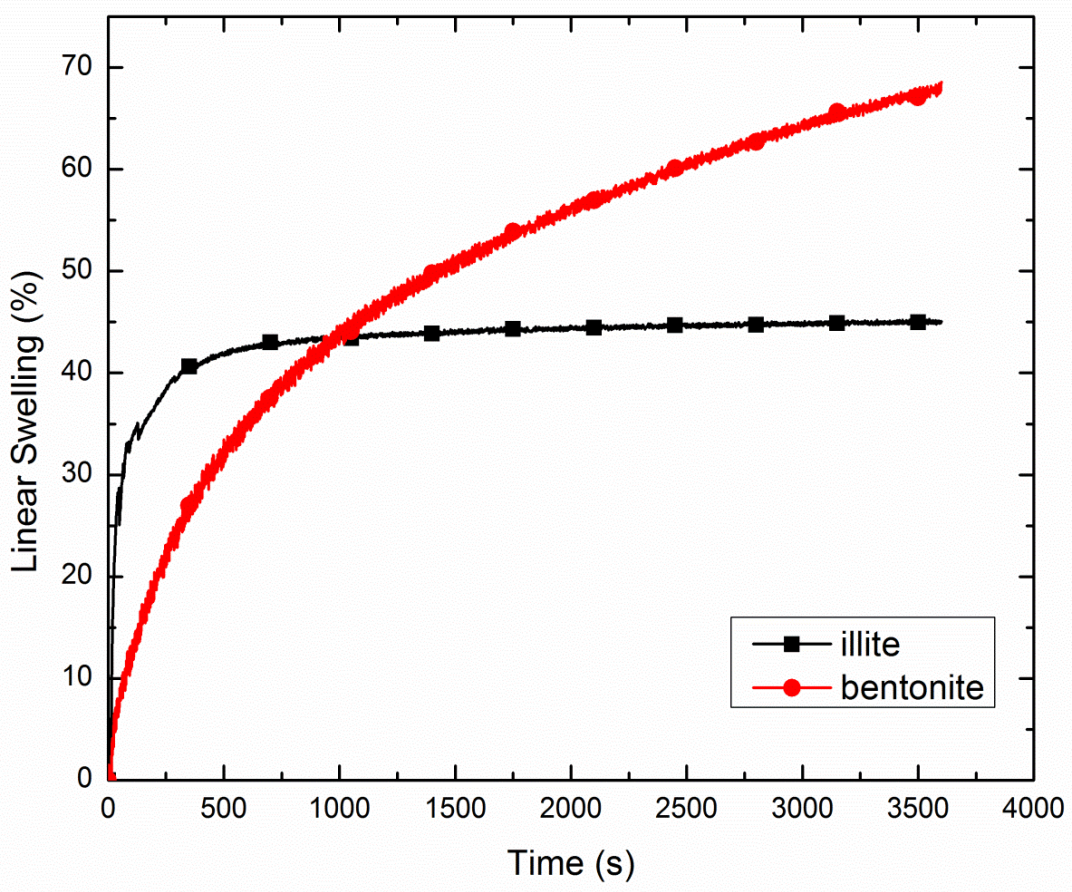

Figure 33. Short term swelling of Na-bentonite and illite cores in water.

Illites are naturally K^+-saturated and generally referred to as non-reactive or non-swelling clay minerals (Wilson and Wilson, 2014). The effects of K^+ saturation are described in the previous section. Therefore, interlayer expansion is not expected in illite minerals. In order to allow comparison with the swelling behaviour of Na^+ saturated Na-bentonite cores, swelling tests of illite cores were carried out in some of the designated aqueous electrolyte solutions and organic solvents. Note that only short term swelling tests were applied to illite cores as they reached their equilibirium swelling state in the short term and extended time-scale tests were unnecessary. It can be clearly seen that swelling behaviour of illite cores are

different than Na-bentonite cores (see Figure 33). In general, illite cores swelled rapidly initially, up to a point, and then stopped swelling. The rapid initial swelling of illites can be related to different pore saturation when compared to the bentonite. As water entering the clay structure is not drawn into interlayers of illite because of its K+ saturated structure, water molecules travel through the pores without interruption and therefore the capillary pressures are higher. Thus, the saturation of the pores is completed in a very short time and pore swelling is faster.

3.4.1. Swelling in Aqueous Electrolyte Solutions

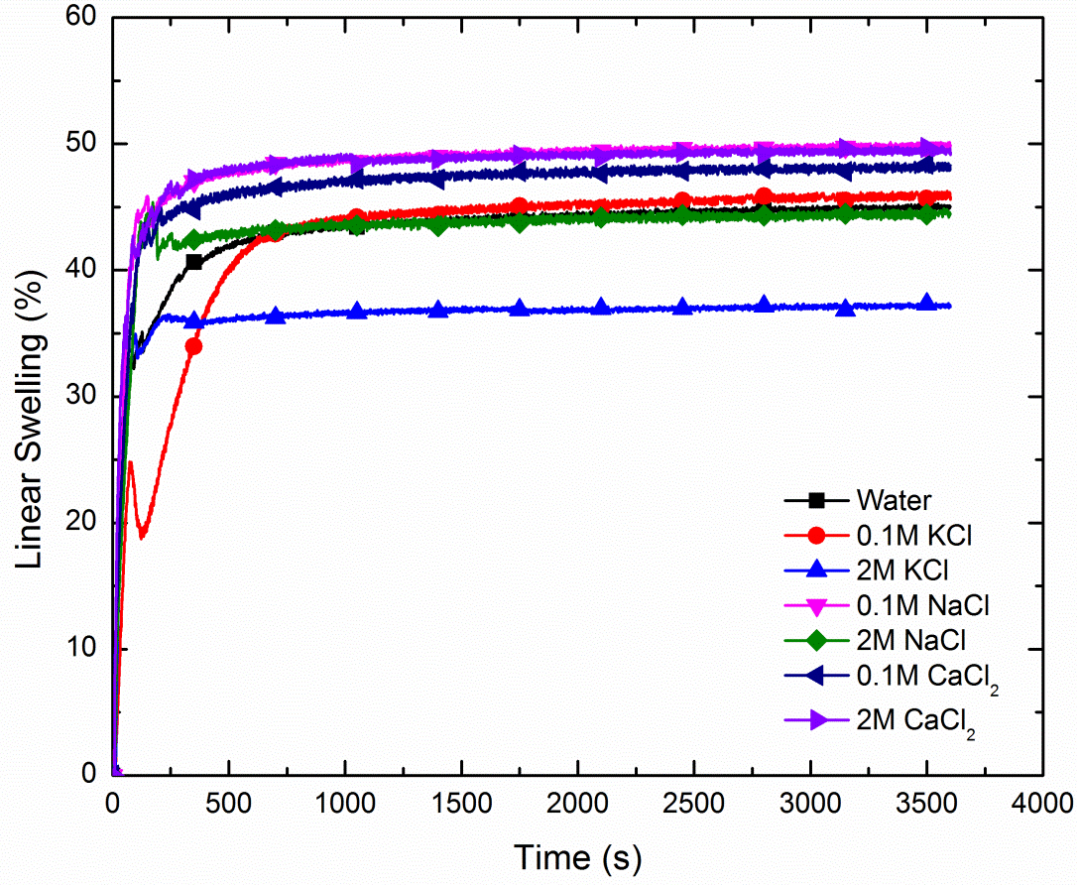

Figure 34. Linear swelling behaviour of compacted illite cores in different concentrations of aqueous KCl, NaCl and $CaCl_2$ solutions

Figure 34 shows the short term swelling of compacted illite cores in water and the solutions of KCl, NaCl and $CaCl_2$. Swelling in electrolyte solutions was almost the same as the swelling in water, regardless to cation type and electrolyte concentration. Cation type and/or the concentration of the electrolyte solutions have no substantial effects on illite swelling. Note that, unlike the coherent structure of Na-bentonite cores after swelling in water, illite cores showed a dispersive and crumbling behaviour.

3.4.2. Swelling of Compacted Illite in Organic Solvents

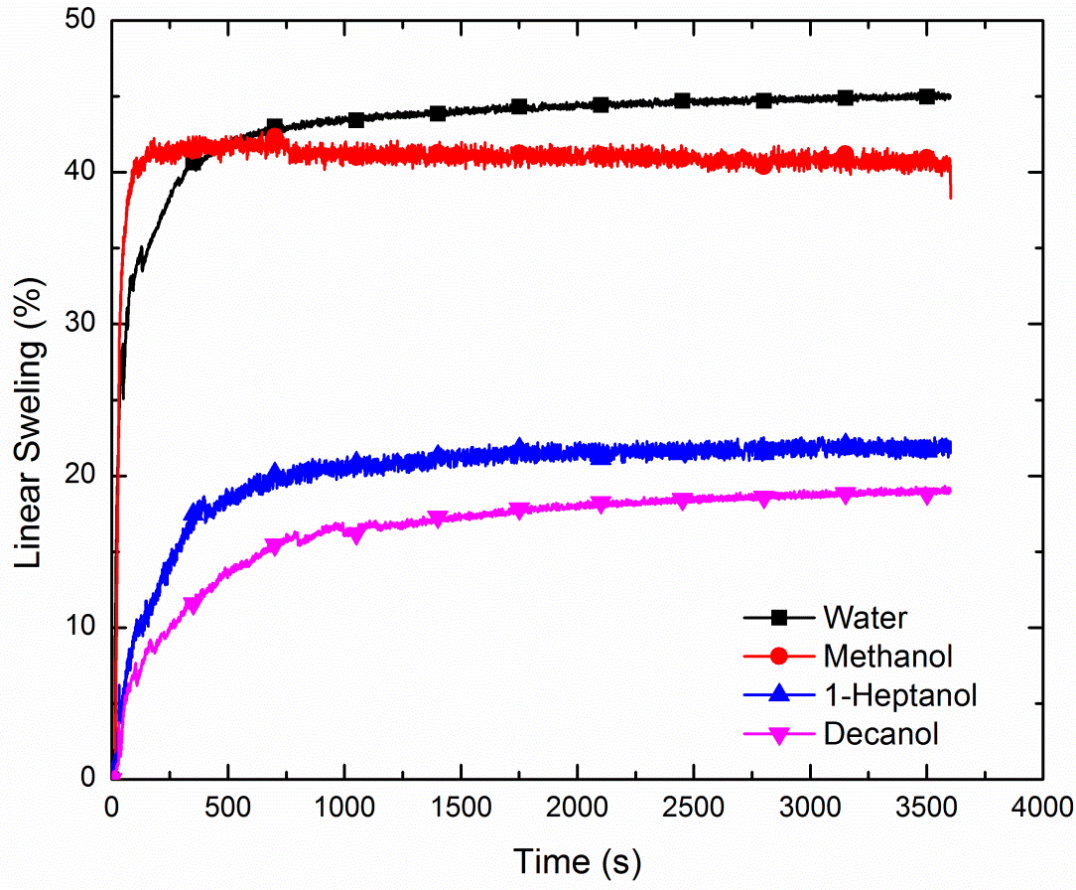

Figure 35. Swelling behaviour of compacted illite cores in water, methanol, 1-heptanol and 1-decanol

Figure 35 shows the swelling behaviour of illite cores in water, methanol, 1-heptanol and 1-decanol. The maximum point of swelling of illite in methanol and

water are almost the same, with 41% and 45% increase in height, respectively. On the other hand, in 1-heptanol and 1-decanol there is an observable difference in the maximum swelling point as it is decreased to 21% and 19%, respectively. The decrease in the swelling in 1-heptanol and 1-decanol can be related to the increase in the viscosity as the viscosity of 1-heptanol and 1-decanol is much higher than water and methanol. This may be inferred as the illite swelling is mainly pore swelling and driven by capillary forces. In order to test this hypothesis, the particle size of illite was changed by sieving to select different particle sizes.

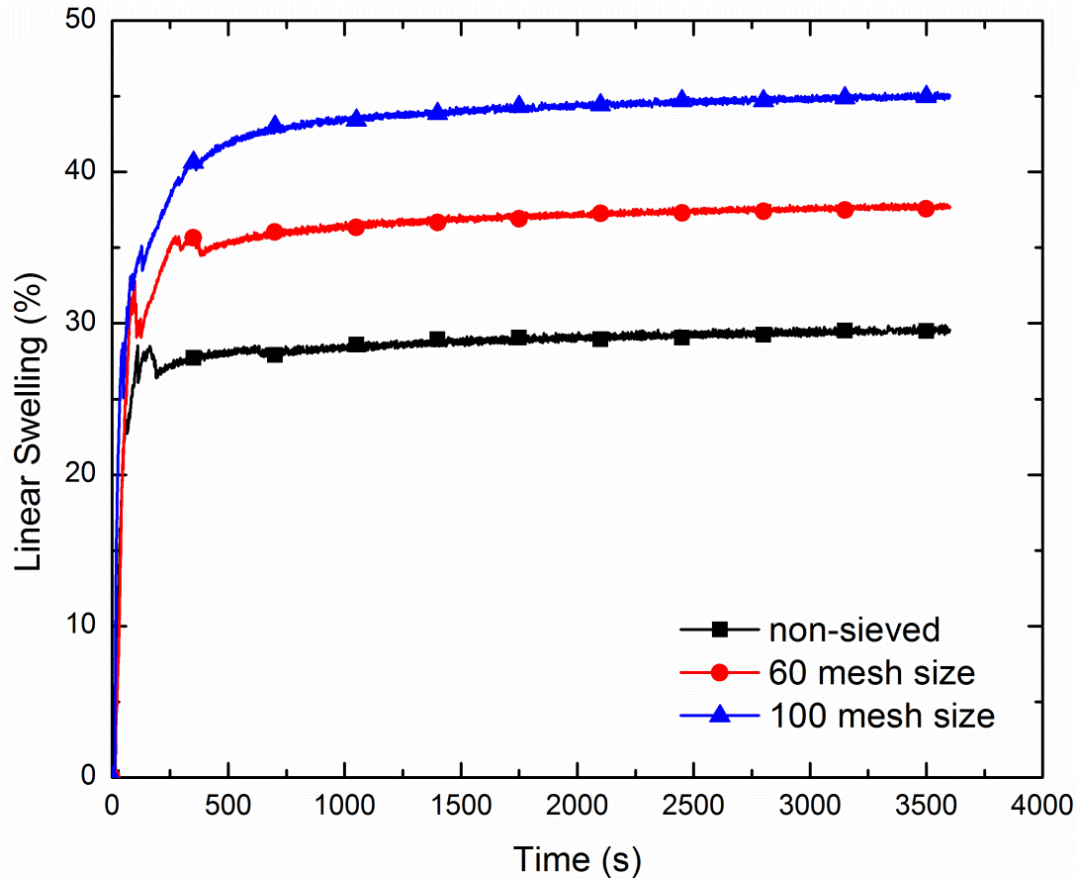

Figure 36. Swelling behaviour of compacted illite cores prepared with different particle sizes

Figure 36 shows the swelling behaviour of illite cores prepared with different particle sizes. It is seen that without sieving, swelling is around 29%, with sieving

to 60 and 100 mesh sizes (250μm and 149μm respectively), the swelling increases to 35% and 45%, respectively. Since the finer the particle size gives rise to a smaller pore size in the compacted core, it is expected that the pore size of the clay cores decreases with decreasing particle size. As seen in Equation 3, the capillary pressures developed in pores are inversely proportional to the pore diameter, in agreement with the results found here. In a similar observation, Forsans and Schmitt (1994) also reported a decrease in the capillary pressures developed in shales with increasing porosity.

4. FURTHER WORK & LIMITATIONS

4.1 Further Possible Tests with NC-LDM

Due to lack of time and resources, intended further tests were postponed to future studies.

1) Tests with illites were restricted with limited organic solvents and limited concentrations of aqueous electrolyte solutions due to lack of time. A full repetition of Na-bentonite tests along with correlations with bulk properties of solvents needs to be applied to illite cores for a full understanding of the swelling behaviour of illites. This will allow a better comparison with Na-bentonite cores and so a better understanding of clay swelling can be attained.
2) Due to laboratory safety regulations, the use of organic solvents was restricted, which didn't allow us to examine the effects of bulk properties of liquids across a wider range of values of solvent properties. NC-LDM along with the computer logging could be moved to a protected area (ie a fume hood) so that more hazardous/volatile chemicals can be used safely.
3) Since the shales in downhole conditions are exposed to high pressures, application of various confining pressure during swelling tests would give more industrially relevant insight.
4) Since the temperature varies along the wellbore throughout the drilling operations, swelling tests in various temperatures could be considered by modifying the swelling chamber to allow efficient heat conduction.

4.2. Development of In-Situ XRD Cell

As was mentioned in the previous "Methods" section, wet-cell XRD technique is an improved way of taking *in situ* XRD measurements allowing recording of changes in basal spacing through time, thereby enabling kinetic measurements of rapid and low temperature crystalline reactions. The method requires no additional modification of the X-ray diffractometer. In this technique, the sample is placed into a novel bespoke designed XRD chamber which allows the kinetic changes to be recorded throughout the analysis. XRD readings are taken at a designated frequency and the results are overlapped on each other enabling to observe the structural changes. Figure 37 shows a favourable graphical outcome of the hydration studies of montmorillonite obtained by this method (Warr and Berger, 2006).

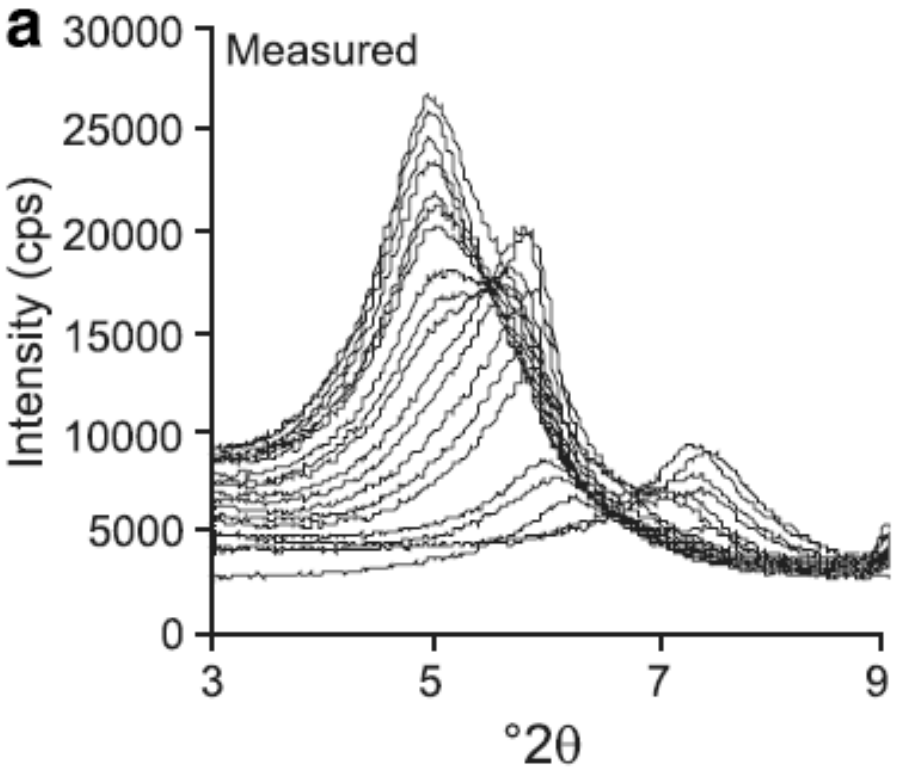

Figure 37. XRD peaks showing the varying hydration states of montmorillonite (Warr and Berger, 2007)

In this present study, the main purpose of using wet-cell XRD technique was to examine the kinetics of clay swelling as well as to find out the role of interlayer expansion in the bulk swelling of clay particles observed in the compacted clay core swelling tests. In order to carry out *in situ* XRD measurements, a custom aluminium cell was designed. The cell consists of a chamber where the clay core is placed in. The chamber was covered with X-ray transparent Kapton® foil. Solvent injection and evacuation of air present in the chamber was facilitated by two 2 mm Ø holes. In order to prevent solvent from spilling through the holes, two nozzles were placed into these holes. The cell was designed with a lid in order to ease the cleaning of the chamber and the capton foil. The designated fluid was injected to the chamber just before the experiment started. Expansion of clay cores were controlled by placing

elastic sponges under them so that the stresses developed during swelling could be absorbed and any possible tear of capton foil could be prevented. Figure 38 shows a schematic sketch of the designed aluminium in-situ XRD cell, while Figure 39 shows the dimensions of the cell.

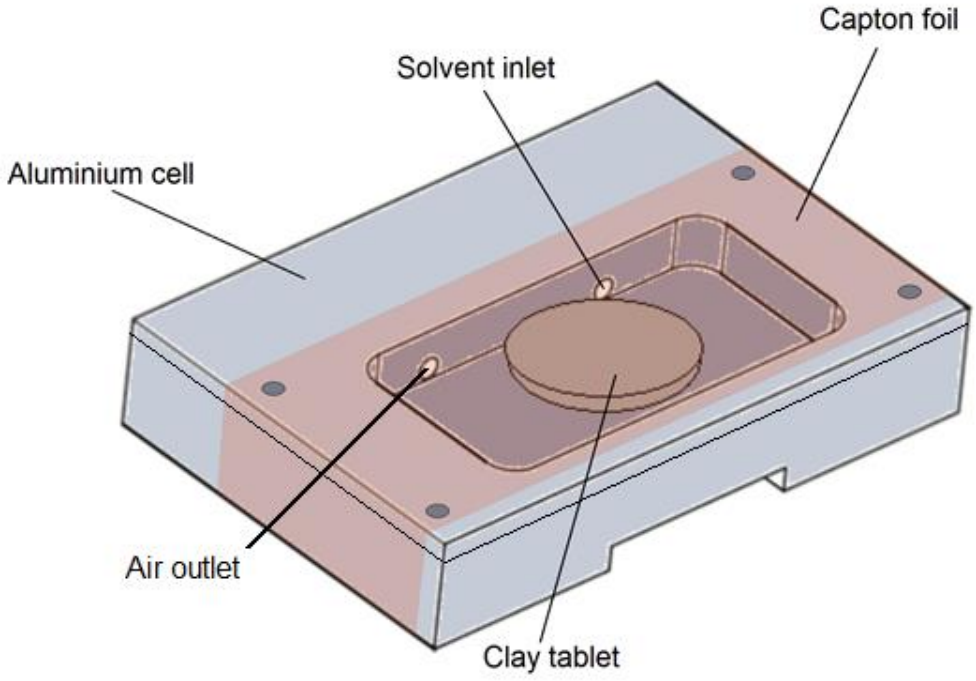

Figure 38. Schematic description of the *in situ* XRD cell used in this study

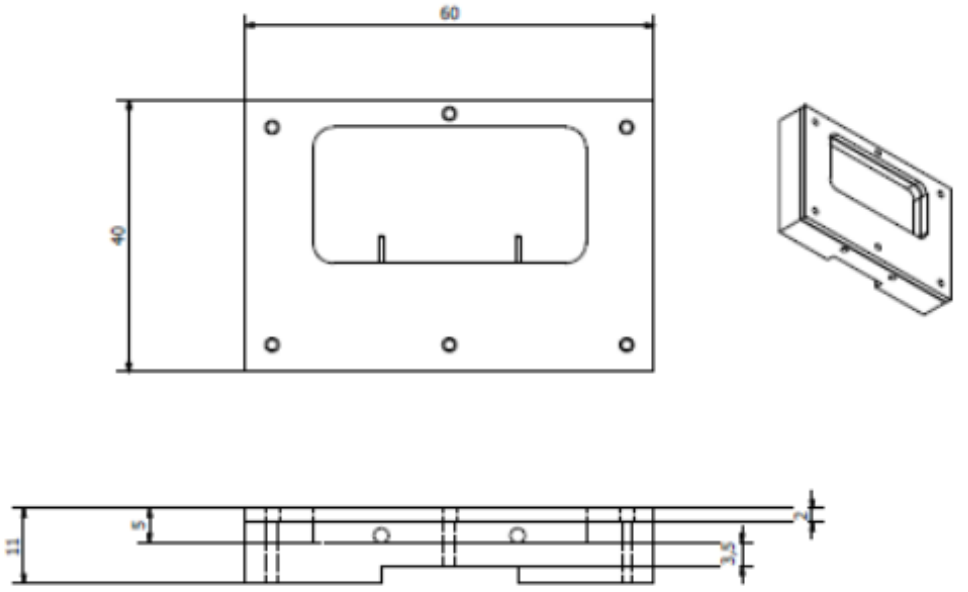

Figure 39. Dimensions of the in-situ XRD cell used in this study

Figure 40 shows the results of one of the trials run within the designed cell. It is seen that at low angles, scanning is problematic and peaks are not observable. The main reason for this was predicted as the reflection of low angle X-Ray beams from the aluminium cell surface, since the data becomes clear after 30°. It is known that the change in the d_{001} spacing of montmorillonite is observed at low diffraction angles, which restricted the use of this cell for swelling experiments. Moreover, since the injection of the liquid is a manual process, injection rate and placing the cell into XRD chamber is prone to human error, which can easily affect the results. Further modifications could not be completed due to time limitations, however this design could be useful in terms of applicability of the *in situ* XRD cells.

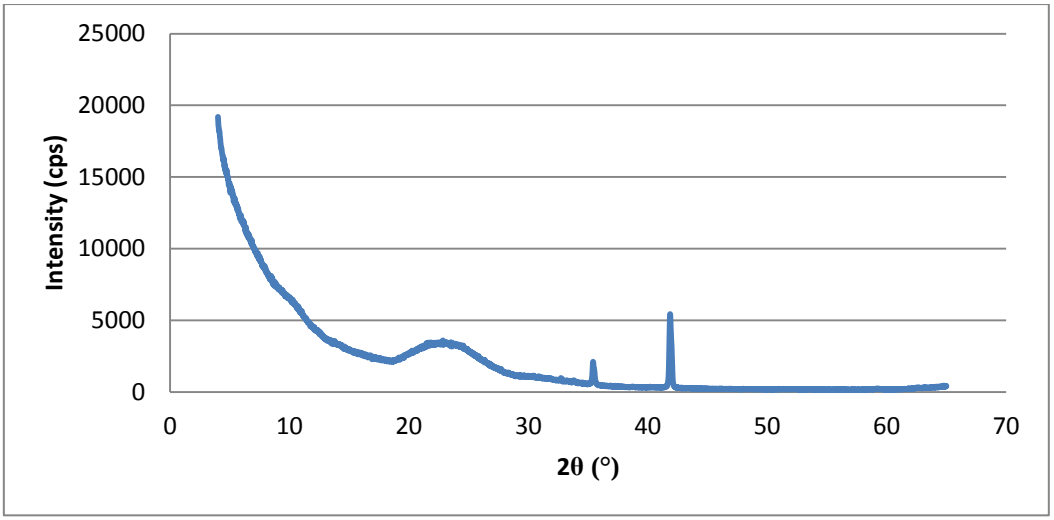

Figure 40. XRD Data obtained from the trials of in-situ XRD cell

5. CONCLUSIONS

The present study is an interpretation of clay swelling in compacted shale/clay cores by using a novel non-contact displacement meter. Time dependent short term swelling tests and equilibrium long term swelling tests were carried out in order to observe the bulk swelling behaviour of artificial Na-bentonite cores in organic solvents for correlations between solvent properties and swelling, and in aqueous electrolyte solutions in order to examine the effects of electrolyte type and concentration.

Swelling tests of Na-bentonite cores in water showed that there are two regimes occurring in water swelling indicating that different forces are dominating the swelling in different times. It is assumed that the first regime is due to pore swelling when water enters the pores and the second regime is due to layer expansion due to water-clay interactions.

In line with DDL theory the dielectric constant of the medium was a key determinant for swelling of smectitic clays. In both short and equilibrium swelling tests, linear swelling rate and total linear swelling of Na-bentonite cores increased with increasing dielectric constant. It was also seen that below a certain value of dielectric constant, (approximately 50-60) the swelling behaviour of smectite cores changed. The effects of dielectric constants higher than water were tested with short term experiments in water/glycine solutions and an increase in the second regime of swelling is observed. Equilibrium swelling and swelling rate of Na-bentonite cores decreased with increasing viscosity of the medium, therefore pore swelling has substantial effects on bulk swelling of Na-bentonites. There are no clear correlations of the dipole moment yet it was seen that having a dipole moment larger than zero is essential for swelling.

Effects of exchangeable cations on swelling were interpreted via swelling tests in different aqueous electrolyte solutions along with DDL theory. In the short term, swelling of Na-bentonite cores was highest in $CaCl_2$ solutions because of higher hydration energy of Ca^{2+} ions leading to higher surface hydration. In addition, it was seen that swelling behaviour of smectites changed above certain concentrations. In long term, when at equilibrium, swelling decreases with increasing electrolyte concentrations because diminishing of double layers. Divalent Ca^{2+} ions are more effective on suppressing clay swelling at low concentrations compared to monovalent K^+ and Na^+ ions. As such, at high concentrations of brine, osmotic swelling is suppressed in all the electrolyte solutions, regardless of the cation properties. In addition, due to having higher hydration affinity, equilibrium swelling of Na-bentonites is higher at high concentrations of $CaCl_2$.

Tests with non-reactive illite clays showed that illite swelling is different than smectite swelling and only viscosity and pore size determine swelling behaviour of illites. This can be concluded as illite swelling is only dominated by capillary action.

In general, swelling behaviour of compacted clay cores is time dependent due to the domination of different swelling components in different periods. At any time of swelling action, several of these components might act simultaneously and their combined influence determines macroscopic effects of swelling.

Further work can be done via in-situ XRD analysis by investigating the role and kinetics of interlayer swelling to overall bulk expansion

APPENDIX A. XRD Data of Na-bentonite and Illite

The XRD diffraction patterns of both Na-bentonite and illite clays are shown in Figure 41 and Figure 42 respectively, with the appropriate crystalline mineral phases labelled above each peak.

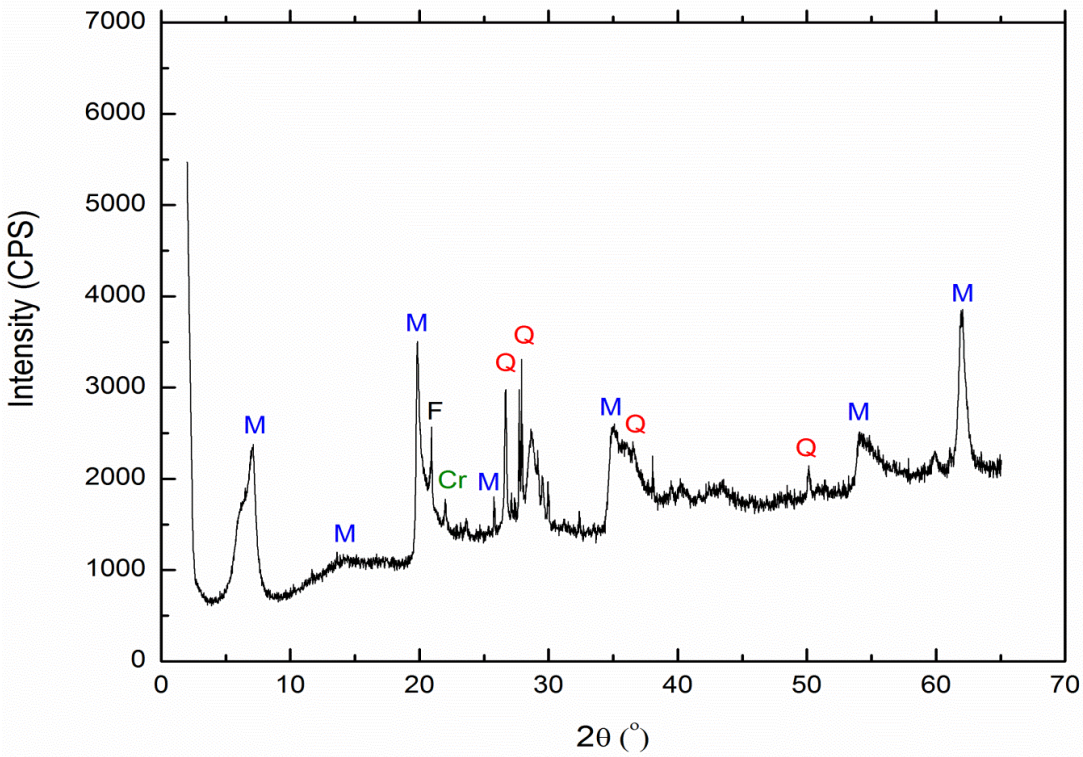

Figure 41. XRD pattern for Na-bentonite cores between a 2-Theta of 2-65°. Where M = Montmorillonite, Q = Quartz, Cr = Cristobalite, F = Feldspar

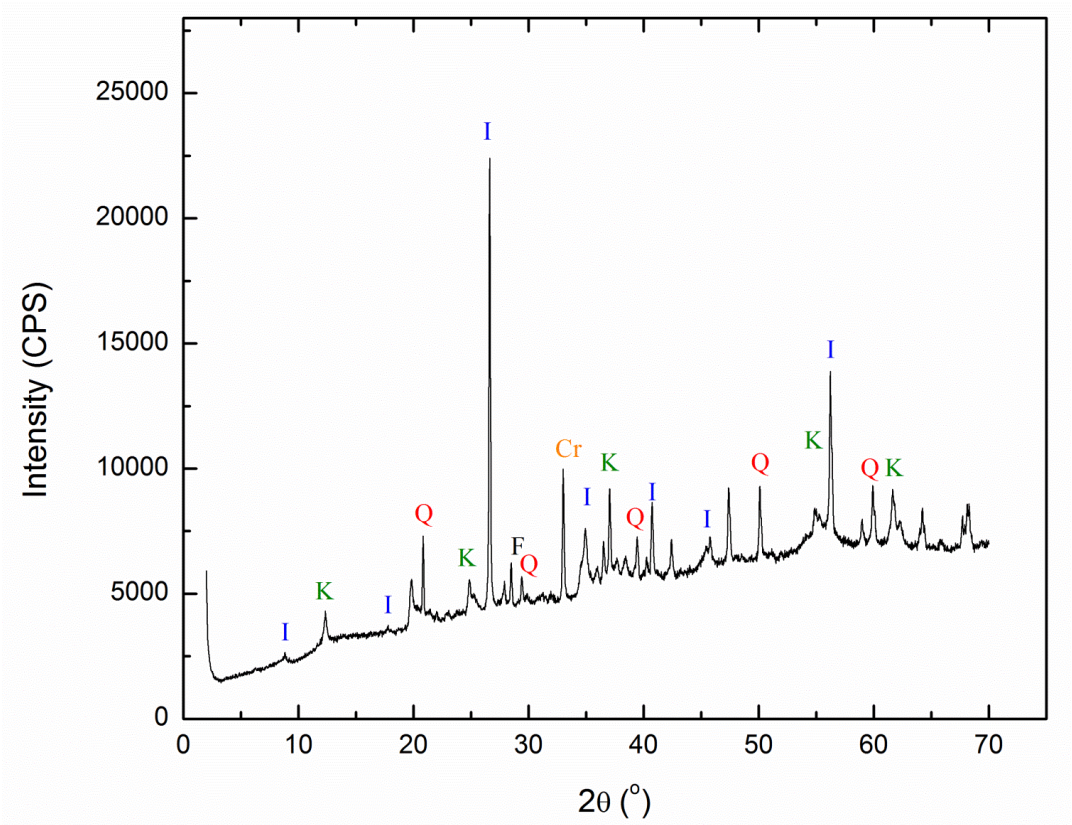

Figure 42. XRD pattern for illite cores between a 2-Theta of 2-70°. Where I = illite, Q = Quartz, K = Kaolinite, Cr = Cristobalite, F = Feldspar

APPENDIX B. Definition of the Solvent Properties

Dielectric constant (ε): The dielectric constant of material represents its ability to reduce the electric force between two charges separated in space is measured with respect to vacuum (1.0) . Dielectric constant is also called "relative permittivity"

Dipole moment (μ): Dipole moment is the measure of net molecular polarity, which is the magnitude of the charge (Q) at either end of the molecular dipole times the distance (r) between the charges.

$$\mu = Q \times r \qquad (4)$$

Dipole moment is a description of the charge separation in a molecule. The larger the difference in electronegativities of bonded atoms, the larger the dipole moment:

$$\frac{\varepsilon_r - 1}{\varepsilon_r + 2} = \frac{\rho N_A}{3M\varepsilon_0}\left(\alpha + \frac{\mu^2}{3kT}\right) \qquad (5)$$

The Debye equation gives the relationship between the dielectric constant and dipole moment, where ε is the dielectric constant, ε_0 is the dielectric constant of vacuum, N_A is Avogadro's number, M is molar mass, T is the temperature, k is the Boltzmann constant. polarizability α, and permanent dipole moment μ in a dielectric material whose molecules are free to rotate.

Surface tension (γ, σ) - The force per unit length in the plane of the interface between a liquid and a gas, which resists an increase in the area of that surface. It can also be equated to the surface Gibbs energy per unit area. In this study the surface tension values are the tension between the organic liquids and the air.

Viscosity (η) - The proportionality factor between sheer rate and sheer stress, defined through the equation $F = \eta A(dv/dx)$, where F is the tangential force required to move a planar surface of area A at velocity v relative to a parallel surface separated from the first by a distance x. Sometimes called dynamic or absolute viscosity. The term kinematic viscosity (symbol ν) is defined as η divided by the mass density (Lide, 2004)

APPENDIX C. Preparation of Electrolyte Solutions

The amounts of the salts used in electrolyte solutions were calculated with the following formula;

The amount of the salt (g) = Mw *(g/mol)* **x Mc** *(mol/L)* **x V** *(L)*

Where;

$\mathbf{M_w}$ is the molecular weight of the salt,

$\mathbf{M_c}$ is the molar concentration of the electrolyte solution,

V is the volume of the solvent.

For short term (200 mL) and equilibrium (20mL) tests, the amount of salts calculated with the formula above is shown in Table 8 and Table 9 respectively.

Table 8. The amounts of salt required for short term swelling tests

	The amount of salt (g)			
Molar Concentration (mol/L)	**KCl**	**NaCl**	**KI**	**$CaCl_2$**
0.02	0.30	0.23	0.66	0.44
0.05	0.75	0.58	1.66	1.11
0.1	1.49	1.17	3.32	2.22
0.3	4.47	3.51	9.96	6.66
0.5	7.46	5.84	16.60	11.10
1	14.91	11.69	33.20	22.20
2	29.82	23.38	66.40	44.39

Table 9. The amounts of salt required for short term swelling tests

	The amount of salt (g)			
Molar Concentration (mol/L)	**KCl**	**NaCl**	**KI**	**$CaCl_2$**
0.02	0.030	0.023	0.066	0.044
0.05	0.075	0.058	0.166	0.111
0.1	0.149	0.117	0.332	0.222
0.3	0.447	0.351	0.996	0.666
0.5	0.746	0.584	1.660	1.110
1	1.491	1.169	3.320	2.220
2	2.982	2.338	6.640	4.439

APPENDIX D. Working Principles of Non-Contact Linear Displacement Meter

The detector has the same working principle with a metal detector, which detects the presence or absence of metal. The detection method is based on the change in the inductance of a coil with the approach of a metal. the inductance increases the coil is approached to an iron object, whereas it decreases if the item is gold. The detector is equivalent to an oscillator including a capacitor and a coil.

One of the essential properties of the metal is its ability to conduct electricity. Metal detectors are based on detecting the flow of an electric current in the metal elements. This detection is based on the induced current flow (see Equation 6, Biot-Savart law) magnetic field.

$$\vec{B}(\vec{r}) = \frac{\mu_0}{4\pi} \oint \frac{I d\vec{l}(\vec{r} - \overrightarrow{r'})}{|\vec{r} - \overrightarrow{r'}|^3} \quad (6)$$

Hence, the presence of a magnetic field induced by a current flowing through a metallic conductor has to be measured. As the sensor of a metal detector is a coil, it is only sensitive to temporal variations of the magnetic flux embracing the coil (see Equation 7, Lentz law).

$$\varepsilon = -\frac{d^{\Phi}}{dt} = -L\frac{di}{dt} \quad (7)$$

However, an electric current does not flow naturally to rest in a conductor. The detection system must first attempt to force the passage of current in order to measure the effects. For this, the same properties as those described above are used. The detector coil, or if one of the coils there are several, is used as the excitation

coil for generating a magnetic field. It is important that this field varies with time, and the electrical circuit supplying the coil generates an alternating current periodically and whose shape is sinusoidal or pulsed. All metallic element immersed in this field is the seat of eddy currents. These currents are established based on the electrical properties of the conductor (see Equation 8, Ohm's law) and the spatial and temporal characteristics of the excitation field.

$$U=R.I \tag{8}$$

In summary, a metal detector is an active sensor, generating a magnetic field varying in time as the excitation source, and measuring the presence of a potential field retro-induct by the metal. Metal detectors are also called magnetic induction detector.

APPENDIX E. Calibration of Non-Contact Linear Displacement Meter

The sensors are inductive coils used to measure the displacement of the nearest metal object to the sensor. The range of the sensor is given as 0-10 mm however the realistic range of the sensor is 2-8 mm. This means 2-8 mm between the sensor and the nearest metal object parallel to the end of the sensor.

Calibration of the sensors is performed by measuring the voltage output of the sensors at given distances. Using Vernier caliper, the distance between the sensor and the metal disk is measured by hand and the voltage output is recorded. Ideally 20 readings are taken every 0.5 mm from 0mm to 10mm (distance between sensor and metal disk). The sensors need to be calibrated to set a 0 value when taking a real measurement.

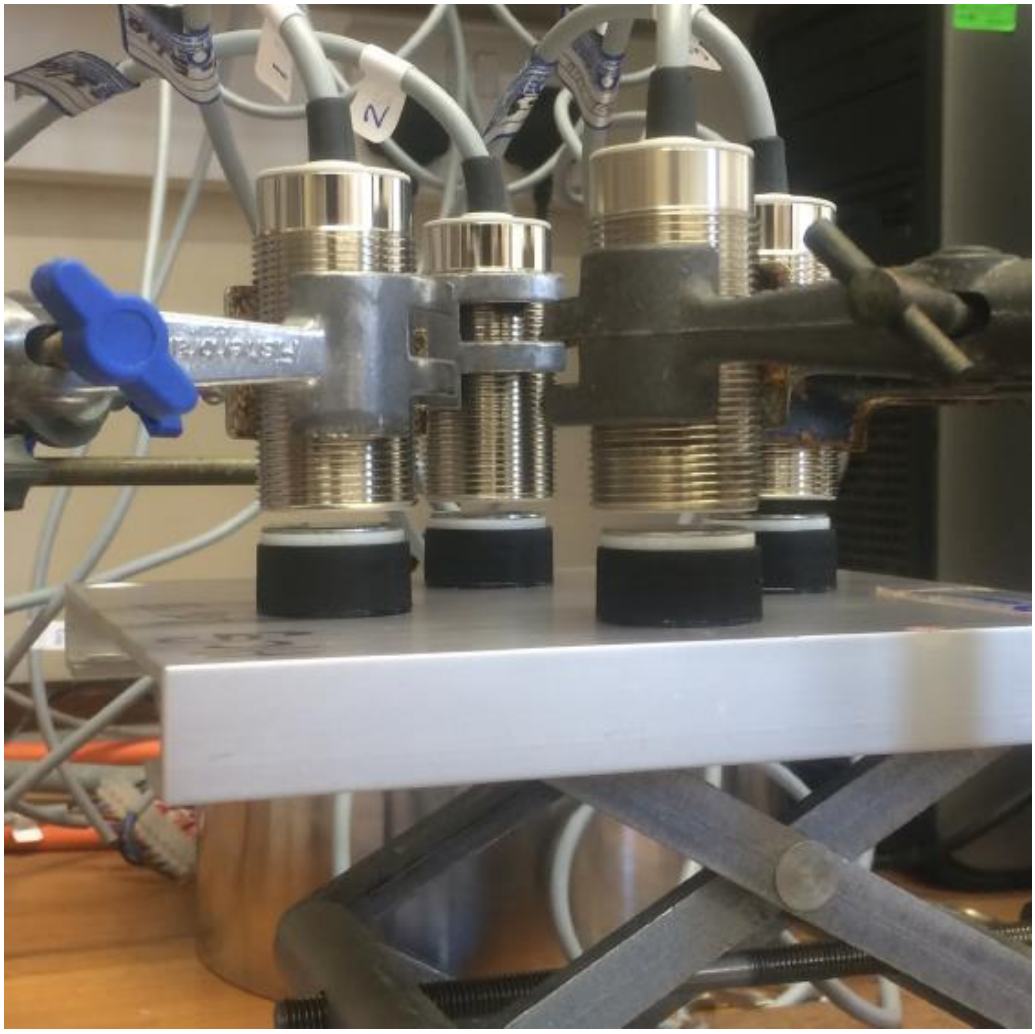

Figure 43. Photographic image of the calibration of the NC-LDM

Figure 43 shows the photographic image of calibration set-up.

At a given distance, the code takes a measurement of the voltage (a snapshot of the output waveform) and calculates the average value of the waveform. It does this 10 times and then it calculates the average and SD of the 10 values. Each waveform graph is setup to show the output signal of each sensor individually, so Waveform1 is for sensor 1 and so on. In the front panel there are 4 input boxes:

1. "**Points**": number of points that is required for a full calibration. I.e the total number of distances at which calibration readings will be taken.

2. "**Vernier**": distance that is recorded between the metal disk and the tip of the sensor using the vernier callipers.

3. "**Rate**": the number of slices that the output signal (waveform) is cut into in 1 second.

4. "**Number of points**": the number of slices used in the calibration reading.

Figure 44 and Figure 45 shows two calibration curves of 25 mm Ø and 20 mm Ø metal disks.

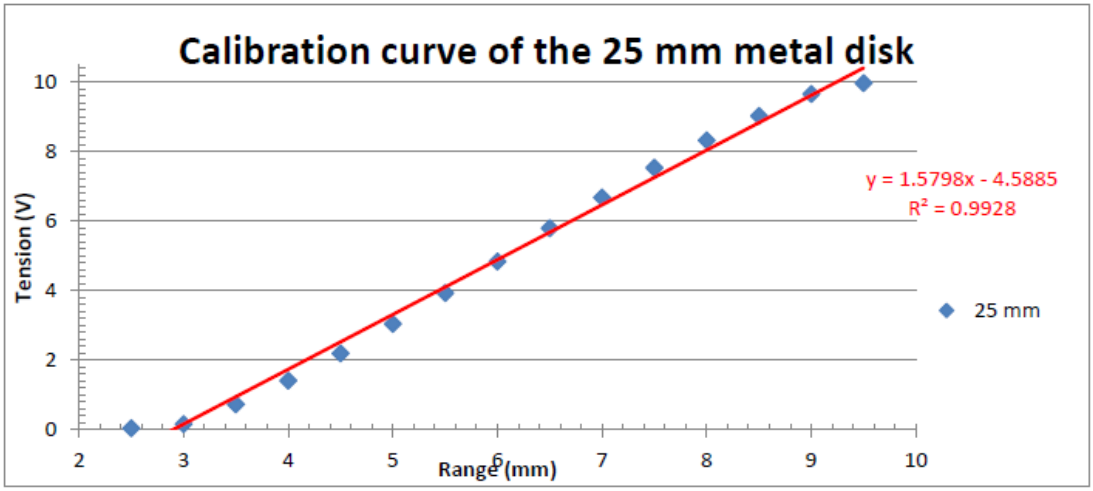

Figure 44. Calibration curve of 25mm metal disk

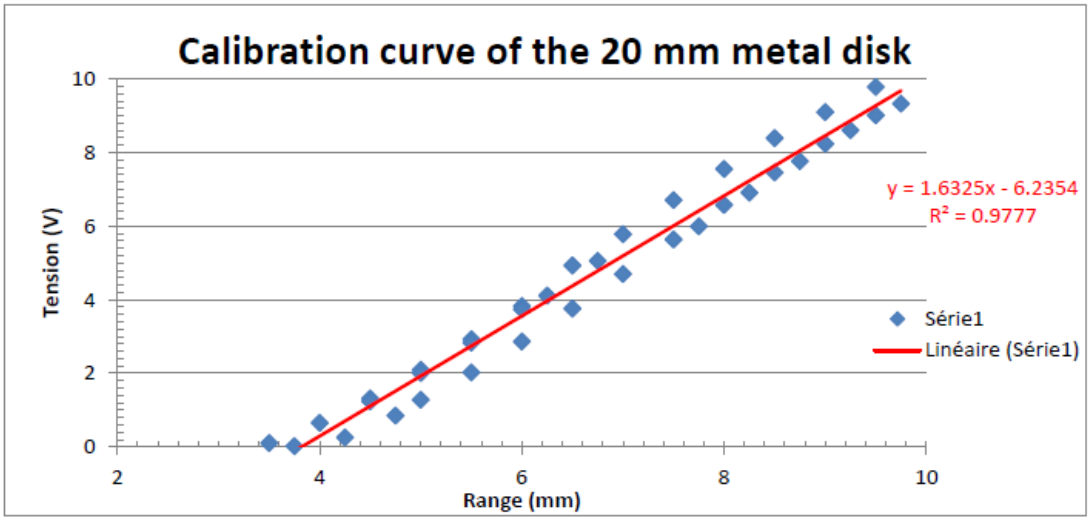

Figure 45. Calibration curve of 20mm metal disk

APPENDIX F. Adjustment of Relative Humidity

The effects of relative humidity of air as well as the saturation of clay cores are tested by using saturated salt solutions. It is known that a saturated solution of a particular salt can be used to maintain certain values of relative humidity inside a sealed container. Table 10 (Rockland, 1960) shows the list of salts to achieve a particular relative humidity value at different temperatures. . In this study, in order to achieve 75% and 82% relative humidity saturated solutions of sodium chloride (NaCl) and potassium chloride (KCl) were used respectively. Note that expected RH value by using saturated KCl solution was 86% RH, however the RH could only go up to 82%.

Table 10. Relative humidity values at saturated salt solutions

Salt	Relative Humidity, % at ° C.							
	5°	10°	15°	20°	25°	30°	35°	40°
GROUP A								
Lithium chloride	16	14	13	12	11	11	11	11
Potassium acetate	25	24	24	23	23	23	23	23
Magnesium bromide	32	31	31	31	31	30	30	30
Magnesium chloride	33	33	33	33	33	32	32	31
Potassium carbonate	..	47	45	44	43	42	41	40
Magnesium nitrate	54	53	53	52	52	52	51	51
Sodium bromide	59	58	58	57	57	57	57	57
Cupric chloride	65	68	68	68	67	67	67	67
Lithium acetate	72	72	71	70	68	66	65	64
Strontium chloride	77	77	75	73	71	69	68	68
Sodium chloride	76	75	75	75	75	75	75	75
Ammonium sulfate	81	80	79	79	79	79	79	79
Cadmium chloride	83	83	83	82	82	82	79	75
Potassium bromide	..	86	85	84	83	82	81	80
Lithium sulfate	84	84	84	85	85	85	85	81
Potassium chloride	88	87	87	86	86	84	84	83
Potassium chromate	89	89	88	88	87	86	84	82
Sodium benzoate	88	88	88	88	88	88	86	83
Barium chloride	93	93	92	91	90	89	88	87
Potassium nitrate	96	95	95	94	93	92	91	89
Potassium sulfate	98	97	97	97	97	97	96	96
Disodium phosphate	98	98	98	98	97	96	93	91[b]
Lead nitrate	99	99	98	98	97	96	96	95
GROUP B								
Zinc nitrate	43	43	41	38	31	24	21	19
Lithium nitrate	61	59	55	49	41	31	19	11
Calcium nitrate	..	66	60	56	54	51	48	46
Cobalt chloride	..	..	73[c]	67	64	62	59	57
Zinc sulfate	95	93	92	90	88	86	85	84

APPENDIX G. Data Processing

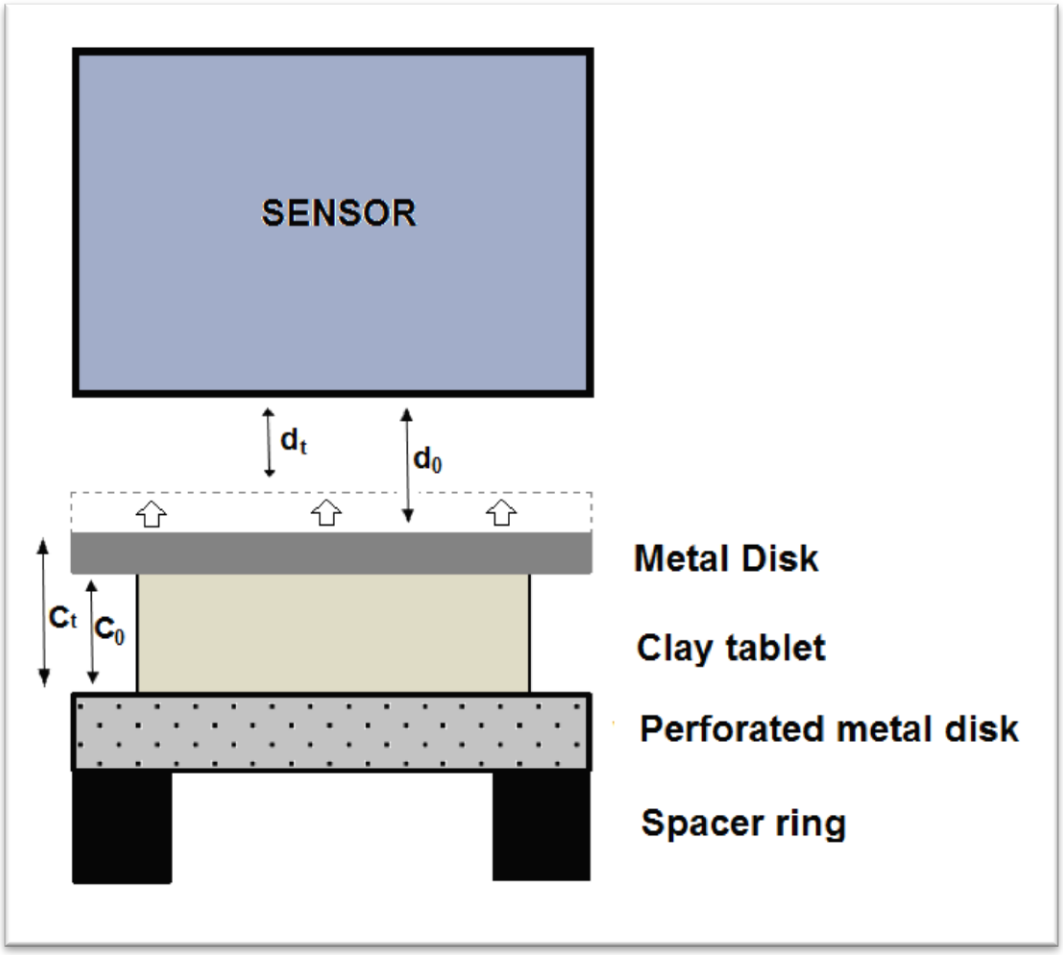

Figure 46. Schematic structure of a single unit of NC-LDM

Figure 46 shows the symbolic structure of a single unit of the non-contact displacement meter. C_0 and C_t are the thickness of the clay core initially and after swelling in a time "t" respectively. d_0 is the initial distance between metal disk and sensor, while d_t is the same distance at time "t". In this study, as only linear swelling is discussed, quantitative representation of clay swelling is addressed to the change in the thickness (y-direction) of clay cores. Thus percentile clay swelling (S%) is shown as;

$$S\% = \frac{\Delta C}{C0} x100 = \frac{Ct - C0}{C0} \; x \; 100$$

Due to the fact that clays are non-conductive, sensors can't measure the expansion of clay cores. Hence, 0.7 thick metal disks are placed on each clay core in order to measure the increase in core thickness as a function on the displacement of the metal disk in y-direction. Sensors measure the distance "d" at any time "t". With the knowledge of initial distance "d_0", the difference between d_t and d_0 is equal to the difference in core thickness in time "t" (C_t-C_0) and the percentile swelling equation becomes;

$$S\% = \frac{Ct - C0}{C0} \; x \; 100 = \frac{-(dt - d0)}{C0} \; x \; 100$$

Each test is performed with four core samples simultaneously in order to achieve consistency. The final swelling data is revealed after calculating the arithmetic mean of these data. Figure 47 and Figure 48 show how the swelling data looks before and after processing respectively.

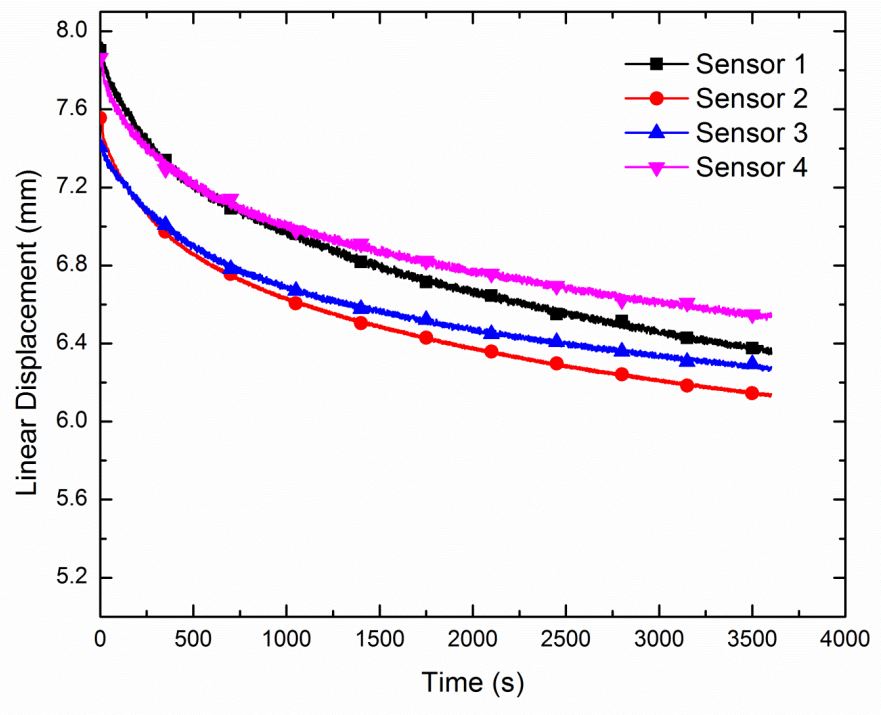

Figure 47. Swelling data before processing

For swelling rate calculations in organic solvents, slope of linear regression data (via Microsoft Excel®) of the plots were taken for certain swelling times. If the expansion exceeded the sensor height, observable swelling and time data were considered. Therefore the swelling rate was calculating by the following formula;

$$\text{Swelling rate} = (S\%)/\Delta t$$

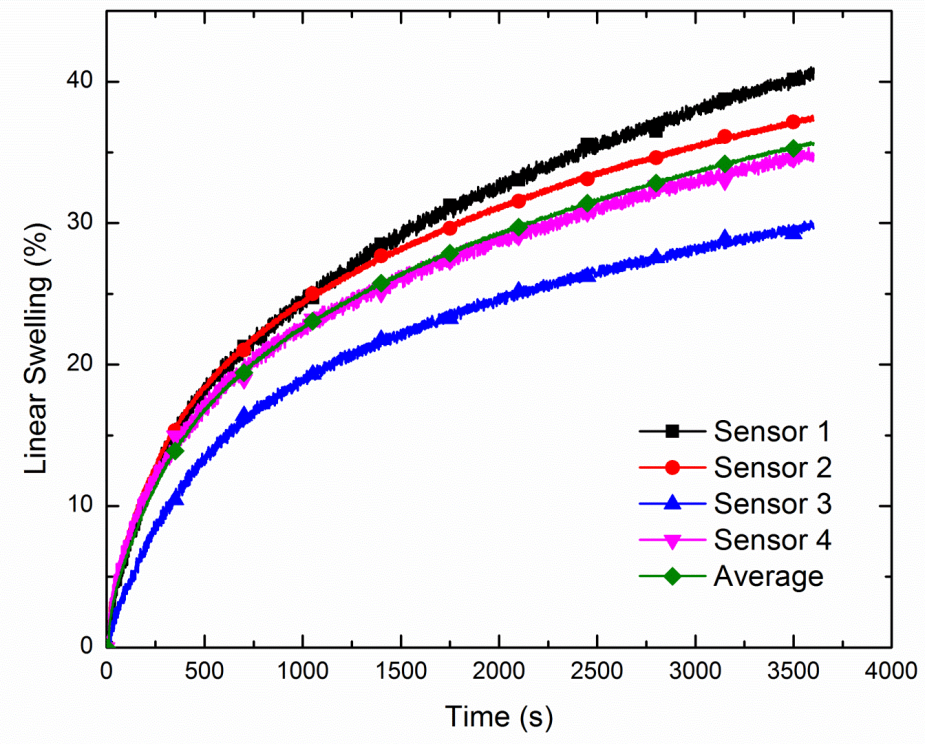

Figure 48. Swelling data after processing

5. REFERENCES

ANDERSON, R. L., RATCLIFFE, I., GREENWELL, H. C., WILLIAMS, P. A., CLIFFE, S. & COVENEY, P. V. 2010. Clay swelling — A challenge in the oilfield. Earth-Science Reviews, 98, 201-216.

BARSHAD, I. 1952. Factors affecting the interlayer expansion of vermiculite and montmorillonite with organic substances. Soil Science Society of America Journal, 16, 176-182.

BERGAYA, F. & LAGALY, G. 2013. Handbook of clay science. Newnes, 5.

BERKHEISER, V. & MORTLAND, M. M. 1975. Variability in Exchange Ion Position in Smectite: Dependence on Interlayer Solvent. Clays and Clay Minerals, 23, 404-410.

BESQ, A., MALFOY, C., PANTET, A., MONNET, P. & RIGHI, D. 2003. Physicochemical characterisation and flow properties of some Na-bentonite muds. Applied Clay Science, 23, 275-286.

BOEK, E. S., COVENEY, P. V. & SKIPPER, N. T. 1995. Monte Carlo molecular modeling studies of hydrated Li-, Na-, and K-smectites: Understanding the role of potassium as a clay swelling inhibitor. Journal of the American Chemical Society, 117, 12608-12617.

BRINDLEY, G. W., WIEWIORA, K. & WIEWIORA, A. 1969. Intracrystalline swelling of montmorillonite in some water-organic mixtures. The American Mineralogist, 54, 1635.

BROWN, G. W. & BRINDLEY, G. W. 1980. Crystal structures of clay minerals and their X-ray identification. Mineralogical Society, London, 5.

CHAPMAN, D. L. 1913. LI. A contribution to the theory of electrocapillarity. The London, Edinburgh, and Dublin philosophical magazine and journal of science, 25, 475-481.

CHEATHAM, C. A. & NAHM, J. J. 1990. Bit balling in water-reactive shale during full-scale drilling rate tests. SPE/IADC Drilling Conference.

CHEN, S., LOW, P. F., CUSHMAN, J. H. & ROTH, C. B. 1987. Organic compound effects on swelling and flocculation of Upton montmorillonite. Soil Science Society of America Journal, 51, 1444-1450.

CHENEVERT, M. E. & OSISANYA, S. O. 1989. Shale mud inhibition defined with rig-site methods. SPE Drilling Engineering, 4, 261-268.

CHRISTIDIS, G. E., BLUM, A. E. & EBERL, D. D. 2006. Influence of layer charge and charge distribution of smectites on the flow behaviour and swelling of Na-bentonites. Applied Clay Science, 34, 125-138.

DARLEY, H. C. & GRAY, G. R. 1988. Composition and properties of drilling and completion fluids.

FORSANS, T. M. & SCHMITT, L. 1994. Capillary forces: The neglected factor in shale instability studies? Rock Mechanics in Petroleum Engineering. Society of Petroleum Engineers.

FOSTER, W. R., SAVINS, J. G. & WAITE, J. M. 1954. Lattice Expansion and Rheological Behaviour Relationships in Water-Montmorillonite Systems. Clays and Clay Minerals, 3, 296-316.

GOUY, G. 1910. Sur la constitution de la charge electrique a la surface d'un electrolyte. J. phys, 9, 457-468.

GREEN, W. J., LEE, G. F., JONES, R. A. & PALIT, T. 1983. Interaction of clay soils with water and organic solvents: Implications for the disposal of hazardous wastes. Environmental Science & Technology, 17, 278-282.

GRIM, R. E. 1953. Clay mineralogy. Soil Science, 76, 317.

HALE, A. H., MODY, F. K. & SALISBURY, D. P. 1993. The Influence of Chemical Potential on Wellbore Stability. SPE Drilling & Completion.

HALLIKAINEN, M. T., ULABY, F. T., DOBSON, M. C., EL-RAYES, M. A. & WU, L. K. 1985. Microwave dielectric behavior of wet soil-part 1: empirical models and experimental observations. Geoscience and Remote Sensing, IEEE Transactions on, 25-34.

HENDRICKS, S. B., NELSON, R. A. & ALEXANDER, L. T. 1940. Hydration Mechanism of the Clay Mineral Montmorillonite Saturated with Various Cations Journal of the American Chemical Society, 62, 1457-1464.

HOFMANN, U., KURD, E. & DIEDERICH, W. 1933. Kristallstruktur und quellung von montmorillonit. Zeitschrift für Kristallographie-Crystalline Materials, 86, 340-348.

JASPER, J. J. 1972. The surface tension of pure liquid compounds. Journal of physical and chemical reference data, 1, 841-1010.

JOHNSON, G. W. 1997. LabVIEW graphical programming. Tata McGraw-Hill Education.

KITTRICK, J. A. 1969. Interlayer forces in vermiculite and montmroillonite. Soil Science Society of America Journal, 33, 217-222.

LAL, M. 1999. Shale stability: drilling fluid interaction and shale strength. SPE Asia Pacific Oil and Gas Conference and Exhibition.

LIDE, D. R. 2004. Handbook of chemistry and physics 85 Boca Raton (Fla).

LIU, S., MO, X., ZHANG, C., SUN, D. & MU, C. 2004. Swelling Inhibition by Polyglycols in Montmorillonite Dispersions. Journal of Dispersion Science and Technology, 25, 63-66.

LIU, X. D. & LU, X. C. 2006. A thermodynamic understanding of clay-swelling inhibition by potassium ions. Angew Chem Int Ed Engl, 45, 6300-3.

LORET, B., HUECKEL, T. & GAJO, A. 2002. Chemo-mechanical coupling in saturated porous. International Journal of Solids and Structures, 39, 2773–2806.

MILLEN, W. A. & WATTS, D. W. 1967. Theoretical calculations of thermodynamic functions of solvation of ions. Journal of the American Chemical Society, 89, 6051-6056.

MODY, F. K. & HALE, A. K. 1993. Borehole stability in shales. SPE Drilling & Completion.

MONDSHINE, T. C. 1969. New technique determines oil-mud salinity needs in shale drilling. Oil and Gas Journal, 14, 70-75.

MOONEY, R. W., KEENAN, A. G. & WOOD, L. A. 1952. Adsorption of Water Vapor by Montmorillonite. II. Effect of Exchangeable Ions and lattice swelling as

measured by X-ray diffraction. Journal of the American Chemical Society, 74, 1371-1374.

MORAIS, F. I., PAGE, A. L. & LUND, L. J. 1976. The effect of pH, salt concentration, and nature of electrolytes on the charge characteristics of Brazilian tropical soils. Soil Science Society of America Journal, 40, 521-527s.

MURRAY, H. H. 2006. Applied clay mineralogy: occurrences, processing and applications of kaolins, Na-bentonites, palygorskitesepiolite, and common clays. Elsevier, 2.

MURRAY, R. S. & QUIRK, J. P. 1982. The physical swelling of clays in solvents. Soil Science Society of America Journal, 46, 865-868.

NORRISH, K. 1954. The Swelling of Montmorillonite. Discussions of the Faraday Society, 18, 120-134.

O'BRIEN, D. E. & CHENEVERT, M. E. 1973. Stabilizing sensitive shales with inhibited, potassium-based drilling fluids. Journal of Petroleum Technology, 25, 1089.

OLEJNIK, S., POSNER, A. M. & QUIRK, J. P. 1974. Swelling of Montmorillonite in Polar Organic Liquids. Clays and Clay Minerals, 22, 361-365.

ONIKATA, M., K., M. & Y., S. 1999. Swelling of formamide-montmorillonite complexes in polar liquids. Clays and clay minerals, 47, 678.

PARKS, G. A. & DE BRUYN, P. L. 1962. The zero point charge of oxides. The Journal of Physical Chemistry, 66, 967-973.

RATCLIFFE, I., WILLIAMS, P. A., ANDERSON, R. L., GREENWELL, H. C., CLIFFE, S., L., S. J. & COVENEY, P. V. 2009. Clay swelling inhibitor structure-activity relationships: a combined molecular simulation and experimental study. RSC Chemistry in the Oilfield IX, 324-337.

ROCKLAND, L. B. 1960. Saturated salt solutions for static control of relative humidity between 5° and 40° C. Analytical Chemistry, 32, 1375-1376.

ROEHL, E. A. & HACKETT, J. L. 1982. A Laboratory Technique for Screening Shale Swelling Inhibitors. SPE Annual Technical Conference and Exhibition. Society of Petroleum Engineers.

SANTARELLI, F. J. & CARMINATI, S. 1995. Do Shales Swell? A Critical Review of Available Evidence. SPE/IADC Drilling Conference. Society of Petroleum Engineers.

SCHMITT, L., FORSANS, T. M. & SANTARELLI, F. J. 1994. Shale Testing and Capillary Phenomena. International journal of rock mechanics and mining sciences & geomechanics abstracts, 31, 411-427.

SING, K. S. W. & GREGG, S. J. 1982. Adsorption, surface area and porosity. Academic Press, London.

SMALLWOOD, I. 2012. Handbook of organic solvent properties. Butterworth-Heinemann.

SMITH, D. W. 1977. Ionic hydration enthalpies. Journal of Chemical Education, 54, 540.

SOGA, K. & MITCHELL, J. K. 2005. Fundamentals of Soil Behaviour. Wiley. Third Edition, ISBN 10, 0-471.

SPOSITO, G., SKIPPER, N. T., SUTTON, R., PARK, S., SOPER, A. K. & GREATHOUSE, J. A. 1999. Surface geochemistry of the clay minerals. Proceedings of the National Academy of Sciences, 96, 3358-3364.

SRIDHARAN, A. & PUVVADI, V. S. 1986. Swelling pressure of clays. ASTM geotechnical testing journal, 9, 24-33.

STEIGER, R. P. 1982. Fundamentals and use of potassium polymer drilling fluids to minimize drilling problems. Journal of Petroleum Technology, 34, 661.

STERN, O. 1924. Zur theorie der elektrolytischen doppelschicht. Zeitschrift für Elektrochemie und angewandte physikalische Chemie, 30, 508-516.

SUTER, J. L., COVENEY, P. V., ANDERSON, R. L., GREENWELL, H. C. & CLIFFE, S. 2011. Rule based design of clay-swelling inhibitors. Energy & Environmental Science, 4, 4572.

TARE, U. & MODY, F. 2000. Stabilizing boreholes while drilling reactive shale formations with silicate-base drilling fluids. Drilling Contractor, 5/6, 42-44.

VAN OLPHEN, H. 1965. Thermodynamics of interlayer adsorption of water in clays: I. Sodium vermiculite. Journal of Colloid Science, 20, 822-837.

VAN OORT, E. 2003. On the physical and chemical stability of shales. Journal of Petroleum Science and Engineering, 38, 213-235.

WARR, L. & BERGER, J. 2007. Hydration of Na-bentonite in natural waters: Application of “confined volume” wet-cell X-ray diffractometry. Physics and Chemistry of the Earth, Parts A/B/C, 32, 247-258.

WARR, L. N. & HOFMANN, H. 2003. In situ monitoring of powder reactions in percolating solution by wet-cell X-ray diffraction techniques. Journal of Applied Crystallography, 36, 948-949.

WILSON, M. J. & WILSON, L. 2014. Clay mineralogy and shale instability: an alternative conceptual analysis. Clay Minerals, 49, 127-145.

ZEYNALI, M. E. 2012. Mechanical and physico-chemical aspects of wellbore stability during drilling operations. Journal of Petroleum Science and Engineering, 82-83, 120-124.

ZHANG, L. M. & SUN, B. W. 1999. Inhibition of water-soluble cationic cellulosic polymers to clay hydration. Journal of applied polymer science 74, 3088-3093.